Horisfieldones A and B, Two Aromatic Ring-contracted Dimeric Diarylpropanes with Human DOPA Decarboxylase Inhibitory Activity from *Horsfieldia kingii*

Rui Zhan, [†,#] You-Tian Hu, [‡,#] Li-Dong Shao, [§,#] Xu-Jie Qin, [¶] Fang Kuang, [†] Shou-Zhen Du, [†] Fang Wu, [*,‡] Ye-Gao, Chen[*,†]

[†] School of Chemistry and Chemical Engineering, Yunnan Normal University, Kunming 650500, China

[‡] Key Laboratory of Systems Biomedicine (Ministry of Education), Shanghai Center for Systems Biomedicine, Shanghai Jiao Tong University, Shanghai 200240, China

[§] Department of Traditional Chinese Medicine, Yunnan University of Chinese Medicine, Kunming 650500, China

[¶] State Key Laboratory of Phytochemistry and Plant Resources in West China, Kunming Institute of Botany, Chinese Academy of Sciences, Kunming 650201, China

Table of Contents

Detailed experimental procedures

General Experimental Procedures. Optical rotations were measured using a Jasco P-1020 polarimeter equipped with a 1 dm pathlength cell. UV spectra were obtained using a Shimadzu UV-2401A spectrophotometer equipped with a DAD and a 1 cm pathlength cell. Samples in methanol solution were scanned from 190-400 nm in 1 nm steps. All ^{1}H, ^{13}C, and 2D NMR (HSQC, ^{1}H–^{1}H COSY, HMBC, ROESY) spectra were collected with a Bruker AV III-800 spectrometer at 800 MHz for ^{1}H and 200 MHz for ^{13}C nuclei. Mass spectra were obtained on an Anilent 6540 Q-Tof instrument (ESI and HRESI mode). HRMS data were recorded via positive ion electrospray or electron impact mass spectrometry using a time of flight analyzer. Experimental ECD spectra were measured on a Chirascan instrument. Semi-preparative HPLC was performed on an Agilent 1260 HPLC with a Zorbax XDB-C_{18} (9.4 mm × 25 cm) column. Chiral semi-preparative HPLC was performed on an Agilent 1260 HPLC with the Ultimate Cellu-DR (10 mm × 25 cm) column. Column chromatography (CC) was performed using silica gel (200−300 mesh, Qingdao Marine Chemical Co. Ltd., Qingdao, People's Republic of China), MCI gel (75−150 μm; Mitsubishi Chemical Corporation, Japan), and Sephadex LH-20 (Amersham Biosciences AB, Uppsala, Sweden).

Plant Material. The twigs and leaves of *Horsfieldia kingii* was collected from Xishuangbanna, Yunnan Province, People's Republic of China, and was identified by Mr. Shishun Zhou, Xishuangbanna Tropical Botanical Garden, Chinese Academy of Sciences. A voucher specimen of this collection (No.140418) has been deposited at Herbarium of Yunnan Normal University, Kunming, China.

Extraction and Isolation. The twigs and leaves of *Horsfieldia kingii* (10 kg) were extracted with 70% aqueous acetone (20 L) four times (two days each time) at room temperature and filtered. The filtrate was evaporated in vacuo. Then the concentrate without acetone (6 L) was partitioned between EtOAc and H_2O. The EtOAc-soluble portion (376 g) was subjected to silica gel CC (2000 g, 100-200 mesh). Five fractions were produced from the silica gel column, eluting with $CHCl_3$-Me_2CO (1:0-0:1 gradient system), and were each decolorized on MCI gel, eluted with 90% MeOH-H_2O, to yield fractions A-F.

Fraction B (28 g), a brown gum, was subjected to CC on Sephadex LH-20 and eluted with $CHCl_3$-MeOH (3:2), to provide four fractions, B1-B4. B2 (320 mg) was purification by repeated semi-preparative HPLC was performed on an Agilent 1260 HPLC with a Zorbax XDB-C_{18} (9.4 mm × 25 cm) column (MeOH-H_2O 48:52, v/v, 3 mL/min; Acetonitrile-H_2O 35:65 v/v, 3 mL/min) to afford horisfieldones A (3.7 mg) and B (3.3 mg). Horisfieldones A and B was then chiral separated on Agilent 1260 HPLC with Ultimate Cellu-DR (10 mm × 25 cm) column (MeOH-H_2O 95:5, v/v, 3 mL/min) respectively to provide (+)-horisfieldone A (1.3 mg), (-)-horisfieldone A (1.1 mg), (+)-horisfieldone B (1.2 mg), and (-)-horisfieldone B (1.0 mg).

Horisfieldone A (1): brown oil; UV (MeOH) λ_{max} (log ε) 204 (4.05), 226 (3.60), 288 (3.30) nm; ^1H and ^{13}C NMR data, see Tables **1** and **2**; negative-ion HRESIMS *m/z* 571.1971 $[M-H]^-$ (calcd for $C_{33}H_{32}O_9$, 571.1974).

(+)-horisfieldone A: $[\alpha]_D^{19.2}$ +138.6 (*c* 0.06, MeOH); CD (MeOH), λ_{max} ($\Delta\ \varepsilon$) 330 (1.61).

(−)-horisfieldone A: $[\alpha]_D^{18.9}$ -87.3 (*c* 0.12, MeOH); CD (MeOH), λ_{max} ($\Delta\ \varepsilon$) 333 (-1.67).

Horisfieldone B (2): brown oil; UV (MeOH) λ_{max} (log ε) 204 (3.78), 226 (3.33), 292 (3.05) nm; ^1H and ^{13}C NMR data, see Tables **1** and **2**; negative-ion HRESIMS *m/z* 601.2071 $[M-H]^-$ (calcd for $C_{34}H_{34}O_{10}$, 601.2079).

(+)-horisfieldone B: $[\alpha]_D^{19.0}$ +86.4 (*c* 0.17, MeOH); CD (MeOH), λ_{max} ($\Delta\ \varepsilon$) 335 (1.55).

(−)-horisfieldone B: $[\alpha]_D^{18.8}$ -124.0 (*c* 0.12, MeOH); CD (MeOH), λ_{max} ($\Delta\ \varepsilon$) 334 (-1.68).

ECD Calculations of 1

ECD Calculations were performed by a Gaussian 09 software. More specifically, the 3D structures were first established randomly or according to the ROESY spectra, which were then subjected to conformational analysis using CONFLEX software with MMFF94S force fields to afford six reliable conformations with relative energy of less than 1.00 kcal/mol. The selected conformers were further optimized by using the Density Functional Theory (DFT) at the B3LYP/6-31+G(d) level in gas phase. The optimized geometries were subsequently checked by frequency calculation and resulted in no imaginary frequencies. The optimized conformations were subjected to ECD calculations using Time Dependent DFT (TDDFT) at the B3LYP/6-311++G(2d, p) level in CH3OH. The calculated ECD curves were generated by SpecDis version 1.63 software. (Reference: Frisch, M.J.; Trucks, G. W.; Schlegel, H. B.; et al. *Gaussian* 09, Revision E. 01. Gaussian, Inc: Wallingford, CT, 2013. Bruhn, T.; Schaumlöffel, A., Hemberger, Y., Bringmann, G. *Chirality* **2013**, *25*, 243–249.)

Molecular Modeling

The ligand and receptor were prepared using DiscoveryStudio 4.0 software. Autodock Tools v1.56[1] was used to perform grid and docking. Docking parameters were set as the default values AutoGrid v4.01 and AutoDock v4.01. The Grid box contained the whole active cavity of human DDC (PDB: 3rbf) was chosen.[2] Docking conformations were classified into different clusters by binding energy, and the cluster with the lowest binding energy was selected. In the selected cluster, conformations with the lowest binding energy and RMSD (<2.0 Å) were finally chosen to analyze the receptor-ligand interaction.

The activity assay of human cystathionine γ-lyase (hCSE).

The inhibition of compounds on the activity of hCSE was determined using our previously reported method that is based on a 192-tandem-well plate.[3] Briefly, 25 μl 50 mM HEPES buffer containing 500 nM purified recombinant GST-tagged hCSE protein and 100 μM PLP (final concentrations; pH 7.4) was first incubated with 1 μL DMSO or compounds in the reaction well at a concentration of 100 μM for 45 min. Then, 50 μl detection buffer (300 μM DTNB in 262 mM Tris-HCl and 13 mM EDTA, pH 8.9) was added into the interlinked detection well. Finally, 25 μl 50 mM HEPES buffer containing 5 mM L-Cys (final concentrations) was added in the reaction well and the plate was immediately and tightly sealed with UltraClear film (Platemax PCR-TS from Axygen, Union City, CA). The assay plate was then incubated for additional 60 min at 37 °C before the absorbance was measured at 413 nm with a microplate reader (Cytation5 from BioTek, Winooski, VT).

The activity assay of human DOPA decarboxylase (hDDC).

The DDC assay was performed under standard assay conditions as previously described.[2b] Briefly, 1 μL DMSO or compounds at a concentration of 100 μM were mixed with 24.5 μL of the enzyme mix [50 mM Tris-HCl, 50 mM NaCl, 0.015% (w/v) bovine serum albumin, 5 mM $MgCl_2$, 2 mM β-mercaptoethanol, 760 μM NADH, 330 nM PEPC, 100 μM PLP and 284 nM 6 × His-tagged hDDC, pH 8.05; final concentrations]. Then, the reaction was started by adding 24.5 μL substrate mix [50 mM Tris-HCl containing 50 mM NaCl, 0.015% (w/v) bovine serum albumin, 5 mM $MgCl_2$, 2 mM β-mercaptoethanol, 10 mM phosphoenolpyruvic acid, 0.49 U malate dehydrogenase and 1.5 mM 3,4-dihydroxy-L-phenylalanine, pH 8.05; final concentration]. The plates were then tightly sealed with UltraClear film and incubated for 30 min at 37 °C before the absorbance of 340 nm was measured in a microplate reader. The remaining activity of compound was expressed as percentage of control (DMSO) with the following equation: Remaining activity (%) = $\{[(OD_{0\ min} - OD_{30\ min})$ of compound] − $[(OD_{0\ min} - OD_{30\ min})$ of blank]} / $\{[(OD_{0\ min} - OD_{30\ min})$ of DMSO] − $[(OD_{0\ min} - OD_{30\ min})$ of blank]} × 100.

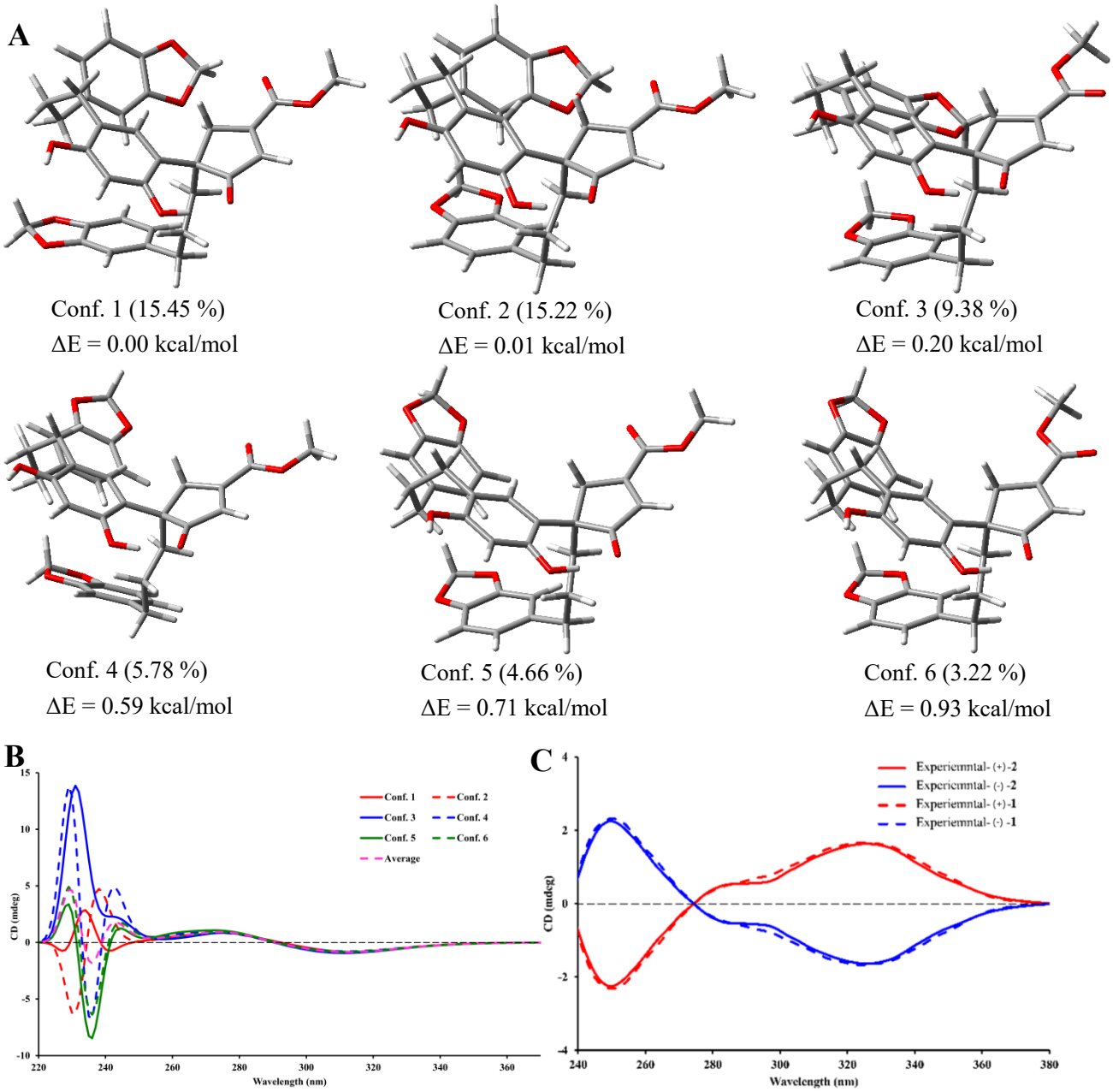

Figure S1. Computational data of **1**. (A) Six receivable conformers with lower relative energy of **1**. (B) Calculated ECD spectra for the low energy structures. (C) Experimental CD spectra of compounds **1** and **2**.

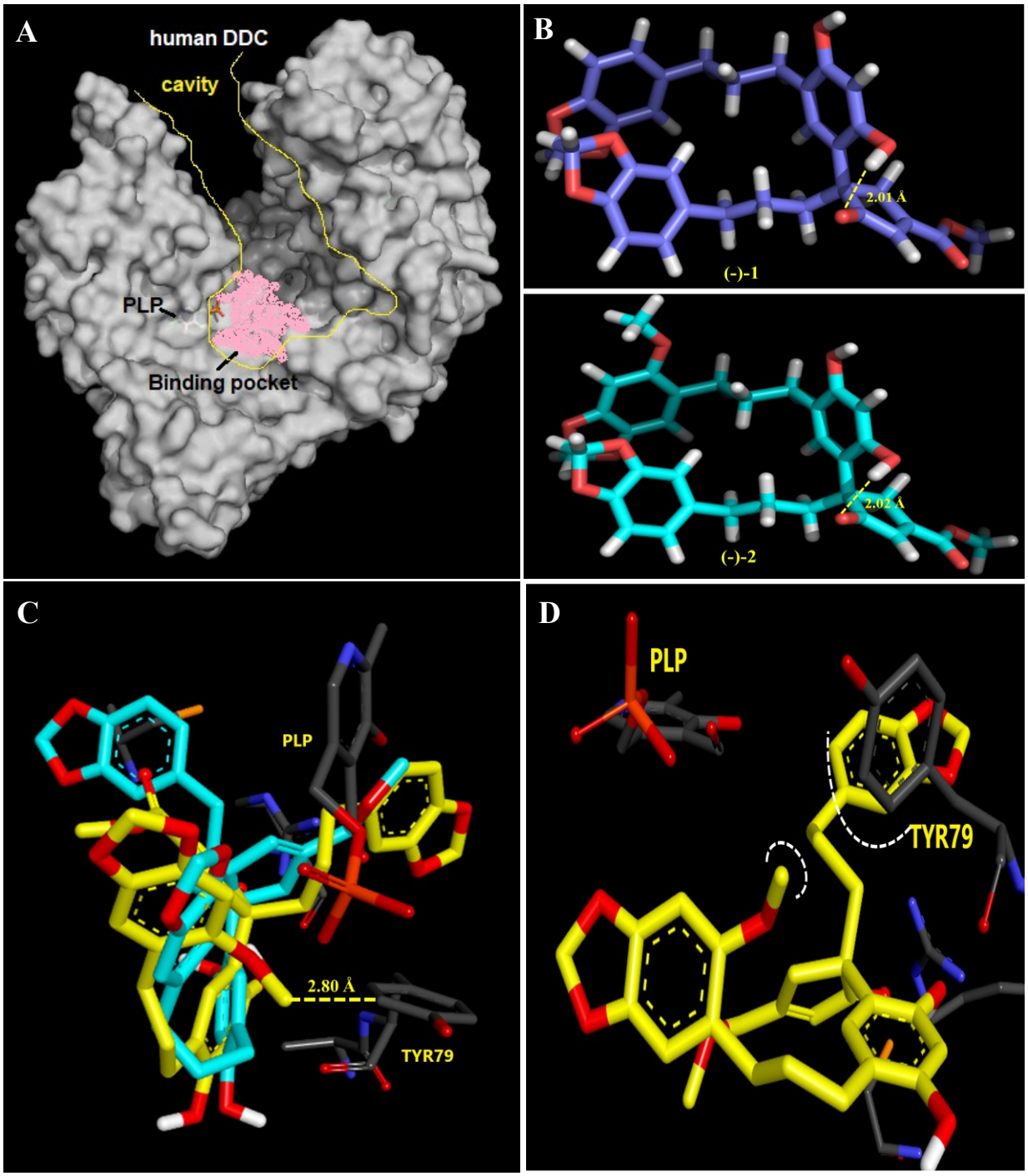

Figure S2. Molecular docking analysis of compounds (-)-**1**, (+)-**1**, (-)-**2**, and (+)-**2** into human DOPA decarboxylase (hDDC) (pdb: 3rbf). (A) The active cavity of hDDC and the calculated binding pocket (shown in pink color, an approximate area overlapped the L-DOPA binding region [ref. 2a]) of compounds (-)-**1**, (+)-**1**, (-)-**2**, and (+)-**2**. The receptor was showed as solid surface in white with 20% transparence. PLP was shown as sticks. Ligands were shown as spheres. (B) Minimized configurations of (-)-**1** and (-)-**2**, yellow-dotted lines represented intramolecular hydrogen bonds with length of 2.01 Å and 2.02 Å, respectively. (C) Superposition of (+)-**1** and (+)-**2** docking into the hDDC. Ligands were shown as sticks. Namely, (+)-**1** was shown in cyan color, and (+)-**2** was shown in yellow color. The key residues were shown as sticks (C, pale; O, red; N, blue; P, orange). (D) Zoomed docking pose of (+)-**2**. The white-dotted arcs represented the steric bump between the C6a″-OMe of (+)-**2** with the aromatic ring of residue TYR79.

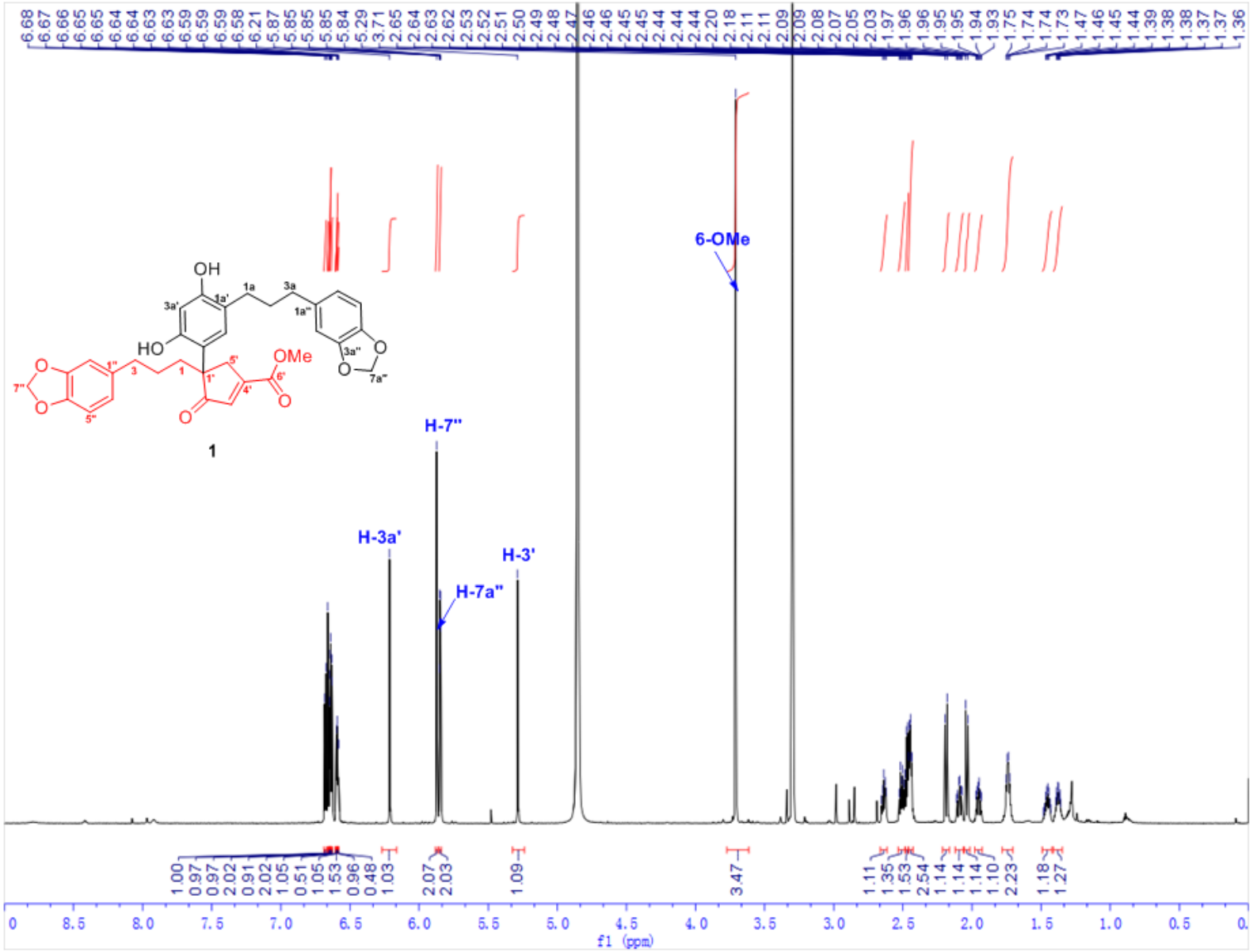

Figure S3. ^{1}H NMR spectrum (0-9 ppm) of compound **1**

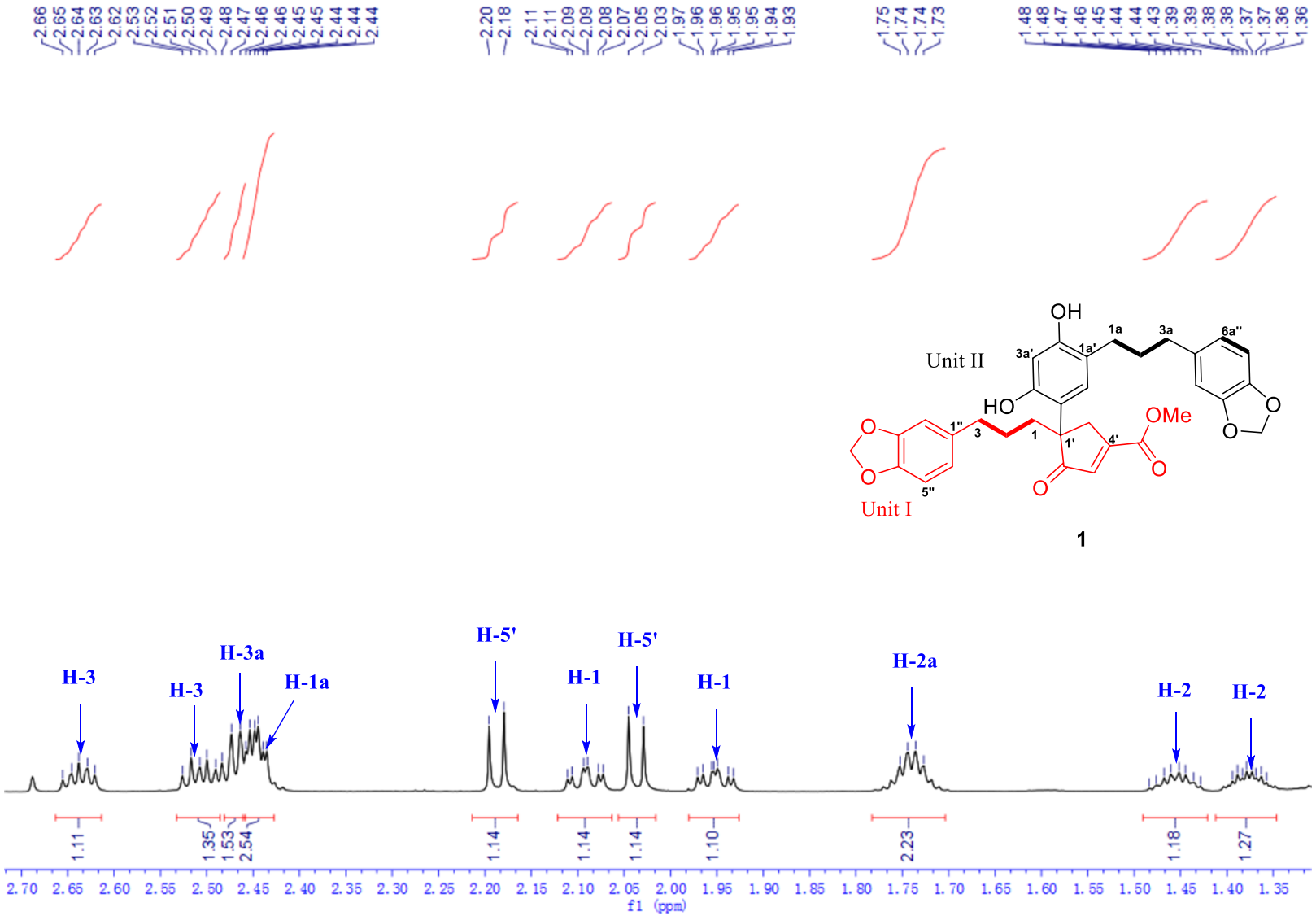

Figure S4. ^{1}H NMR spectrum (1.35-2.70 ppm) of compound **1**

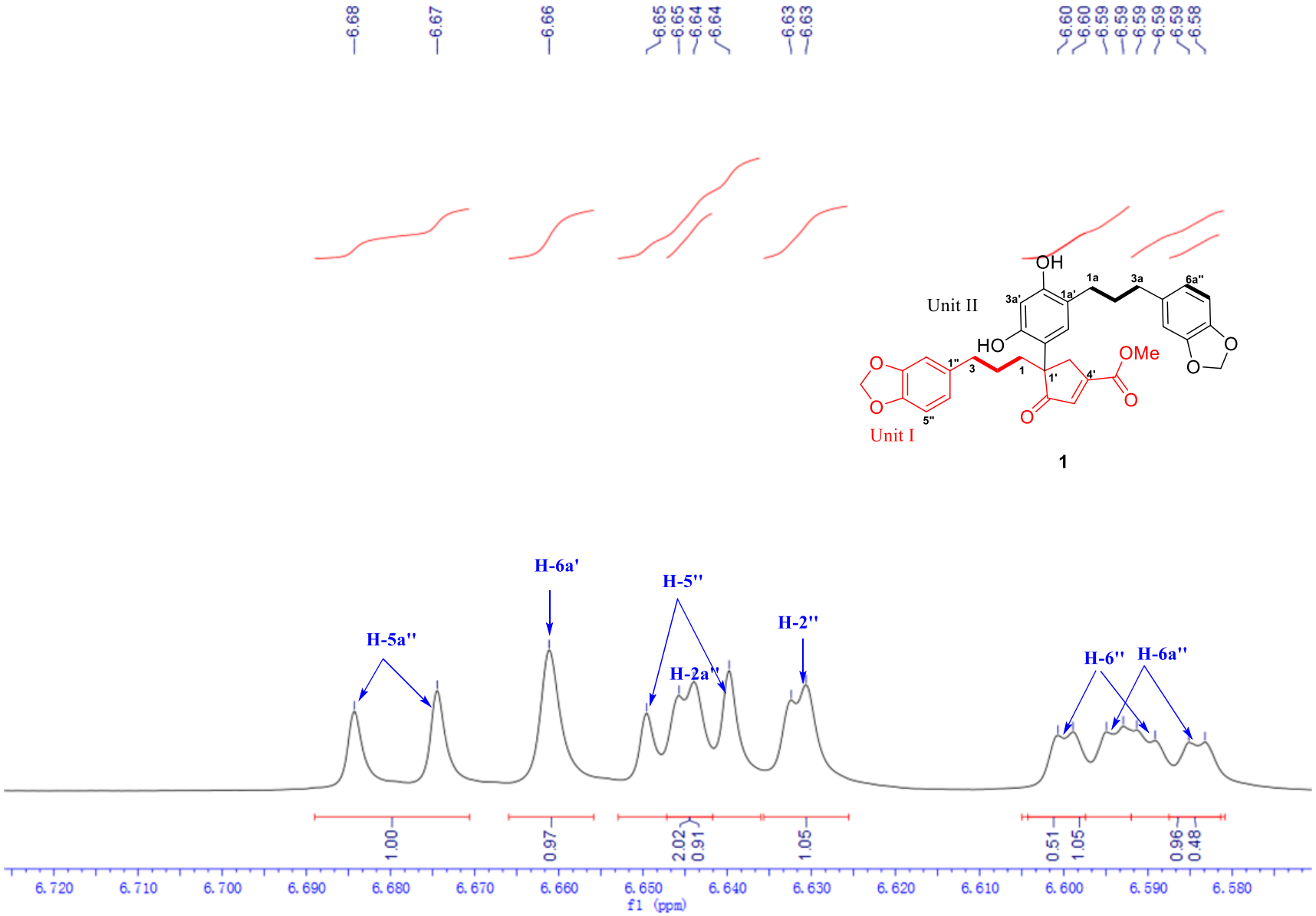

1

Figure S5. ^{1}H NMR spectrum (6.58-6.72 ppm) of compound **1**

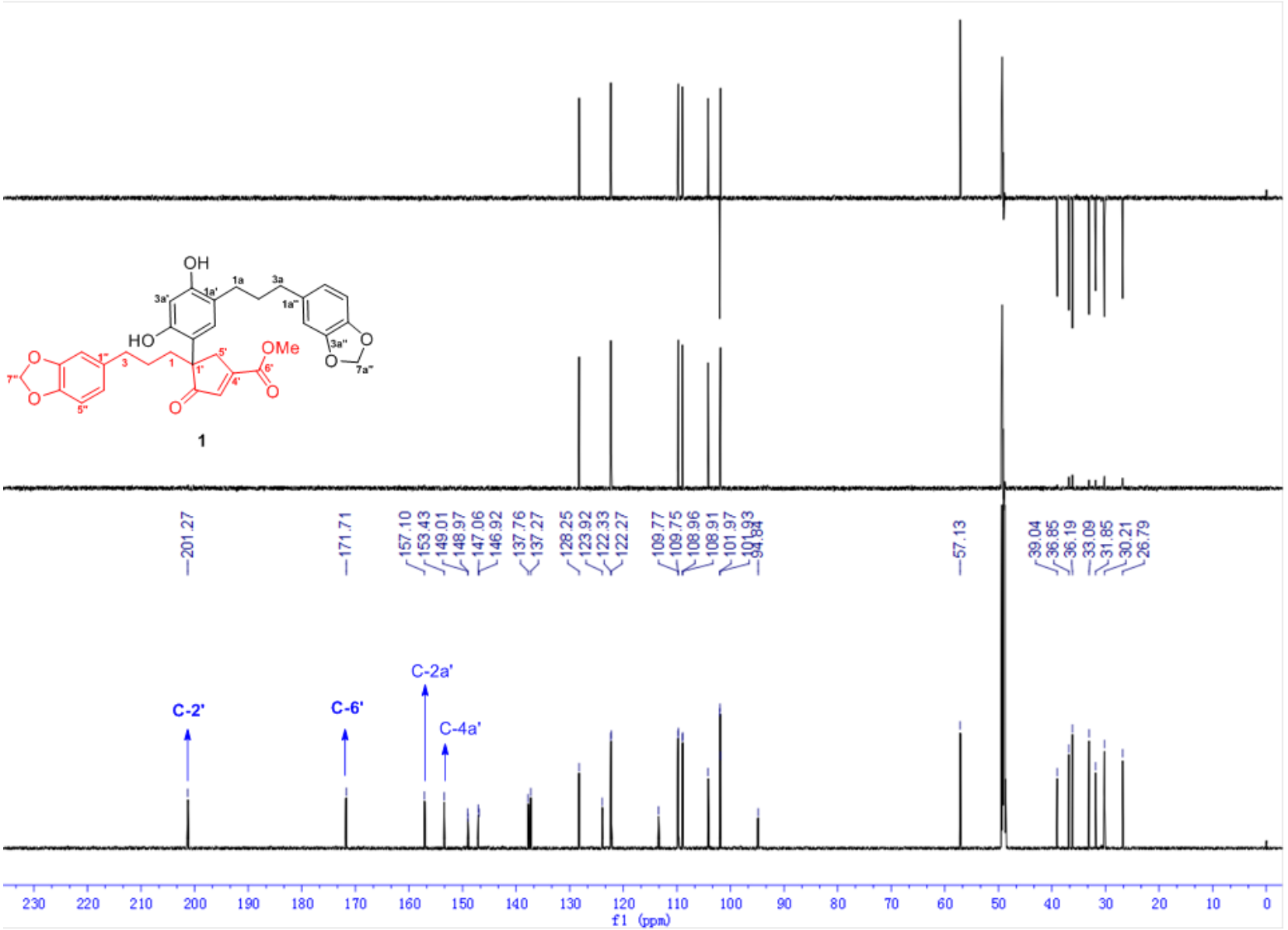

Figure S6. ^{13}C NMR spectra (0-230 ppm) of compound **1**

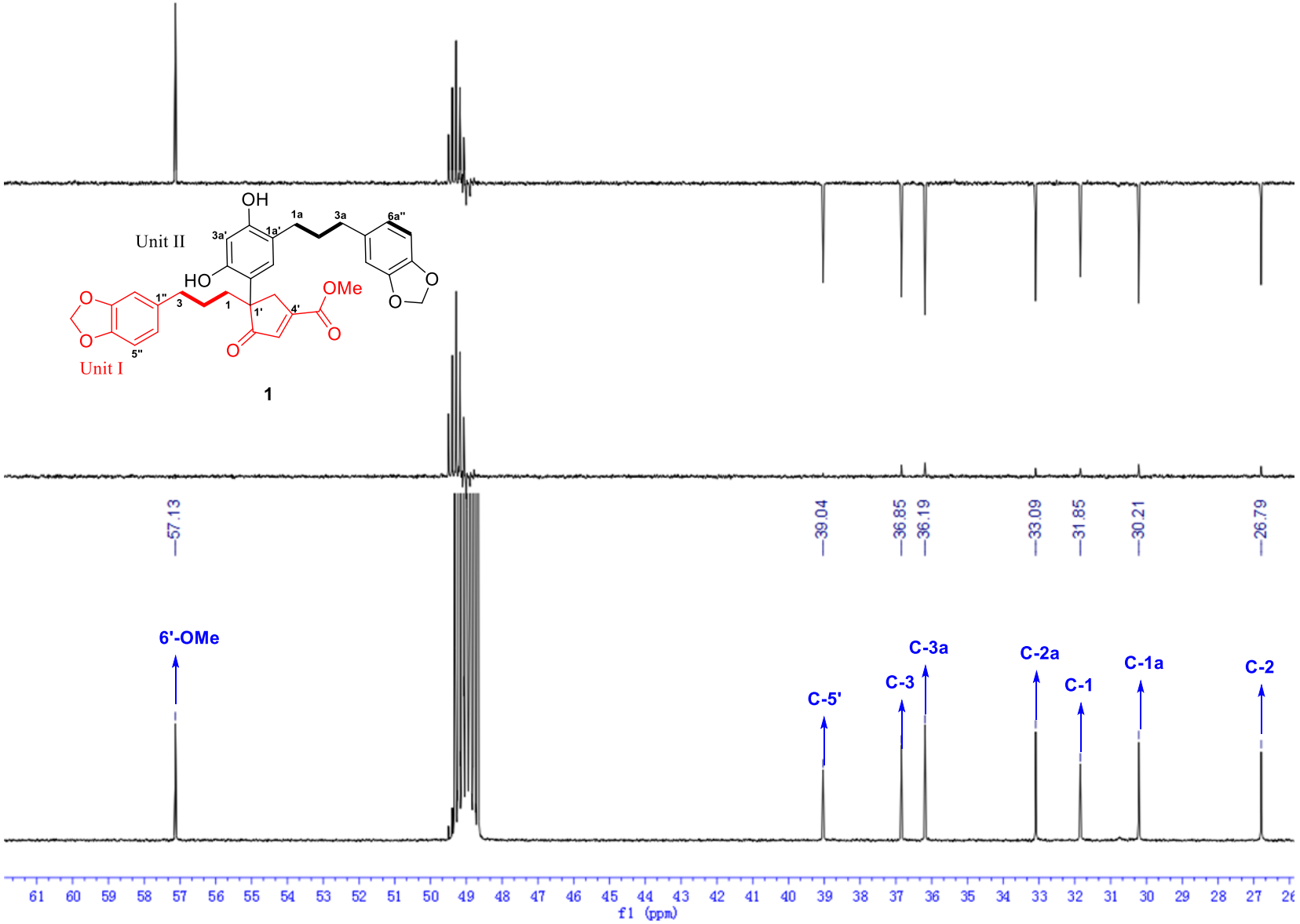

Figure S7. ^{13}C NMR spectra (20-61 ppm) of compound **1**

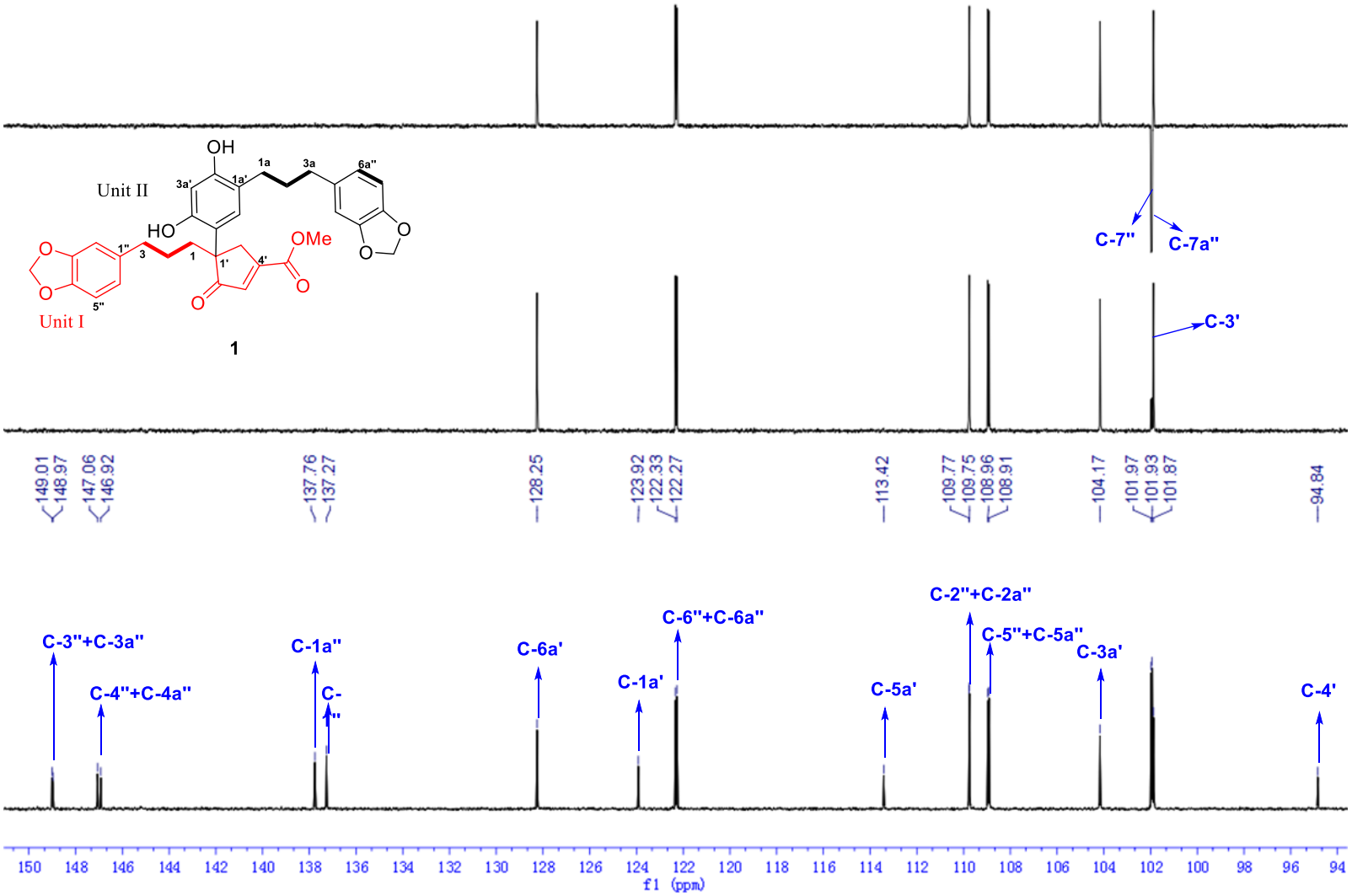

Figure S8. ^{13}C NMR spectra (94-170 ppm) of compound **1**

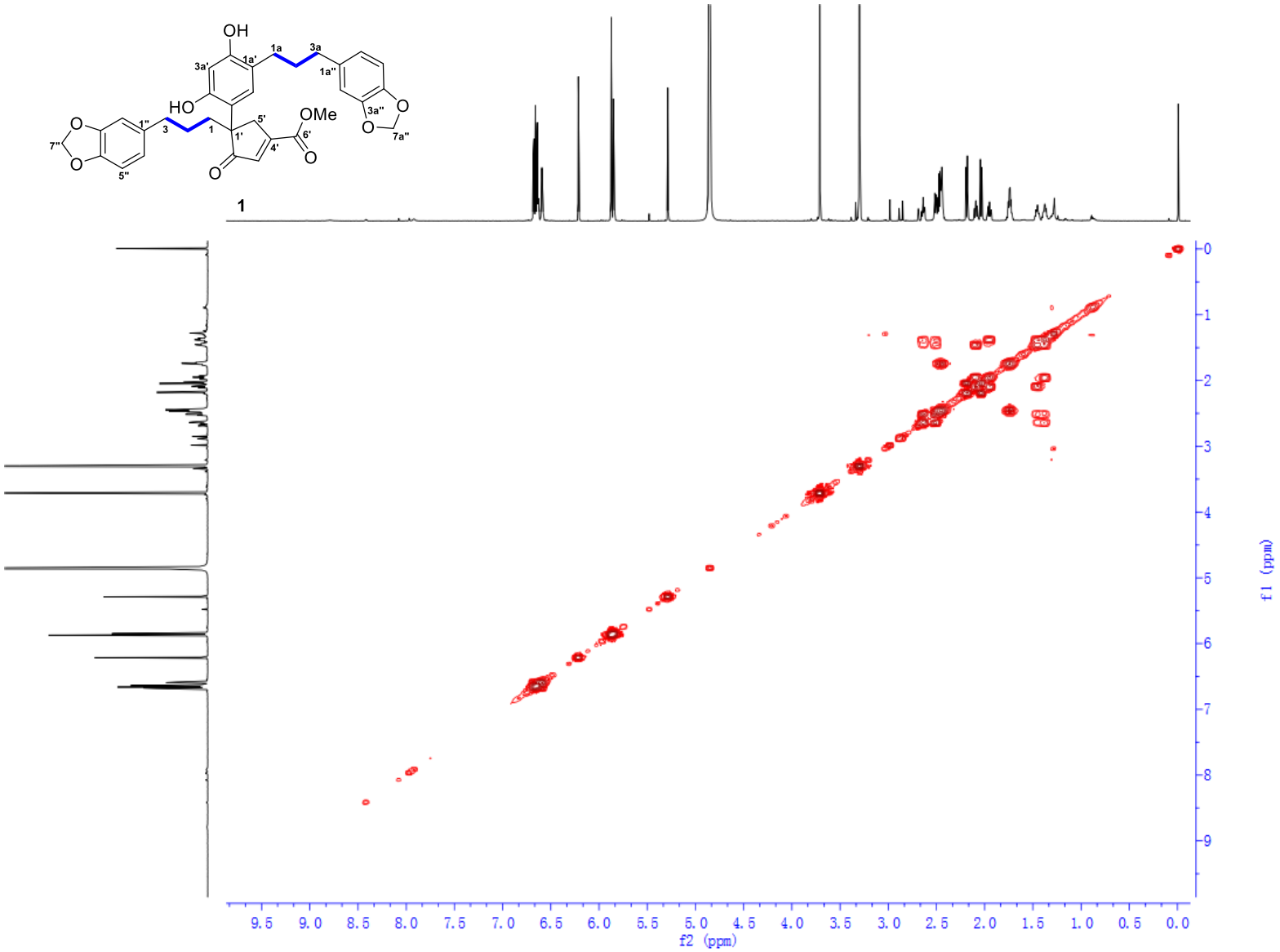

Figure S9. ^{1}H-^{1}H COSY spectrum of compound **1**

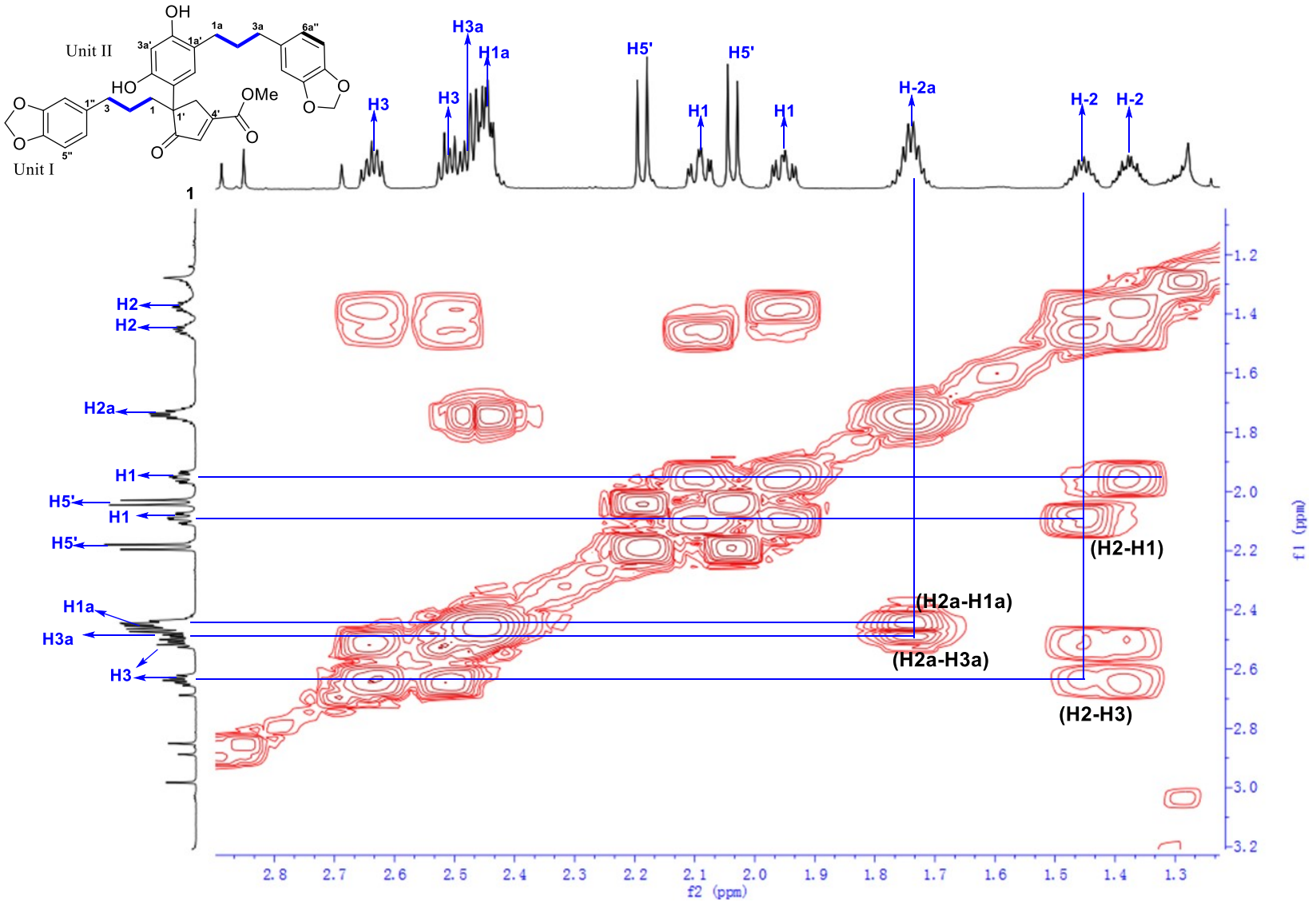

Figure S10. Key ^{1}H-^{1}H COSY spectrum of compound **1**

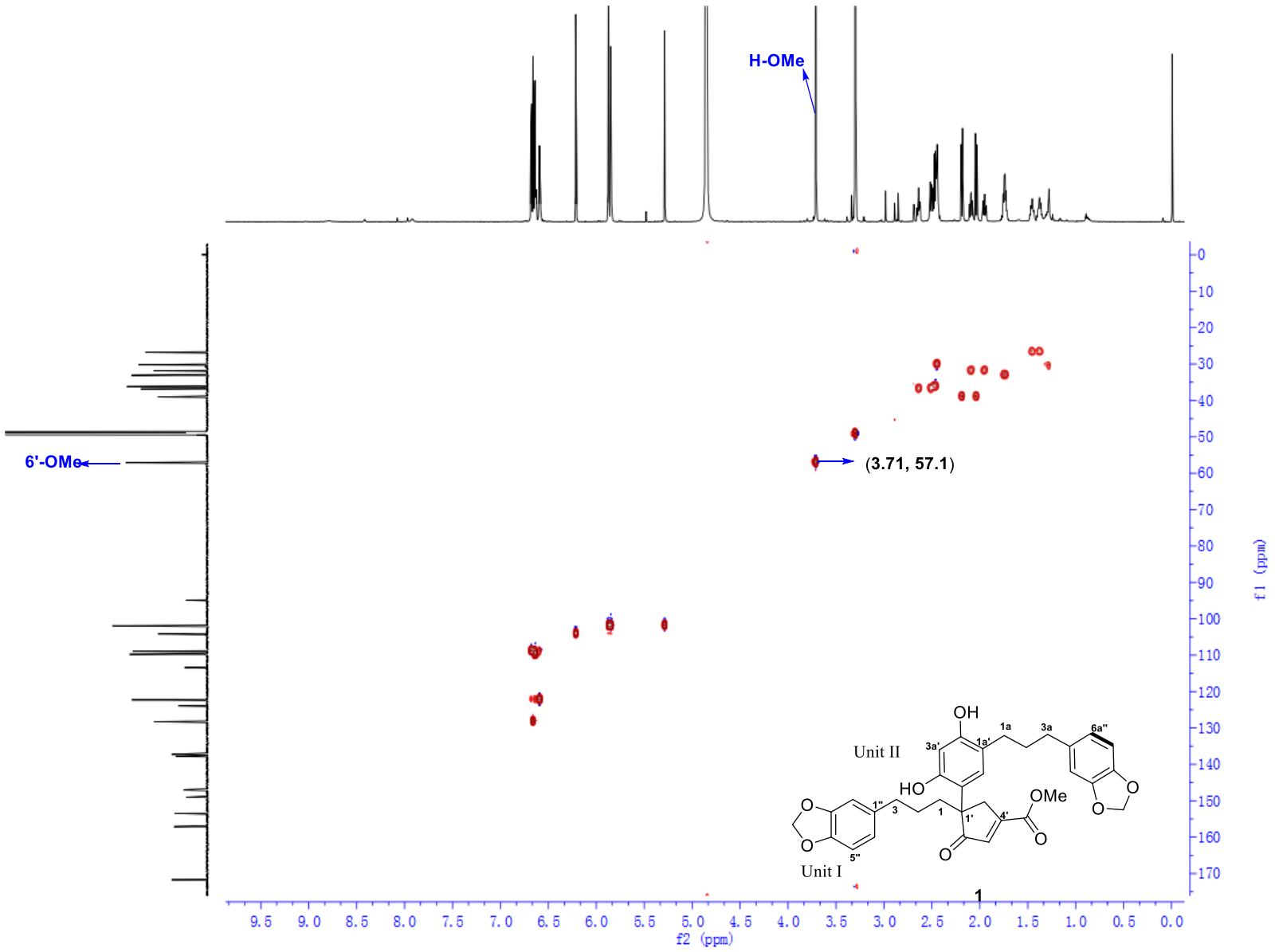

Figure S11. HSQC spectrum of compound **1**

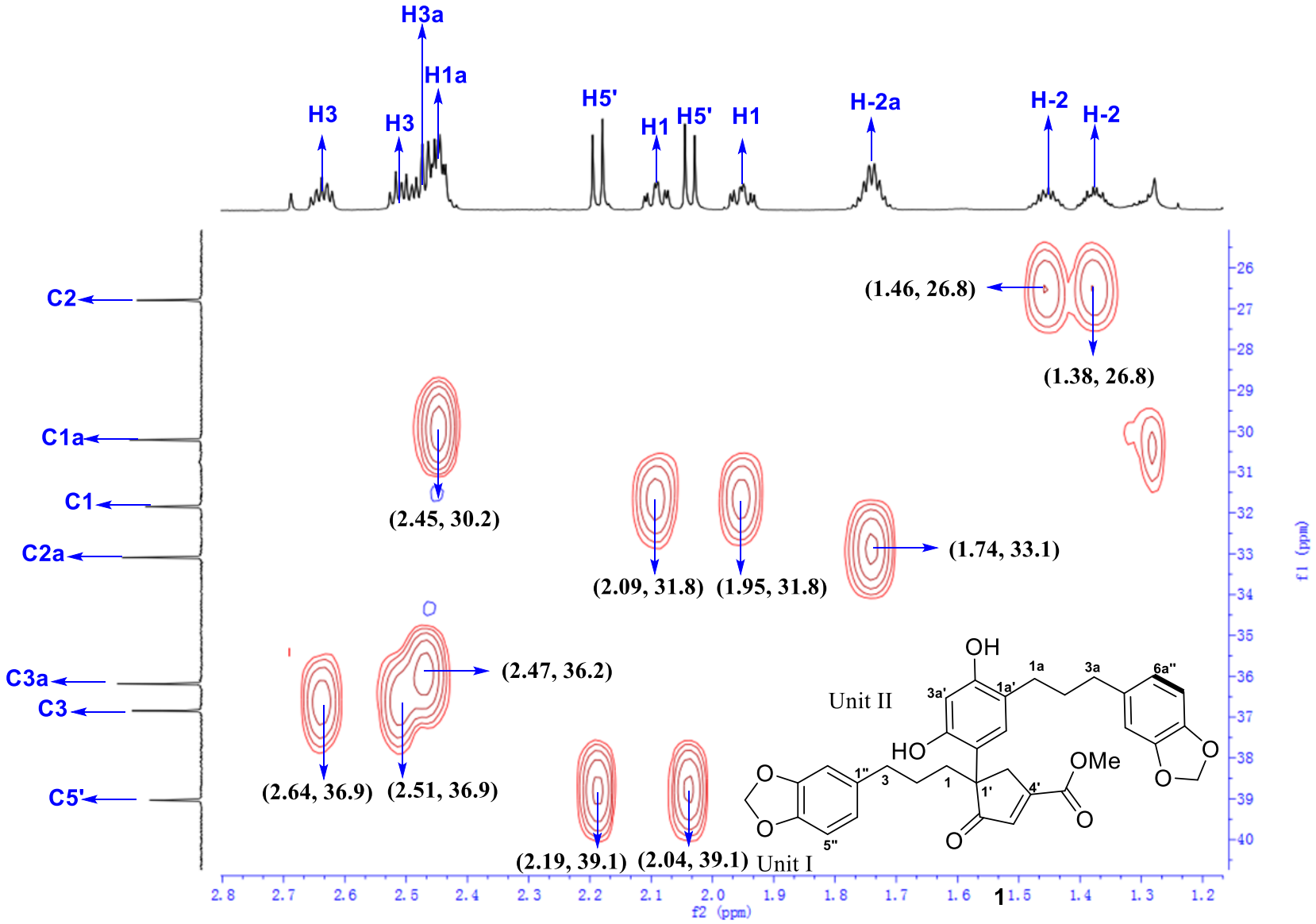

Figure S12. HSQC spectrum (δ_H 1.2–2.8 ppm and δ_C 26–40 ppm) of compound **1**

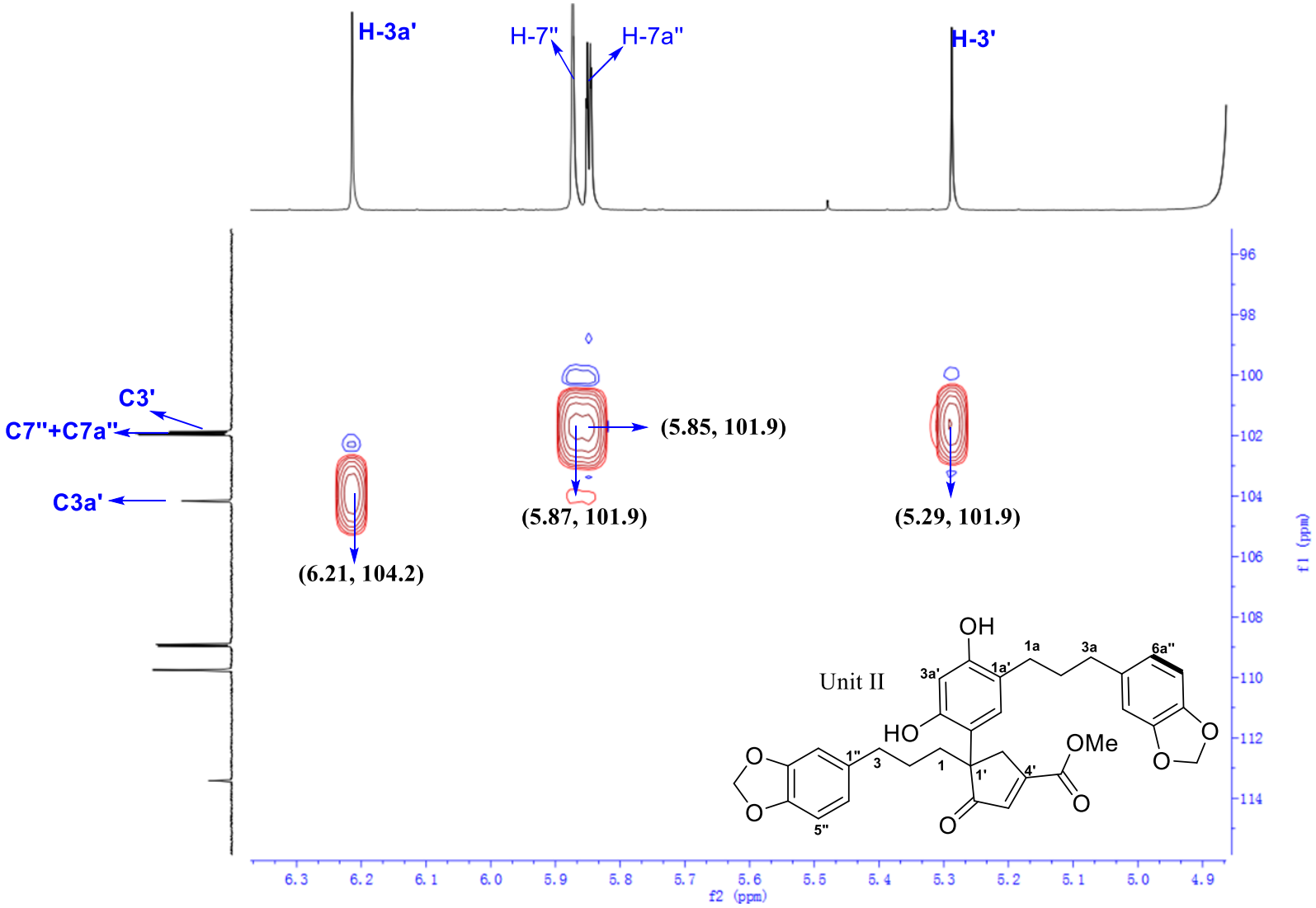

Figure S13. HSQC spectrum (δ_H 4.9–6.5 ppm and δ_C 96–114 ppm) of compound **1**

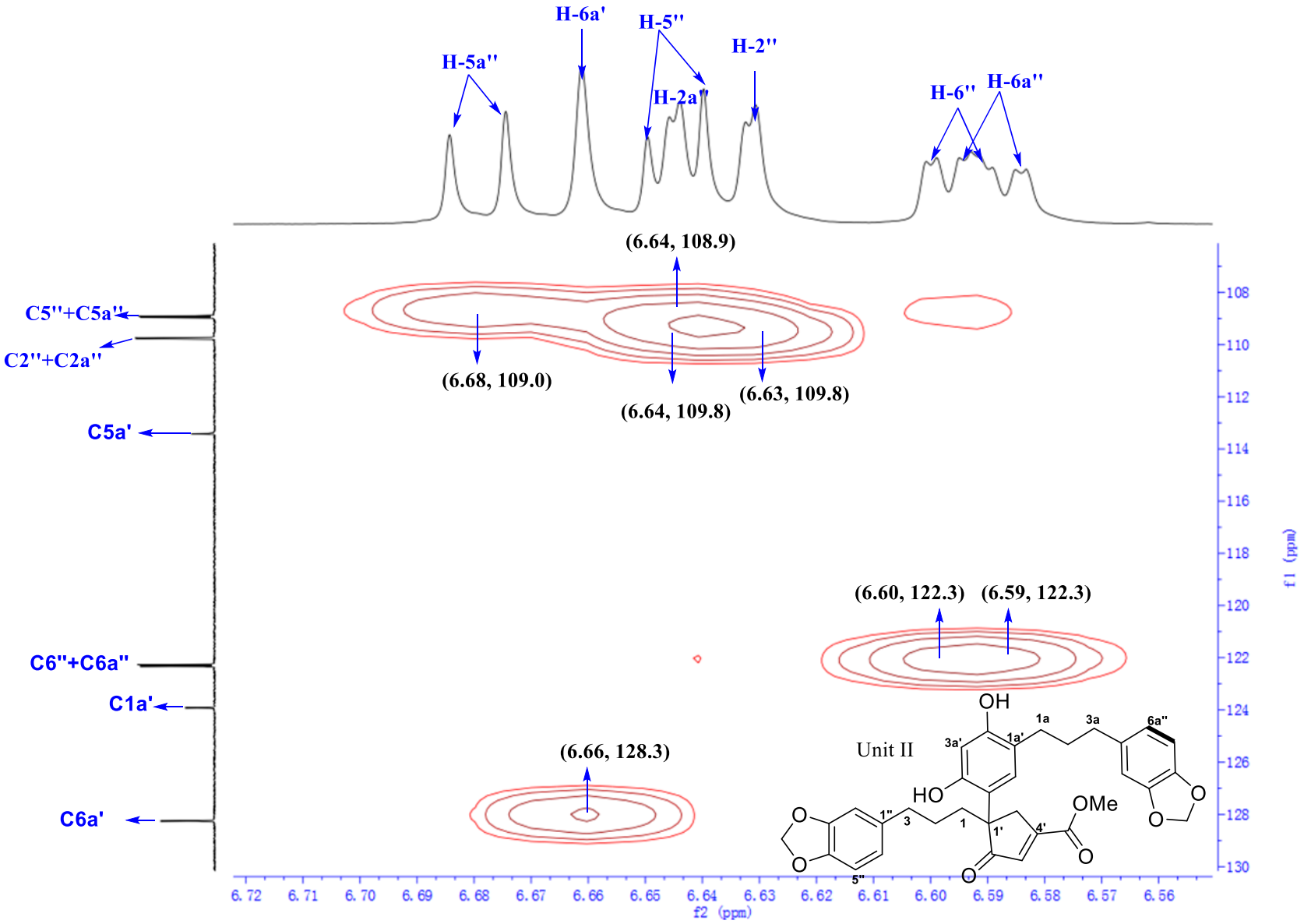

Figure S14. HSQC spectrum (δ_H 6.56–6.72 ppm and δ_C 108–130 ppm) of compound **1**

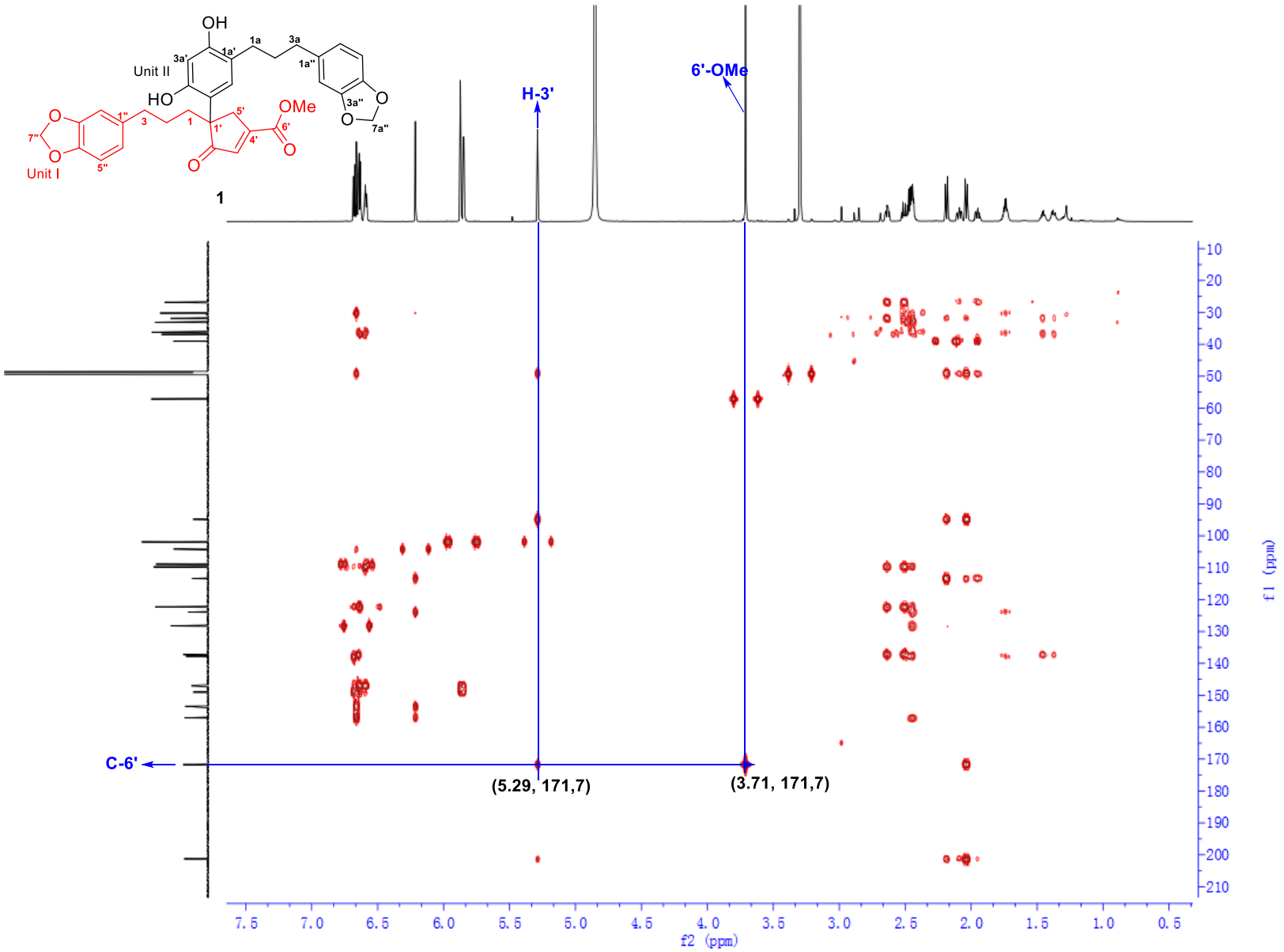

Figure S15. HMBC spectrum of compound **1**

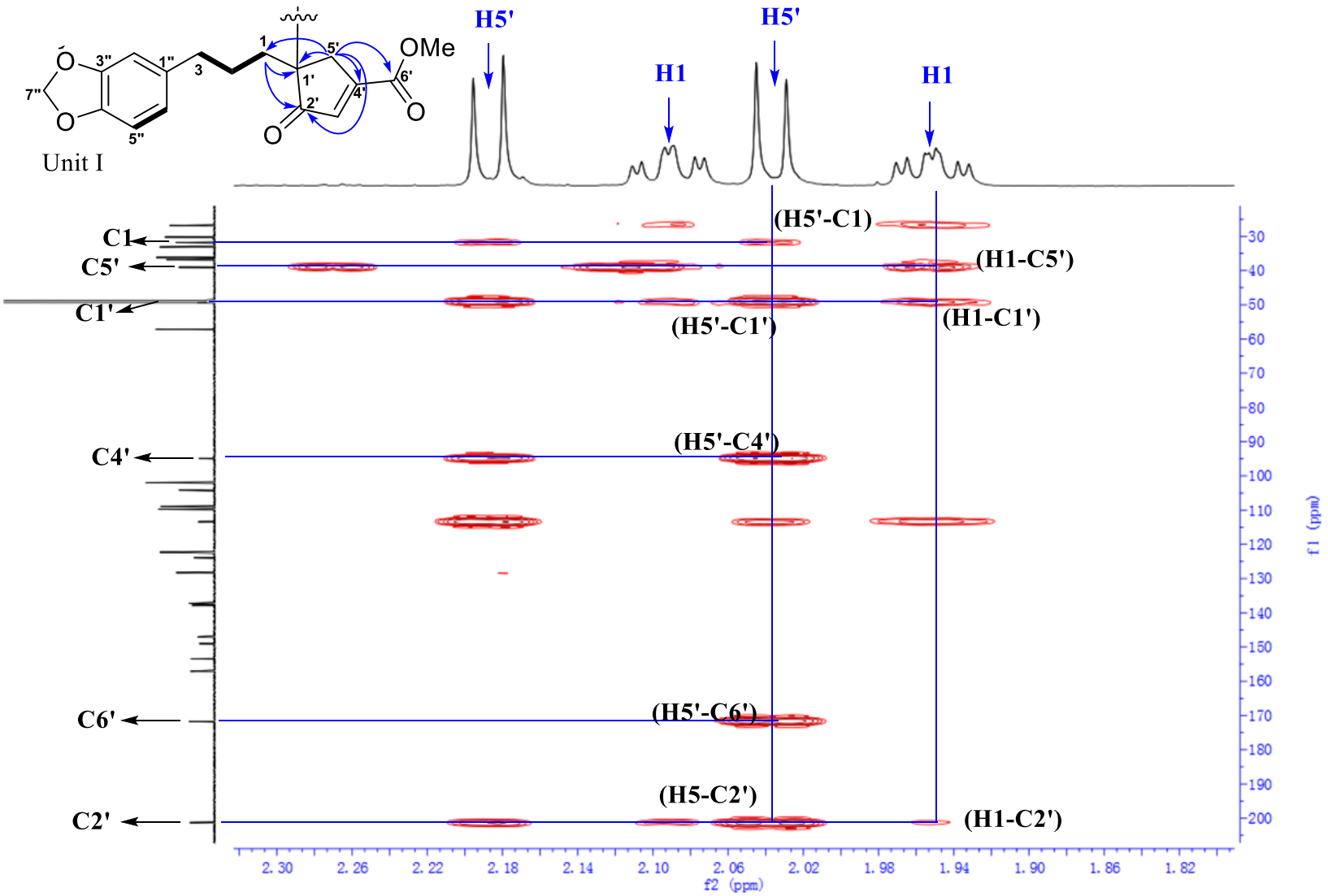

Figure S16. Key HMBC spectrum (δ_H 1.82–2.30 ppm and δ_C 30–200 ppm) of unit I in compound **1**

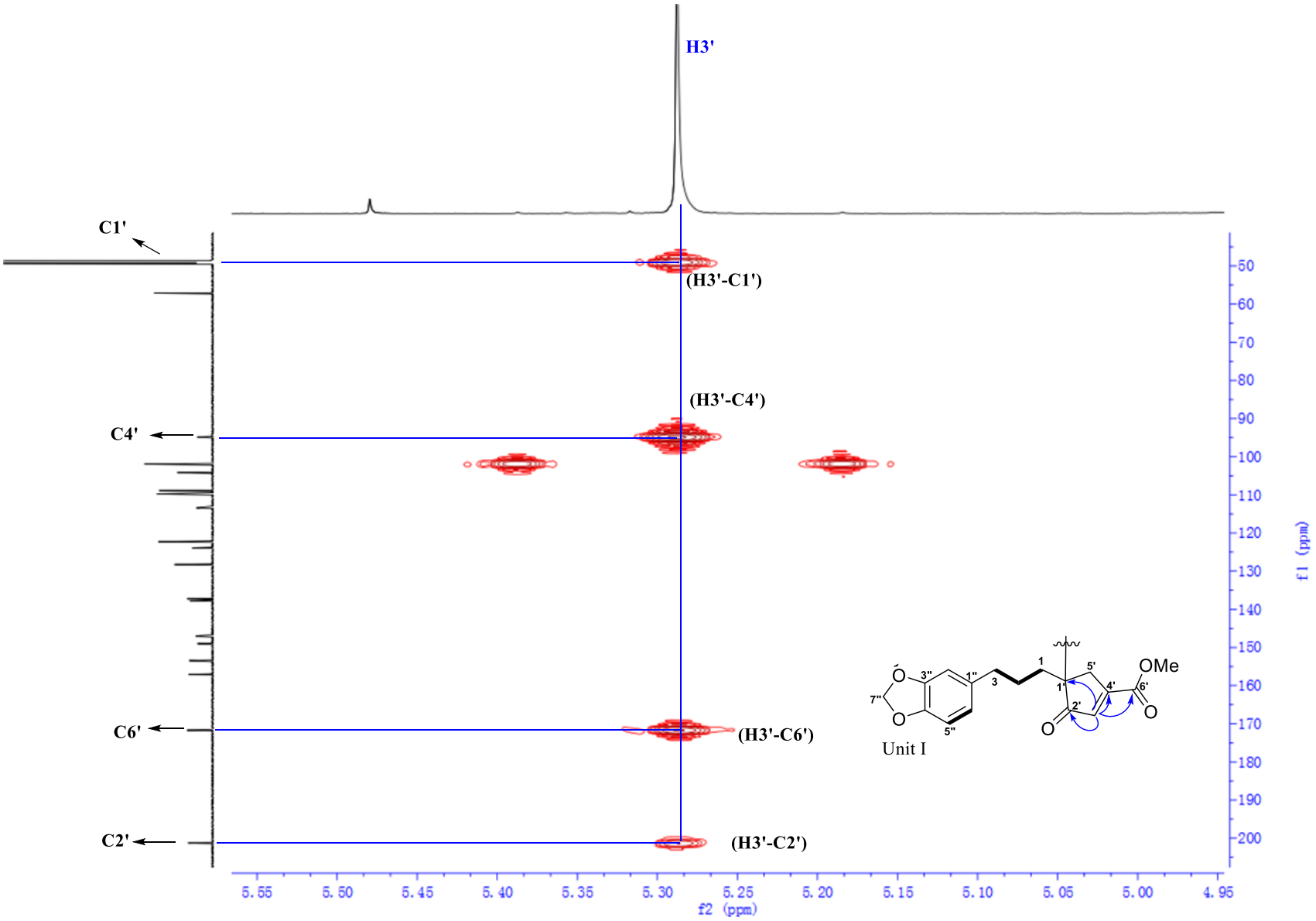

Figure S17. Key HMBC spectrum (δ_H 4.9–5.9 ppm and δ_C 40–200 ppm) of unit I in compound **1**

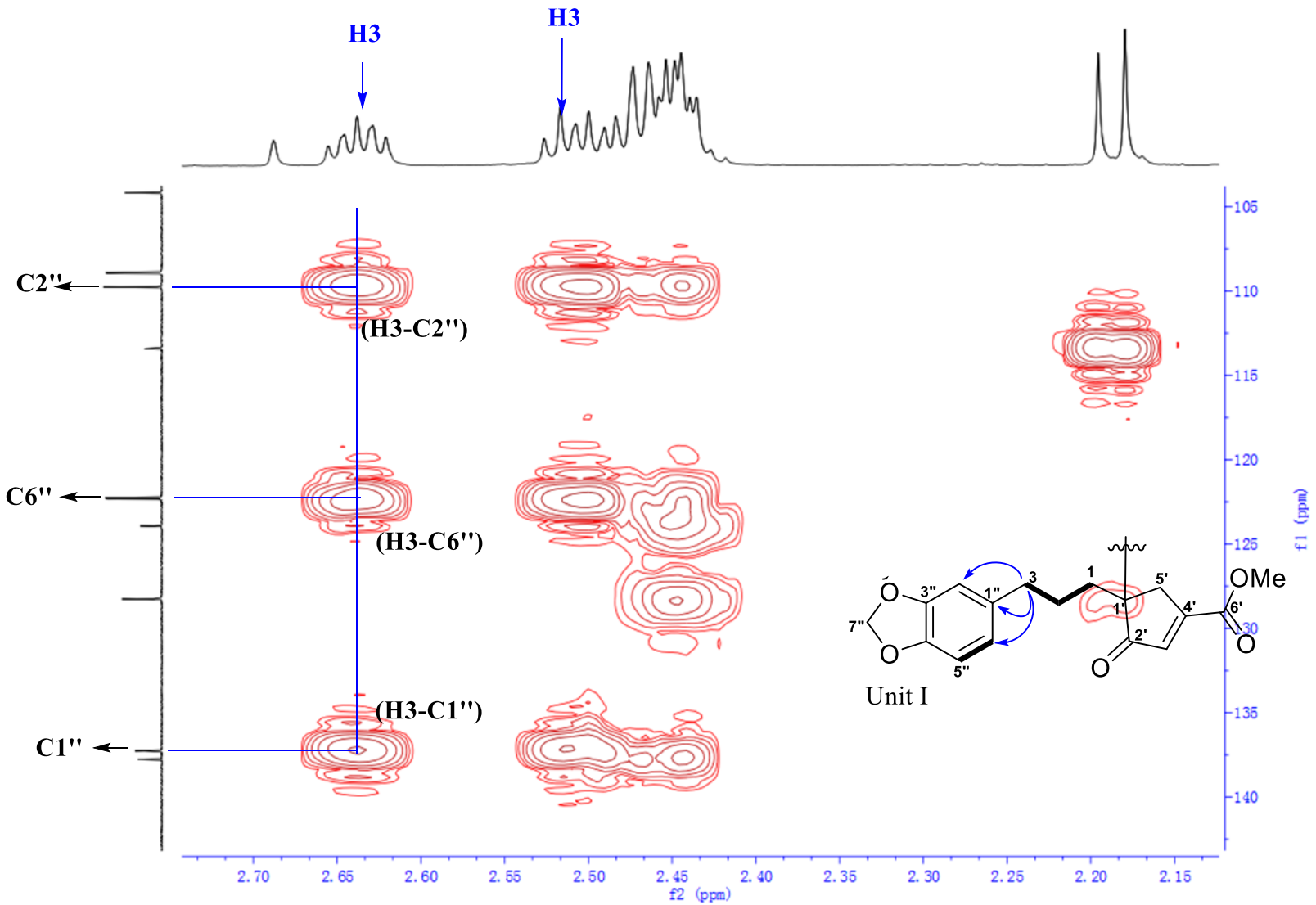

Figure S18. Key HMBC spectrum (δ_H 2.15–2.70 ppm and δ_C 105–140 ppm) of unit I in compound **1**

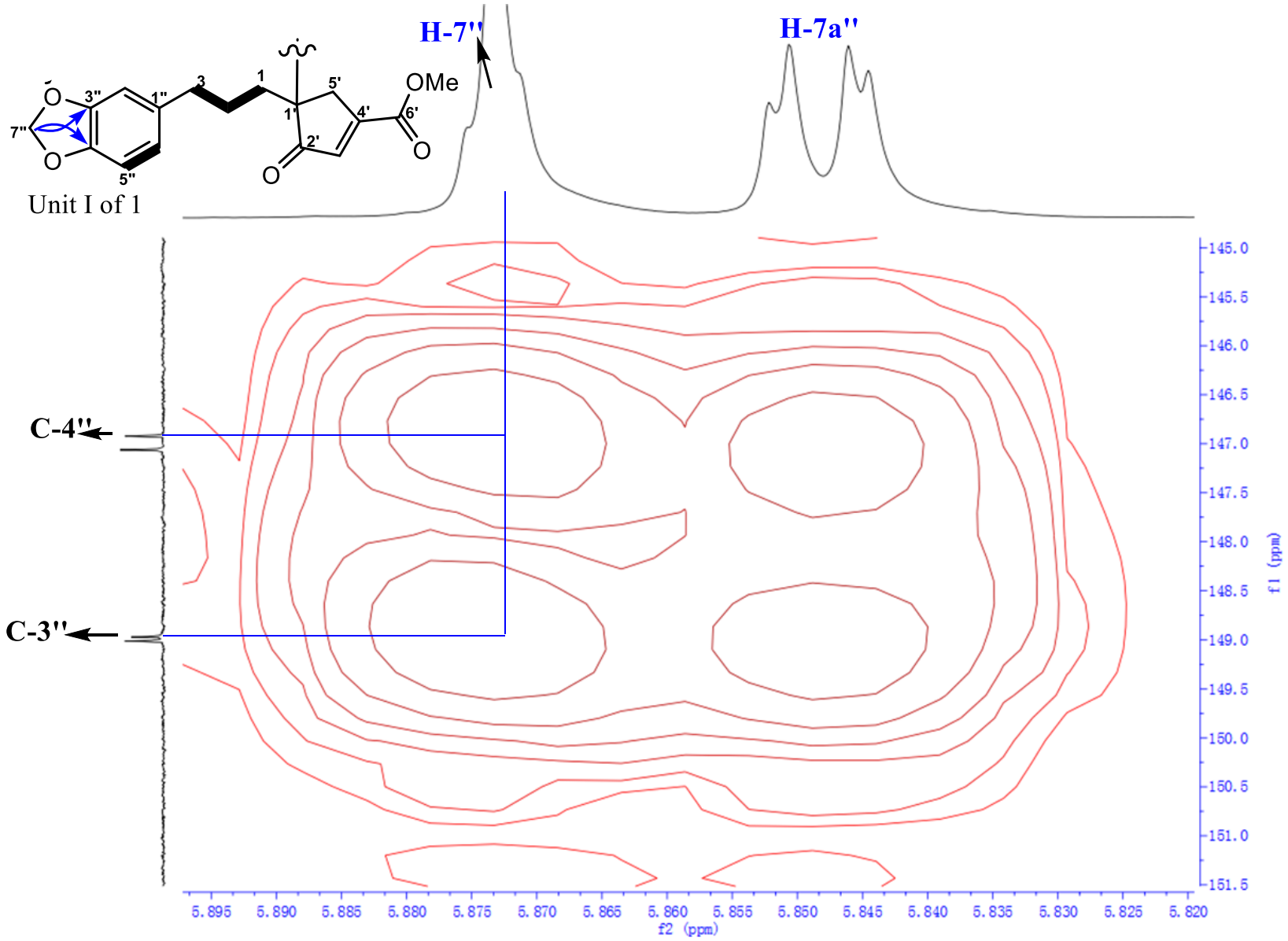

Figure S19. Key HMBC spectrum (δ_H 5.82–5.90 ppm and δ_C 145–151.5 ppm) of unit I in compound **1**

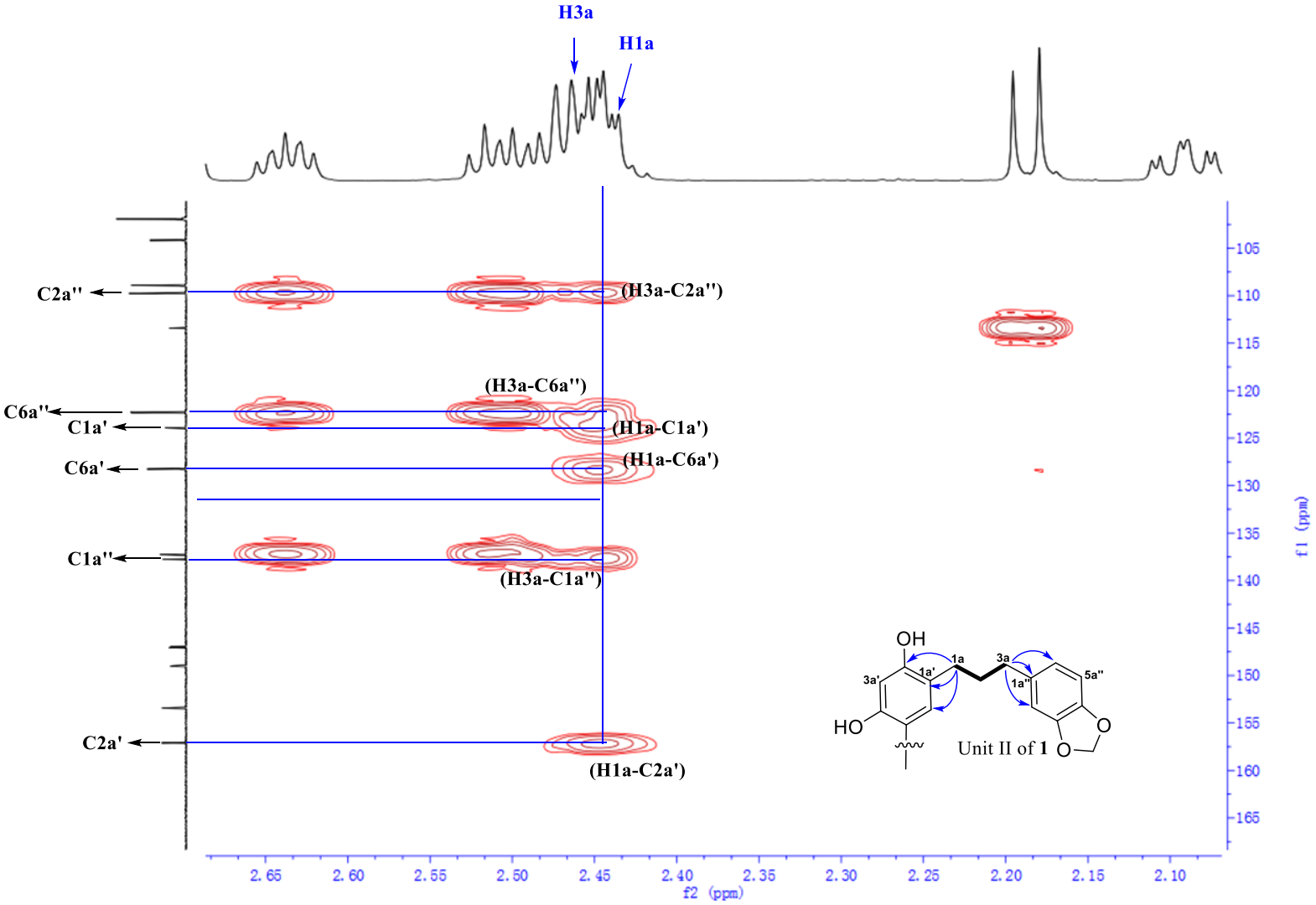

Figure S20. Key HMBC spectrum (δ_H 2.10–2.65 ppm and δ_C 145–165 ppm) of unit II in compound **1**

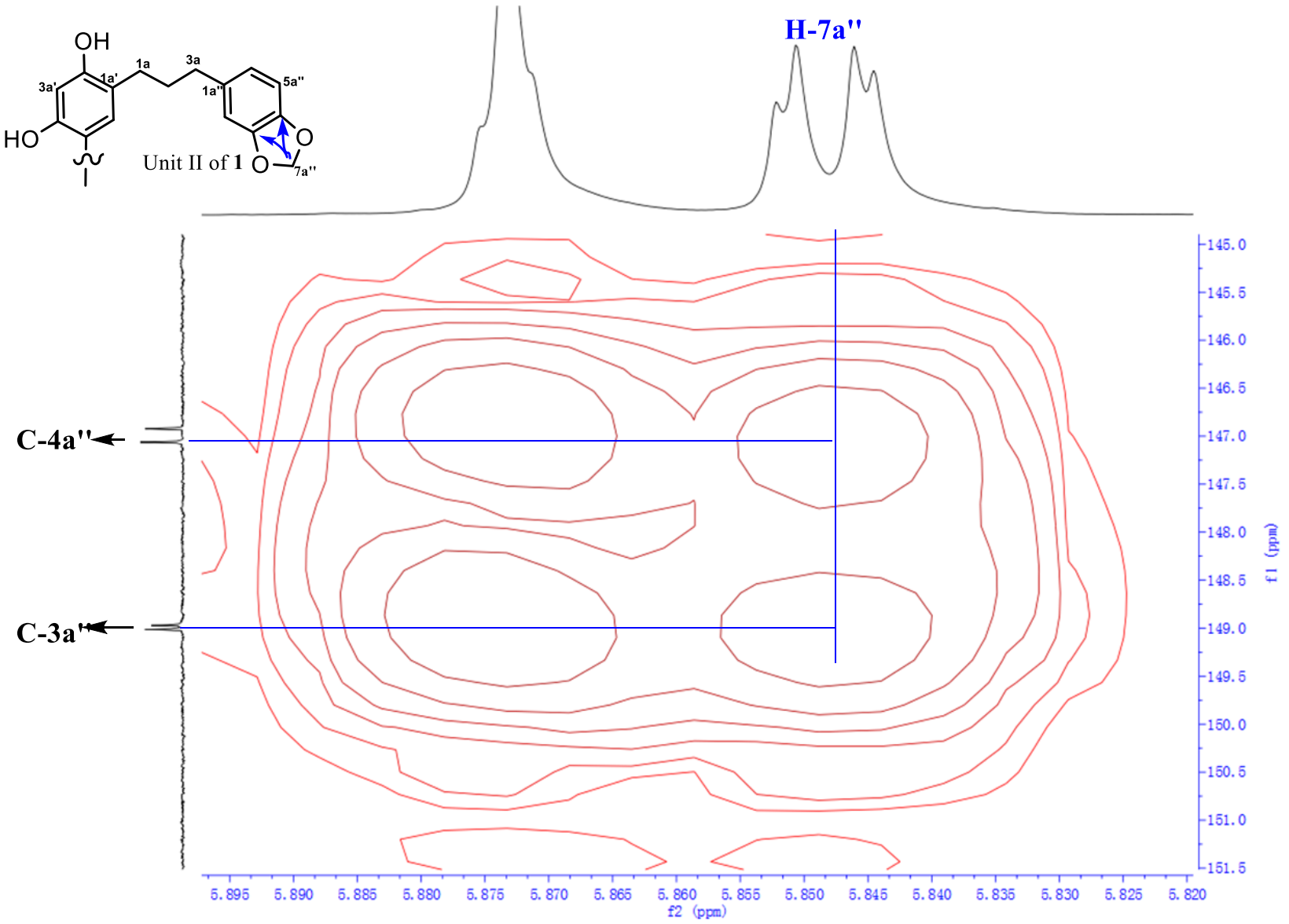

Figure S21. Key HMBC spectrum (δ_H 5.82–5.895 ppm and δ_C 145–150 ppm) of unit II in compound **1**

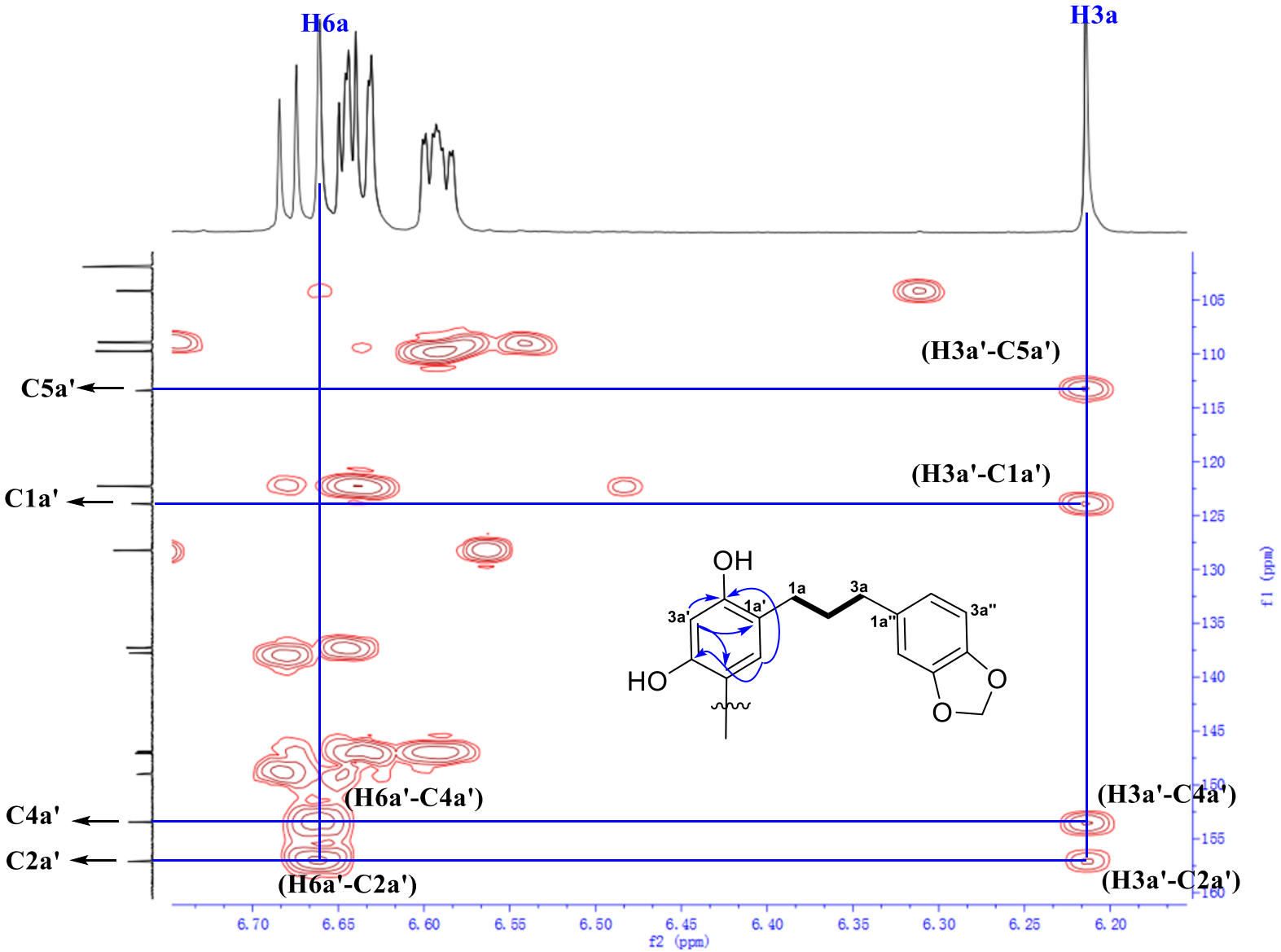

Figure S22. Key HMBC spectrum (δ_H 6.20–6.70ppm and δ_C 105–160 ppm) of unit II in compound **1**

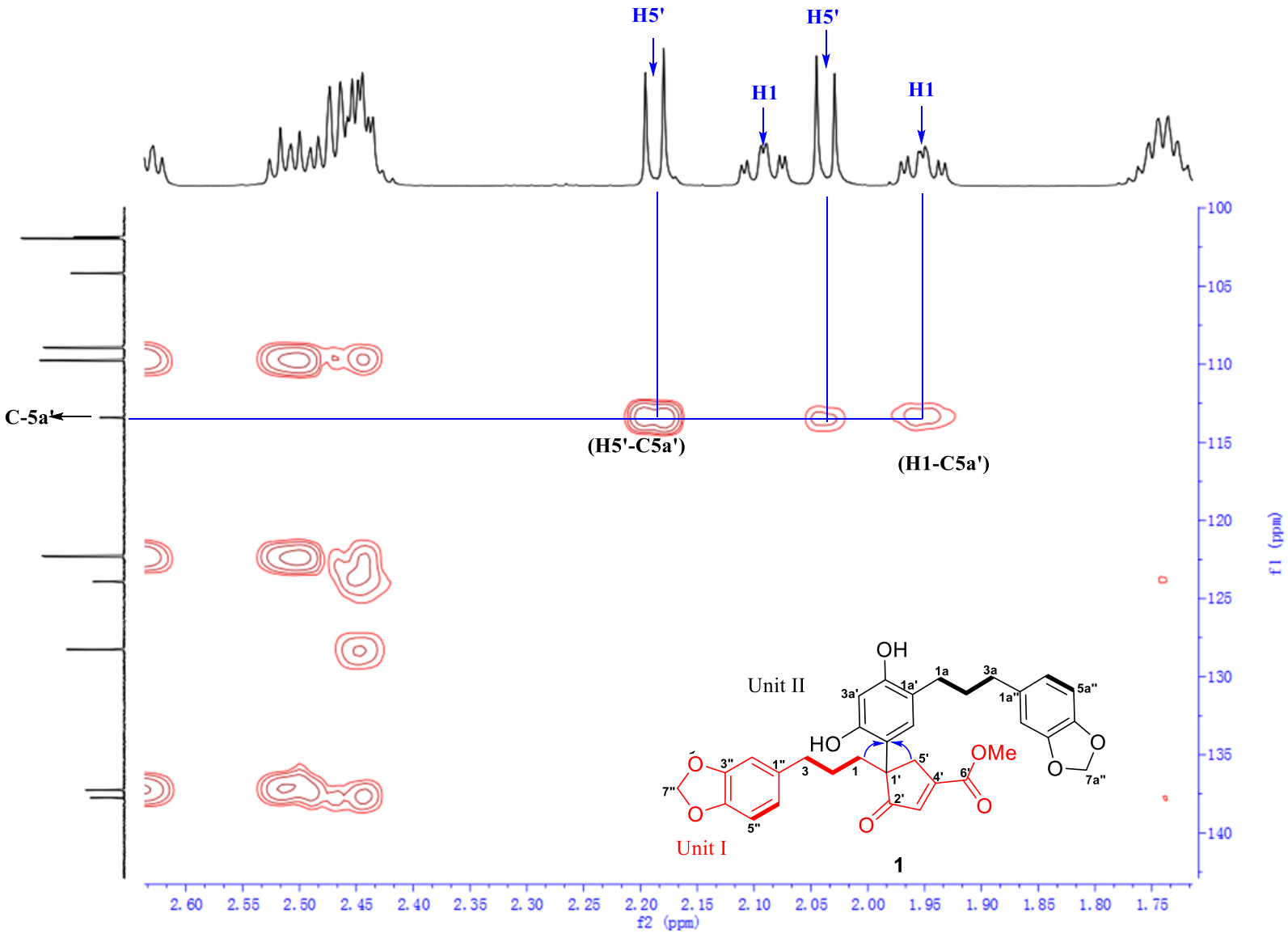

Figure S23. Key HMBC spectrum (δ_H 1.75–2.00 ppm and δ_C 100–140 ppm) ofcompound **1**

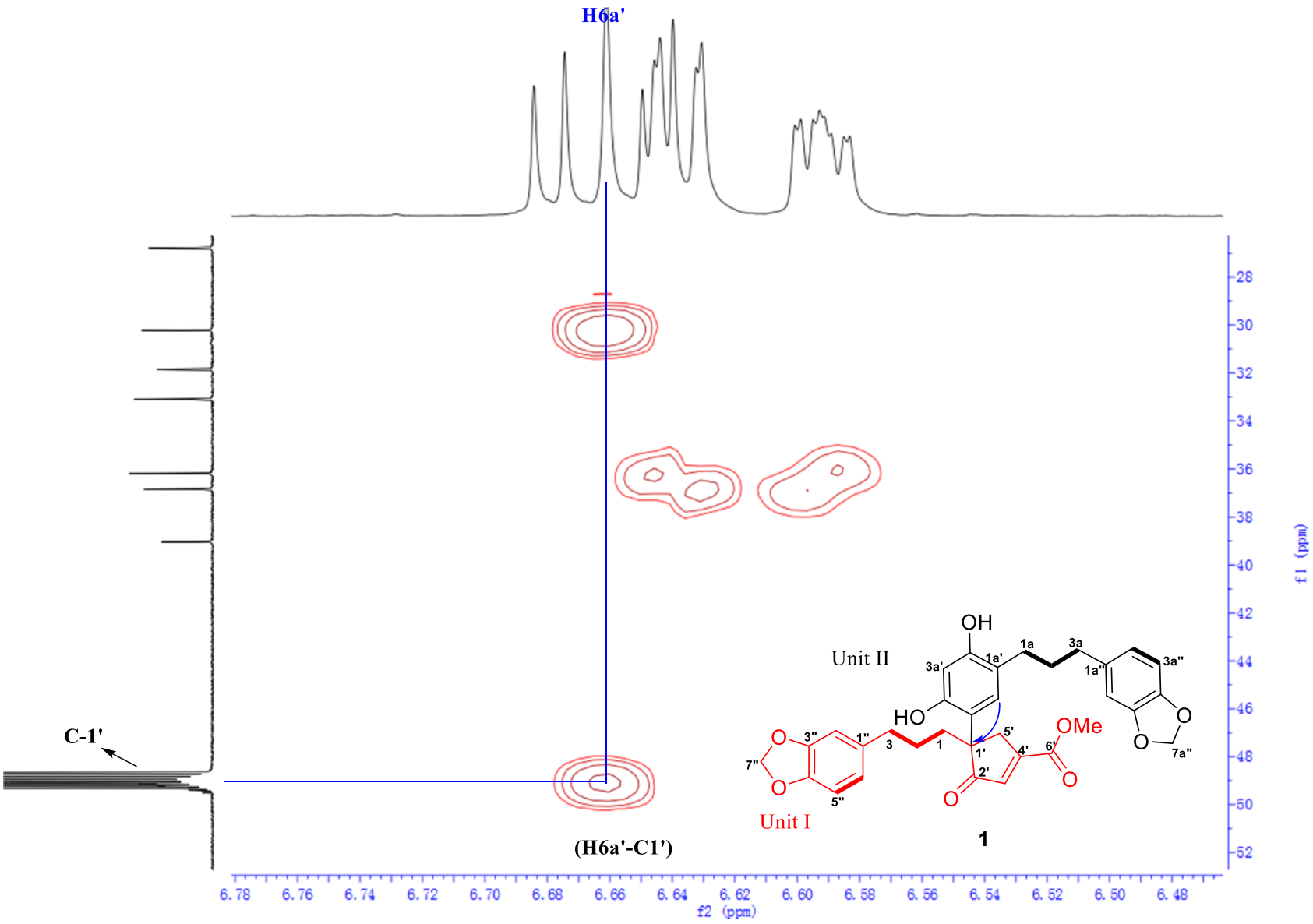

Figure S24. Key HMBC spectrum (δ_H 1.75–2.00 ppm and δ_C 100–140 ppm) ofcompound **1**

User Spectra

Fragmentor Voltage	Collision Energy	Ionization Mode
135	0	ESI

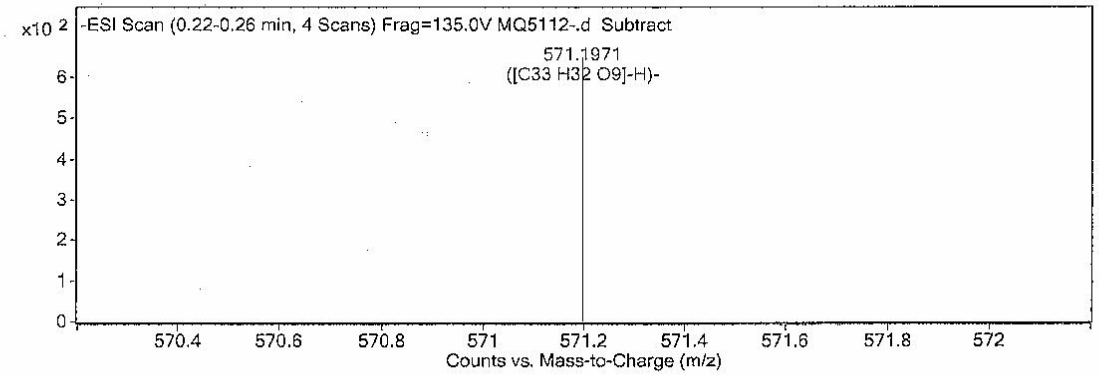

Peak List

m/z	z	Abund
112.9852		4620.68
133.014		4810.29
205.1598	1	4252.88
238.0332	1	5657.29
255.2329	1	9252.09
341.109	1	11531.95
377.0855	1	4949.85
404.1046	1	6599.28

Formula Calculator Element Limits

Element	Min	Max
C	3	60
H	0	120
O	0	30

Formula Calculator Results

Formula	CalculatedMass	CalculatedMz	Mz	Diff. (mDa)	Diff. (ppm)	DBE
C33 H32 O9	572.2046	571.1974	571.1971	-0.1	-0.1	18.0000

--- End Of Report ---

Figure S25. HR-ESIMS spectrum of compound **1**

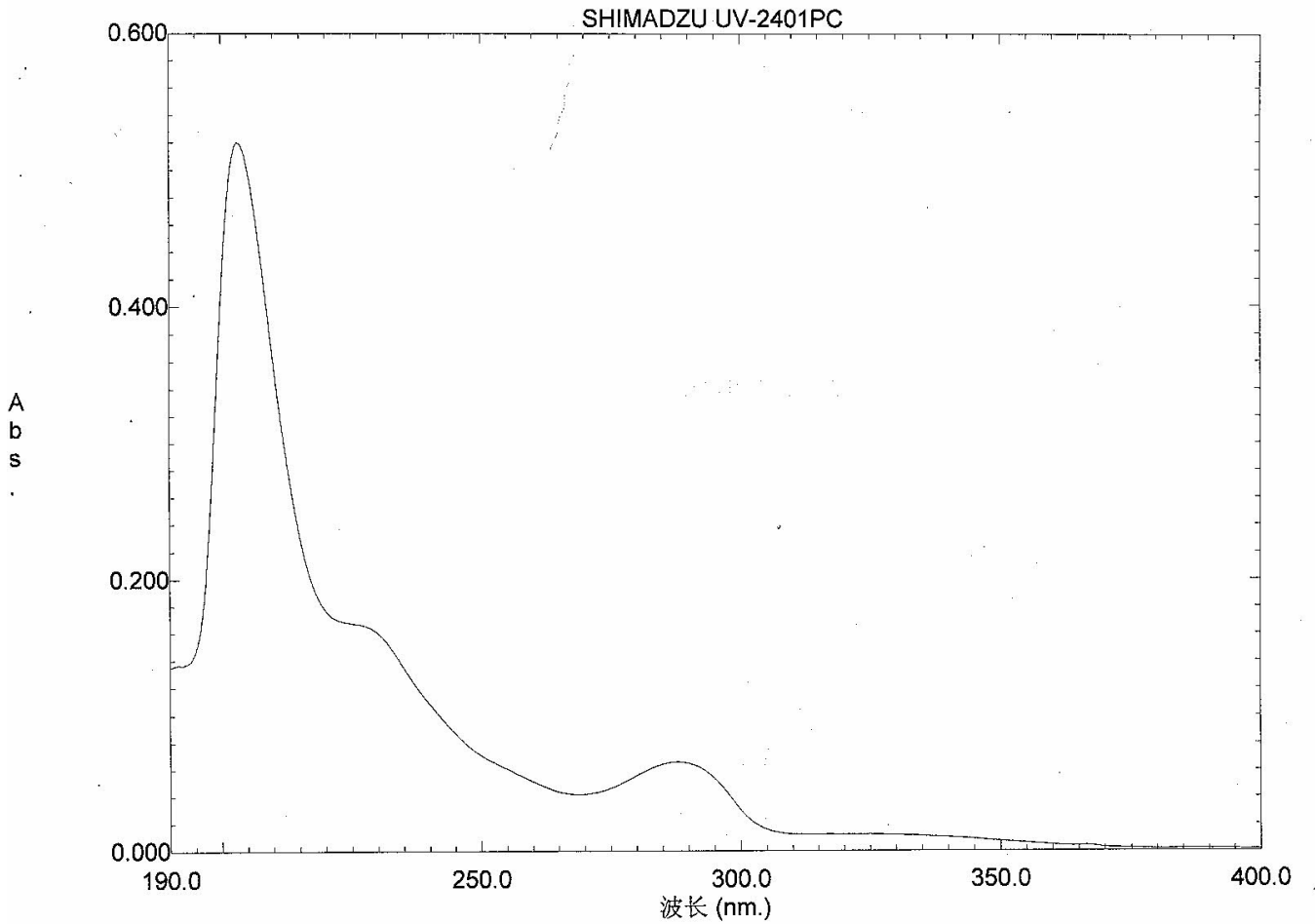

Figure S26. UV spectrum of compound **1**

Optical rotation measurement

Model : P-1020 (A060460638)

No.	Sample	Mode	Data	Monitor Blank	Temp. Cell Temp Point	Date Comment Sample Name	Light Filter Operator	Cycle Time Integ Time
No.1	83 (1/3)	Sp.Rot	134.6670	0.0404	19.2	Thu Jan 18 16:19:57 2018	Na	2 sec
				0.0000	50.00	0.00060g/mL MeOH	589nm	2 sec
					Cell	5112-1		
No.2	83 (2/3)	Sp.Rot	136.3330	0.0409	19.1	Thu Jan 18 16:20:03 2018	Na	2 sec
				0.0000	50.00	0.00060g/mL MeOH	589nm	2 sec
					Cell	5112-1		
No.3	83 (3/3)	Sp.Rot	143.6670	0.0431	19.1	Thu Jan 18 16:20:08 2018	Na	2 sec
				0.0000	50.00	0.00060g/mL MeOH	589nm	2 sec
					Cell	5112-1		
No.4	84 (1/3)	Sp.Rot	147.6670	0.0443	19.1	Thu Jan 18 16:20:24 2018	Na	2 sec
				0.0000	50.00	0.00060g/mL MeOH	589nm	2 sec
					Cell	5112-1		
No.5	84 (2/3)	Sp.Rot	129.6670	0.0389	19.0	Thu Jan 18 16:20:30 2018	Na	2 sec
				0.0000	50.00	0.00060g/mL MeOH	589nm	2 sec
					Cell	5112-1		
No.6	84 (3/3)	Sp.Rot	139.3330	0.0418	19.0	Thu Jan 18 16:20:35 2018	Na	2 sec
				0.0000	50.00	0.00060g/mL MeOH	589nm	2 sec
					Cell	5112-1		

+138.7776°

Figure S27. ORD spectrum of compound (+)-**1**

Optical rotation measurement

Model : P-1020 (A060460638)

No.	Sample	Mode	Data	Monitor Blank	Temp. Cell Temp Point	Date Comment Sample Name	Light Filter Operator	Cycle Time Integ Time
No.1	82 (1/3)	Sp.Rot	-87.5000	-0.0525 0.0000	18.9 50.00 Cell	Thu Jan 18 16:12:33 2018 0.00120g/mL MeOH 5112-2	Na 589nm	2 sec 2 sec
No.2	82 (2/3)	Sp.Rot	-85.6670	-0.0514 0.0000	18.9 50.00 Cell	Thu Jan 18 16:12:39 2018 0.00120g/mL MeOH 5112-2	Na 589nm	2 sec 2 sec
No.3	82 (3/3)	Sp.Rot	-88.8330	-0.0533 0.0000	19.0 50.00 Cell	Thu Jan 18 16:12:44 2018 0.00120g/mL MeOH 5112-2	Na 589nm	2 sec 2 sec

-87.5555°

Figure S28. ORD spectrum of compound (-)-**1**

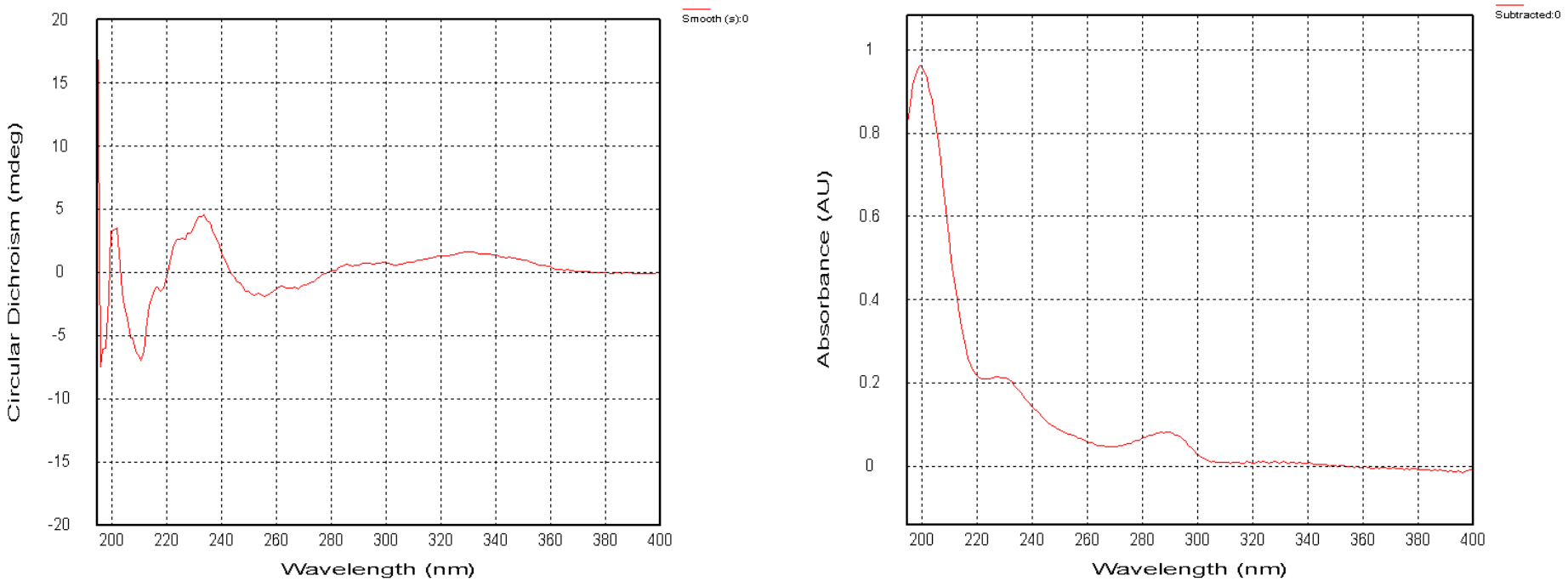

Figure S29. CD spectrum of compound (+)-**1**

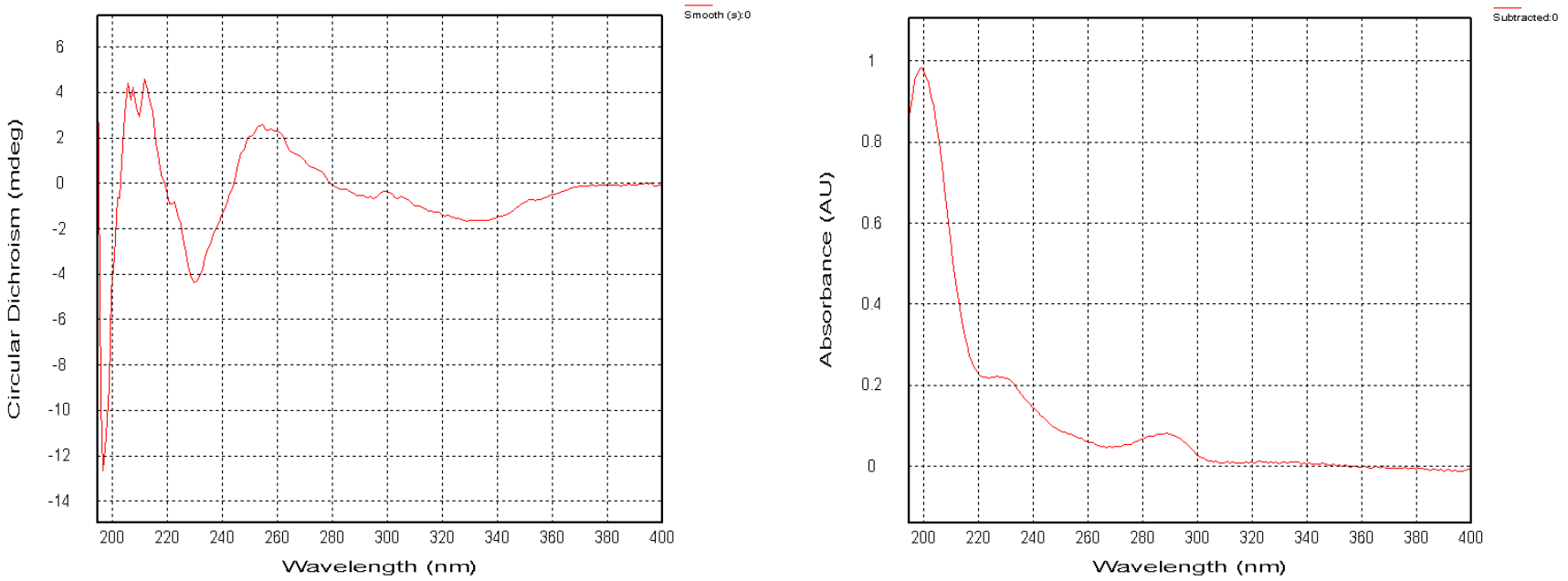

Figure S30. CD spectrum of compound (-)-**1**

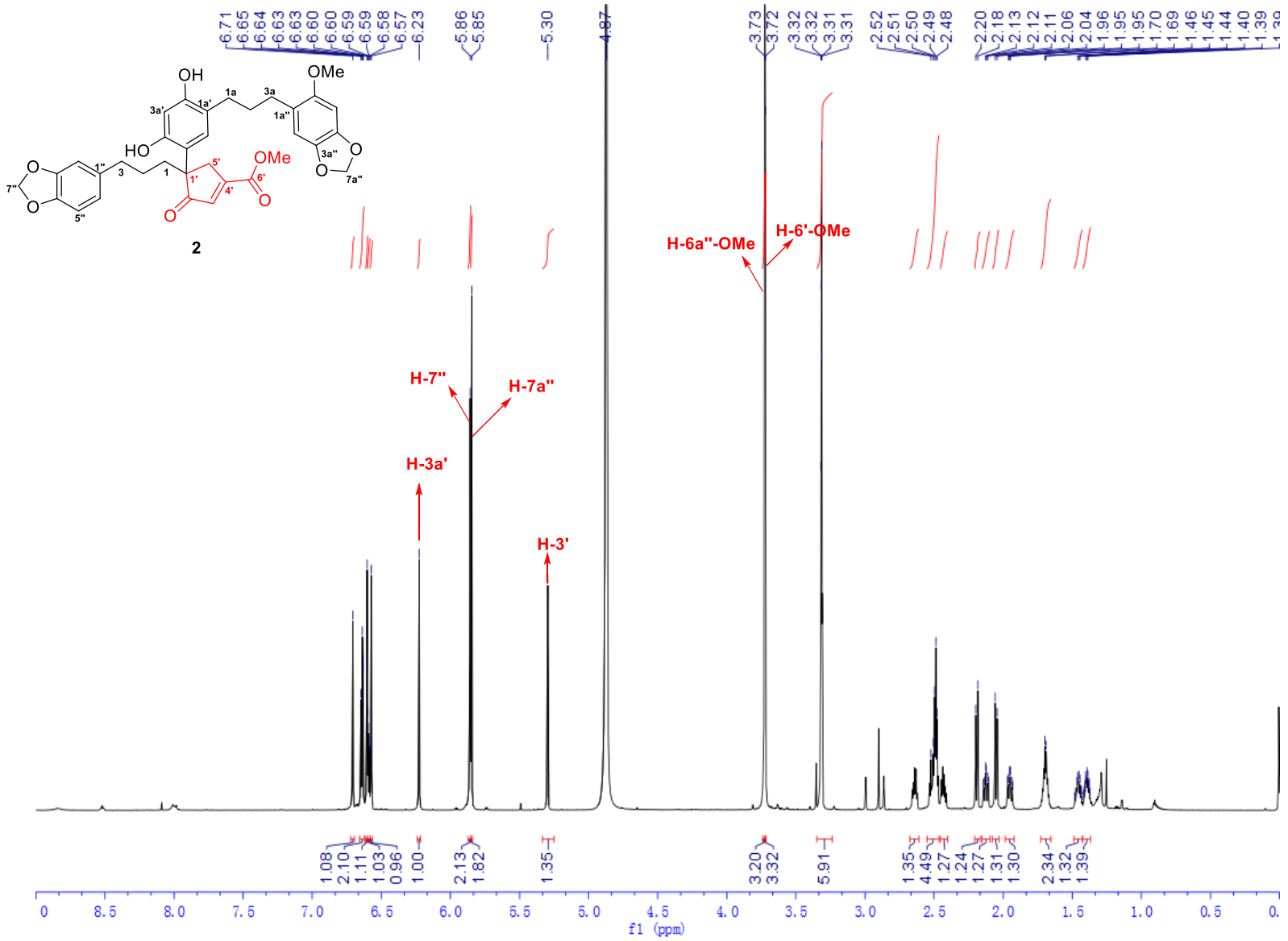

Figure S31. ^{1}H NMR spectrum (0-9 ppm) of compound **2**

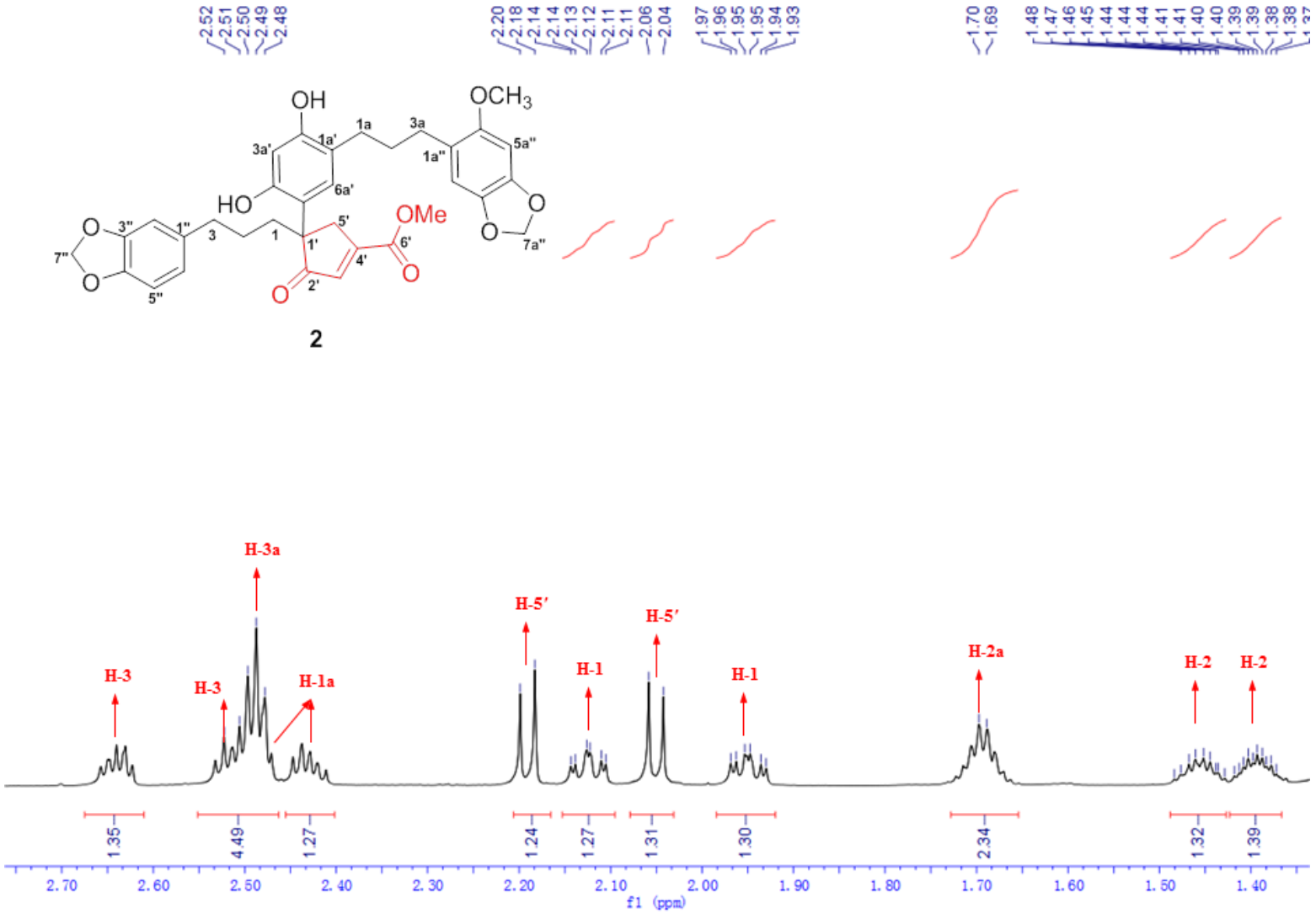

Figure S32. ^{1}H NMR spectrum (1.40-2.70 ppm) of compound **2**

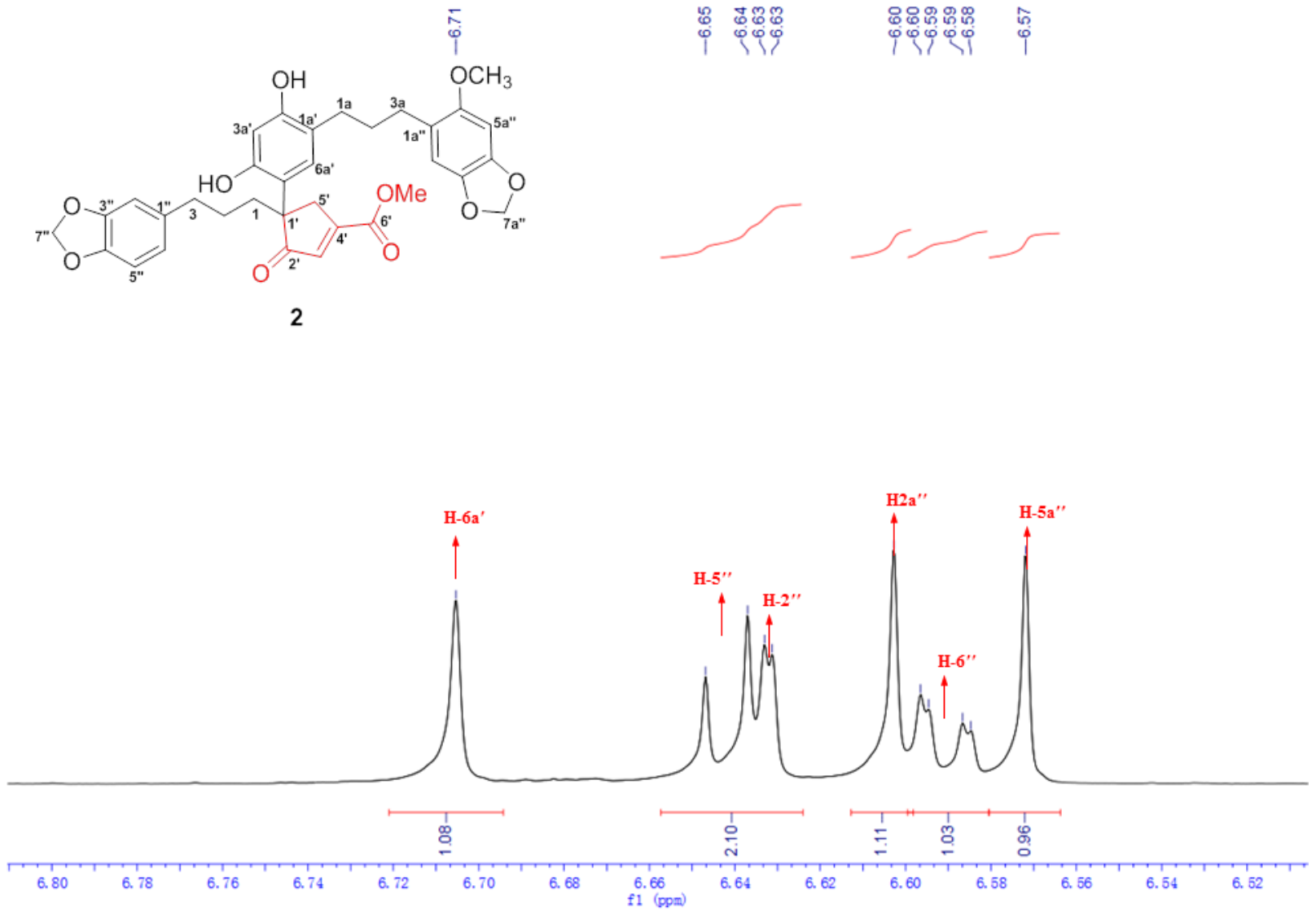

2

Figure S33. ^{1}H NMR spectrum (6.52-6.80 ppm) of compound **2**

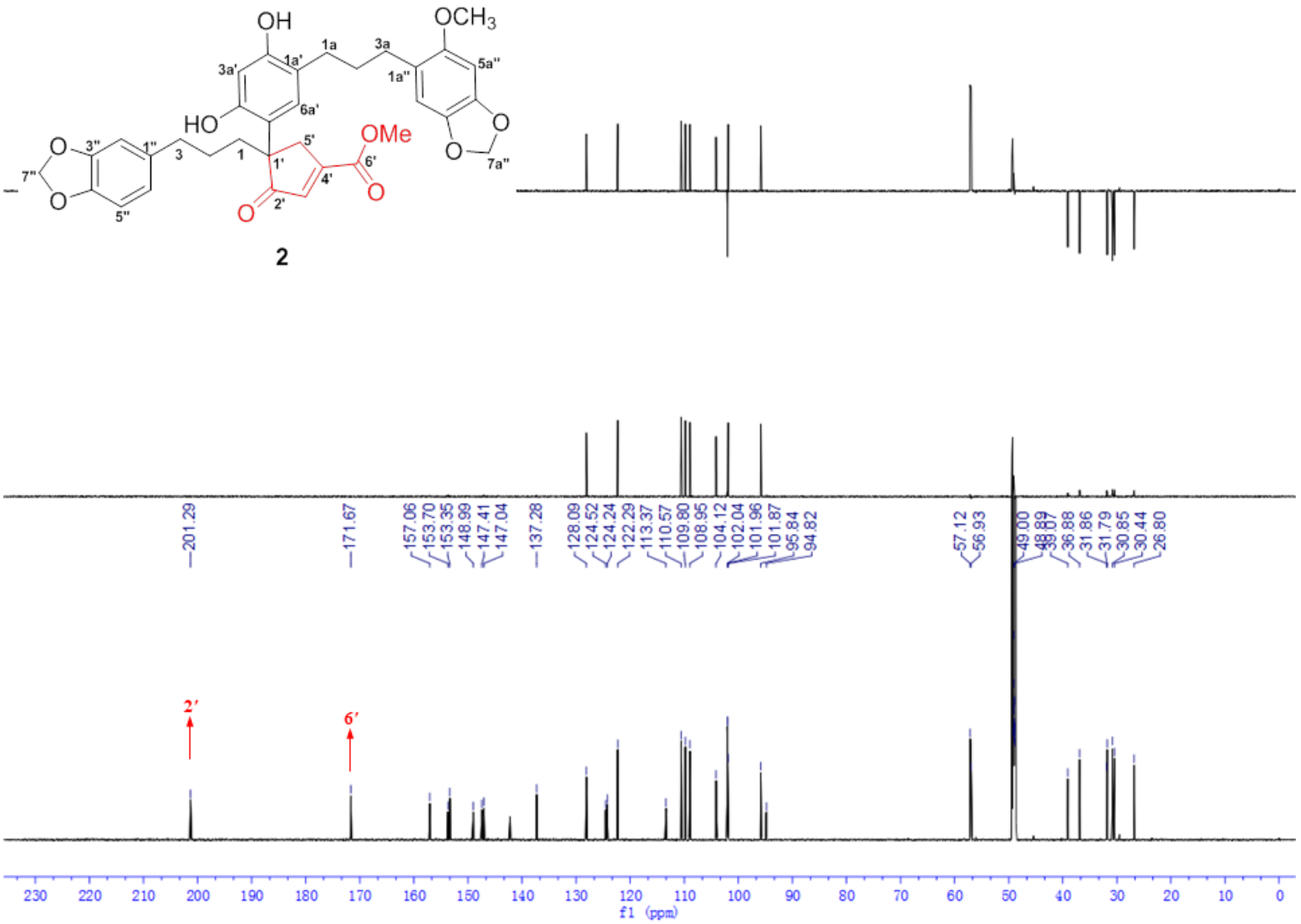

Figure S34. ^{13}C NMR spectra (0-230 ppm) of compound **2**

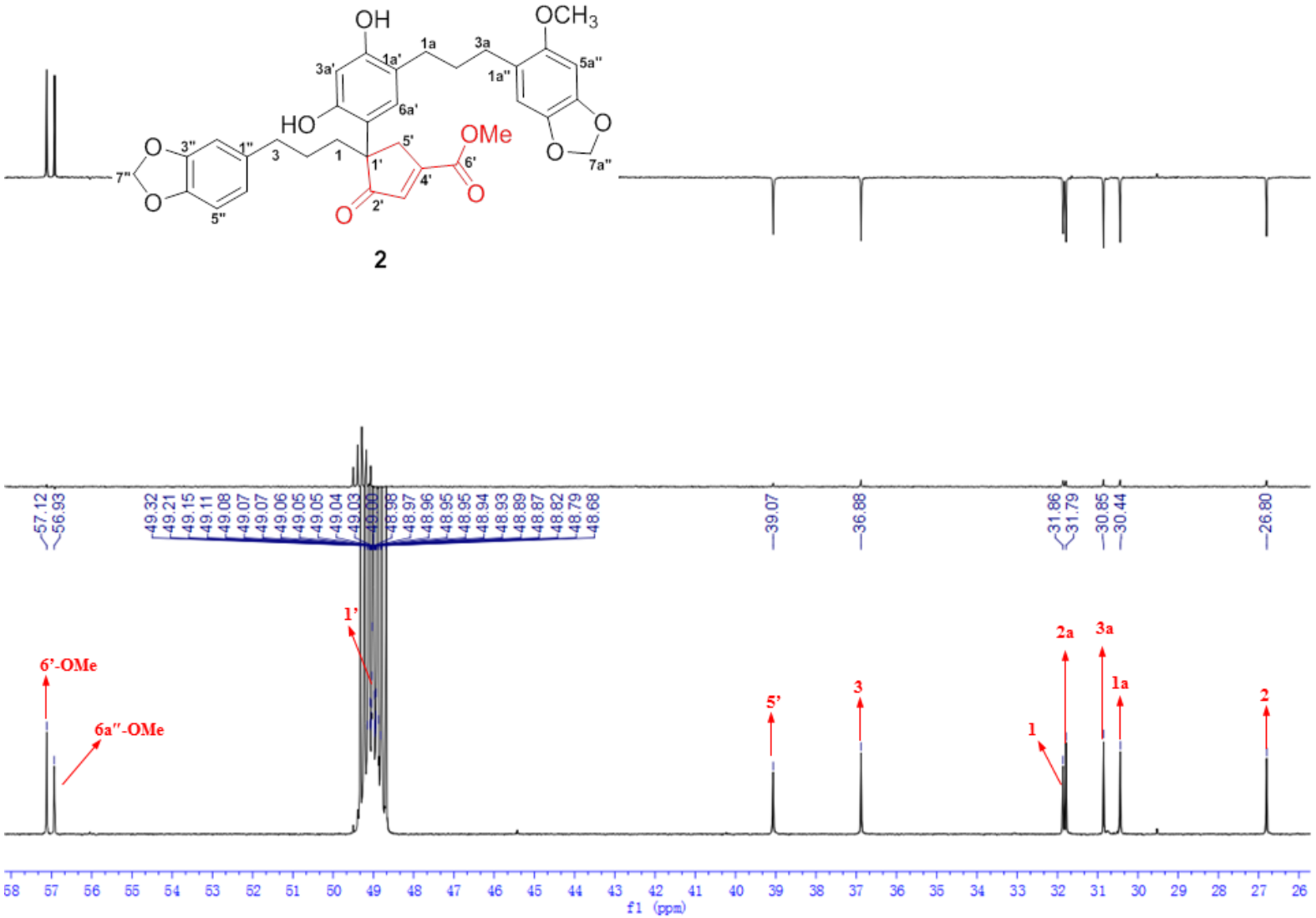

Figure S35. ^{13}C NMR spectra (26-58 ppm)of compound **2**

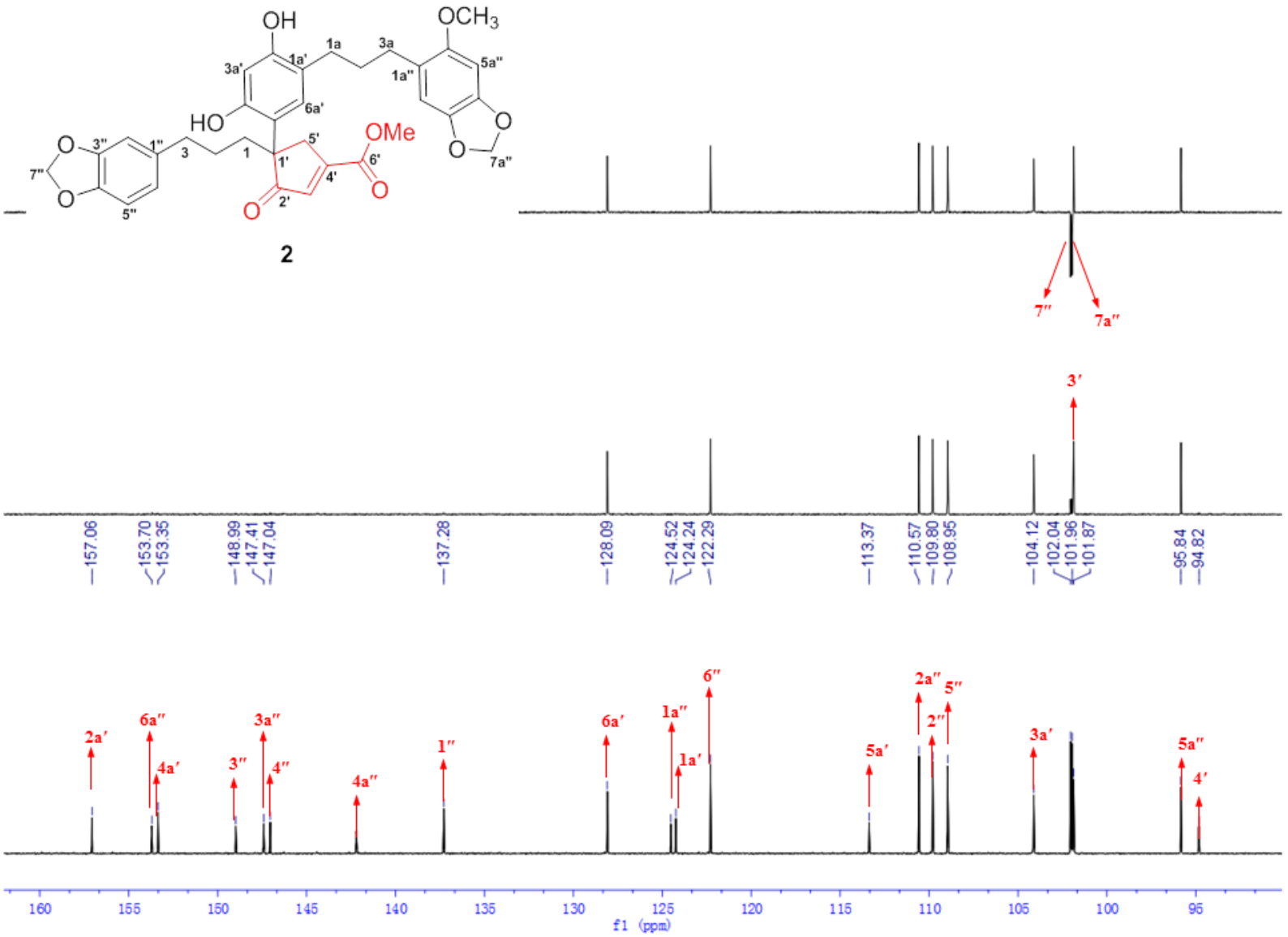

Figure S36. ^{13}C NMR spectra (93-160 ppm) of compound **2**

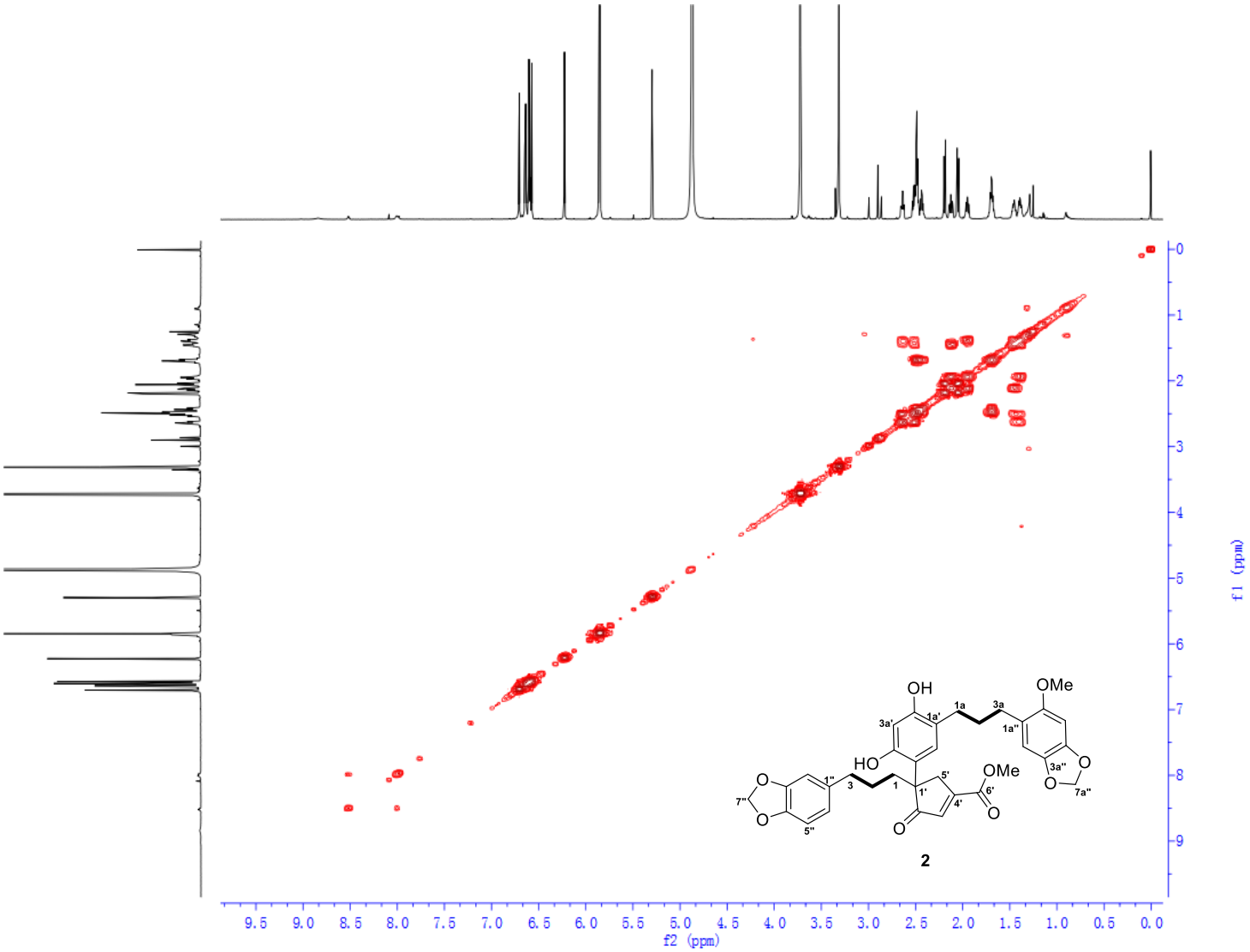

Figure S37. ^{1}H-^{1}H COSY spectrum of compound **2**

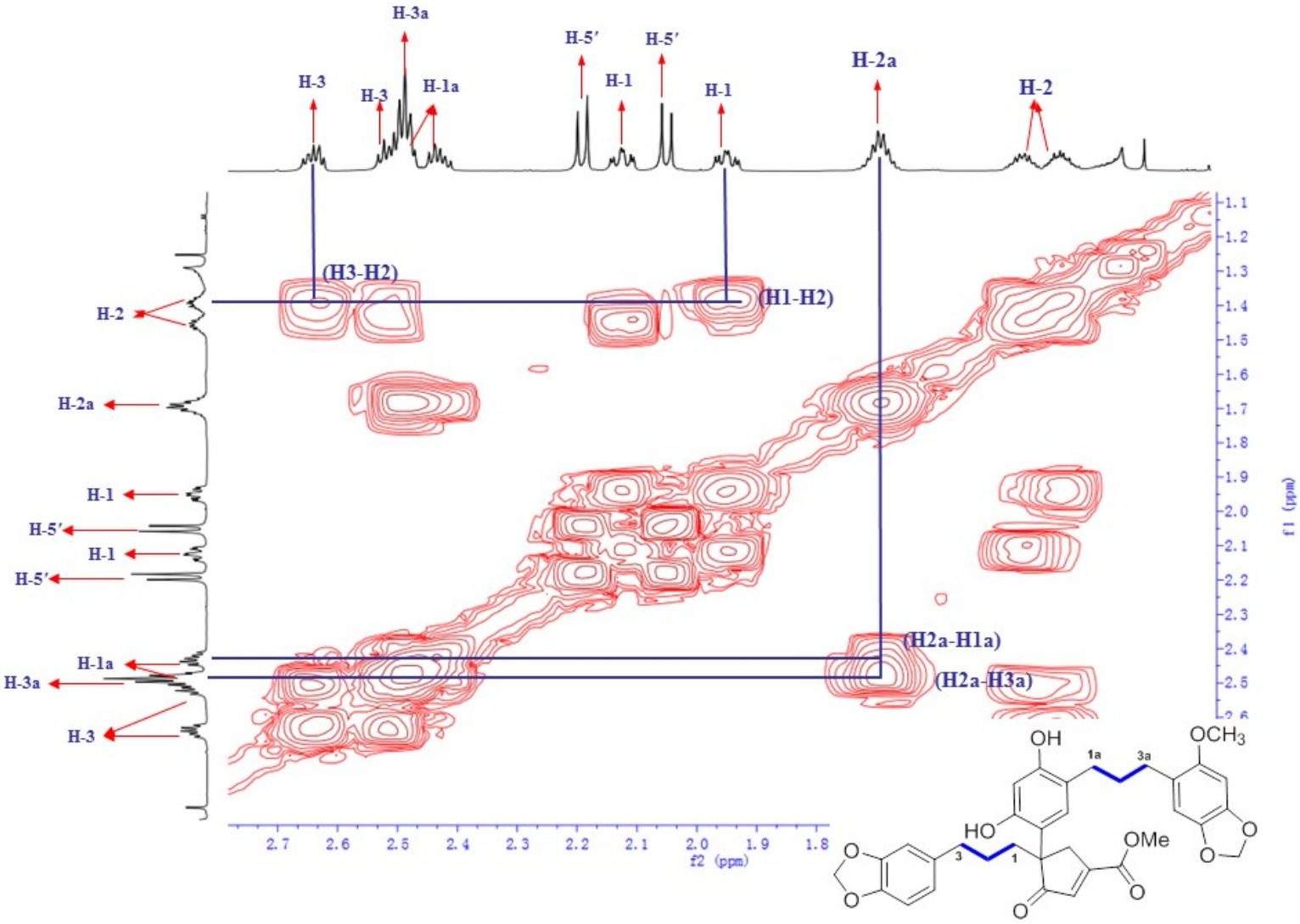

Figure S38. Key ^{1}H-^{1}H COSY spectrum of compound **2**

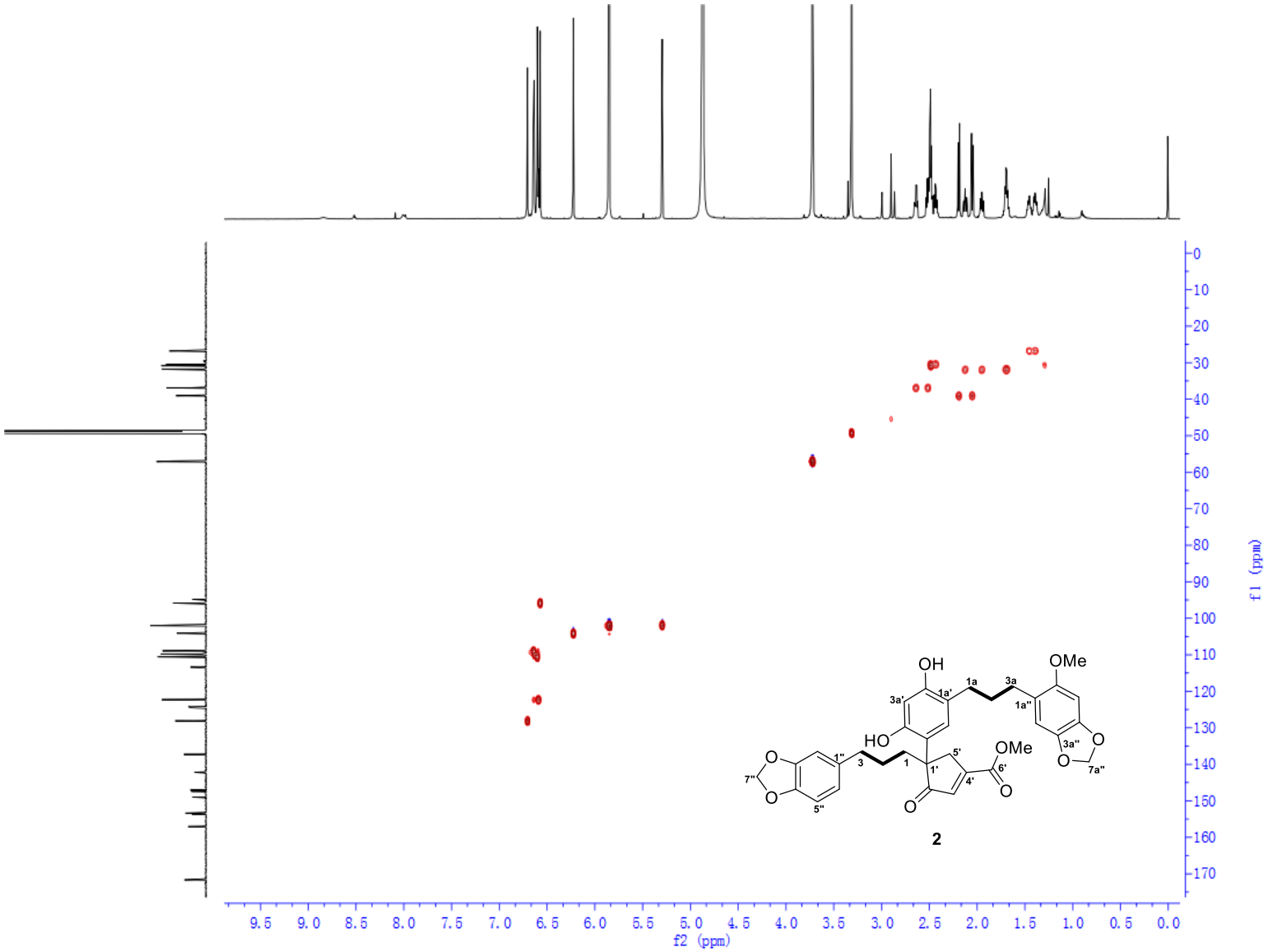

Figure S39. HSQC spectrum of compound **2**

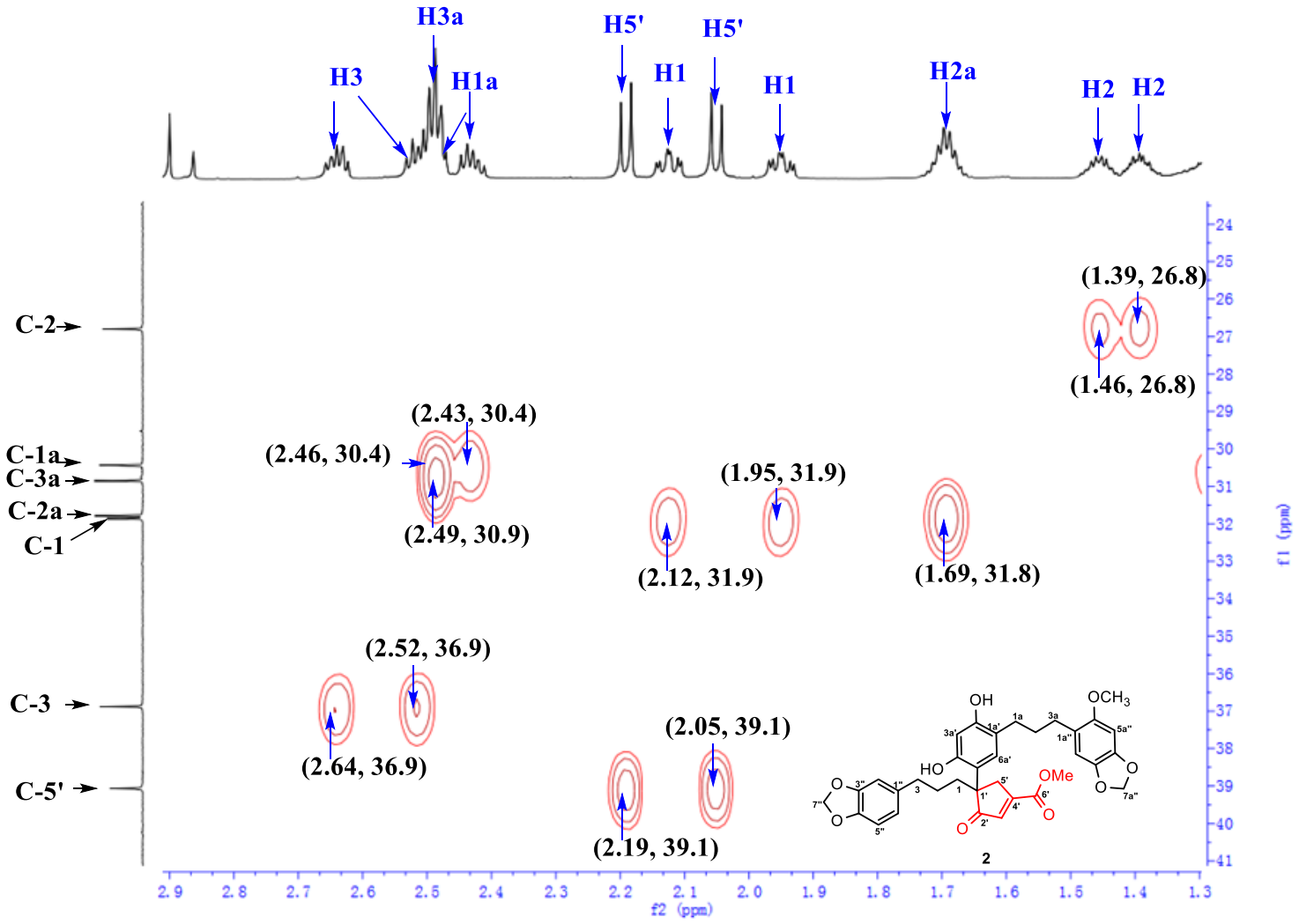

Figure S40. HSQC spectrum (δ_H 1.3-2.9 and δ_C 24-41) of compound **2**

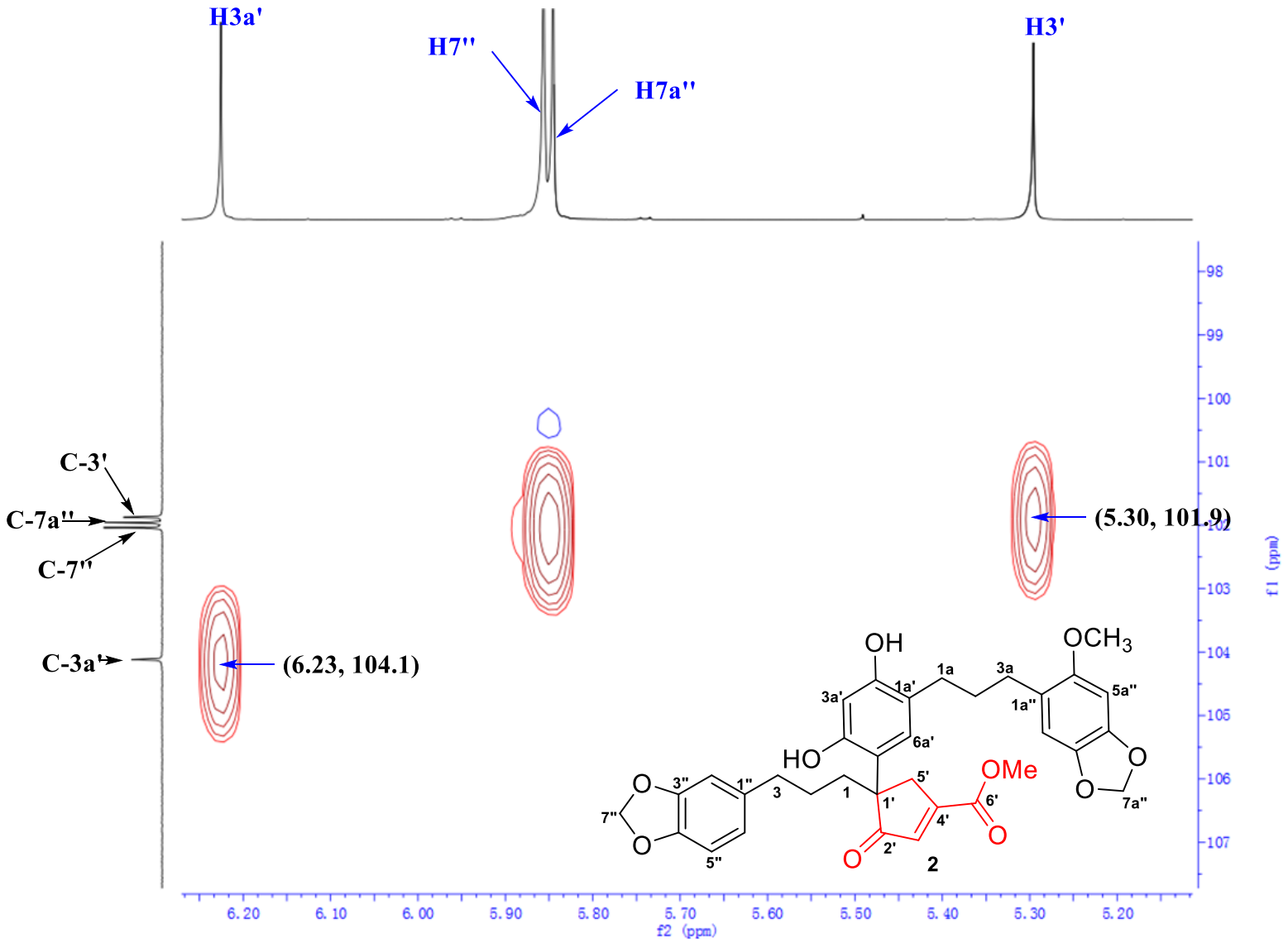

Figure S41. HSQC spectrum (δ_H 5.2-6.2 and δ_C 98-107)) of compound **2**

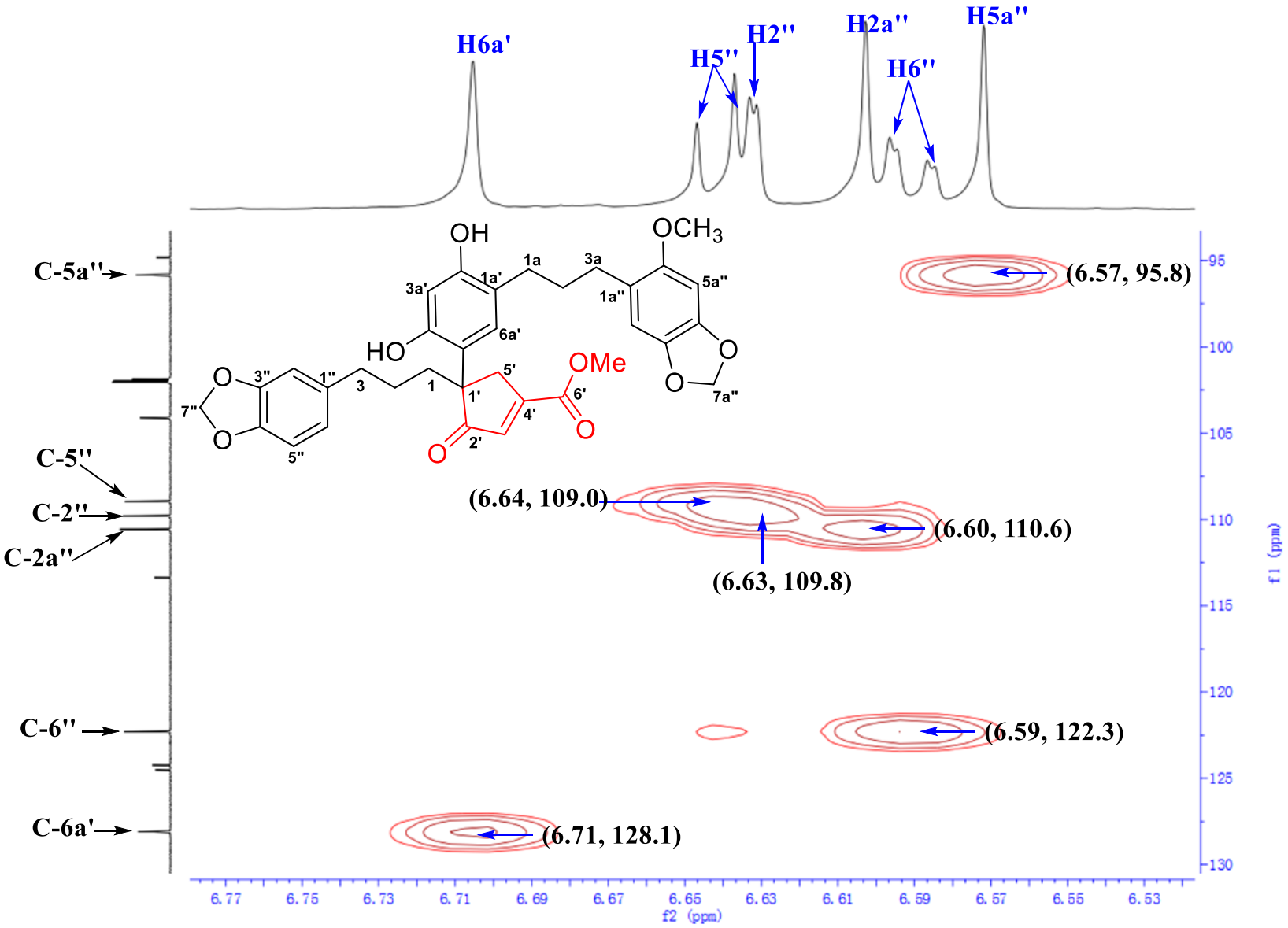

Figure S42. HSQC spectrum (δ_H 6.53-6.77 and δ_C 95-130)) of compound **2**

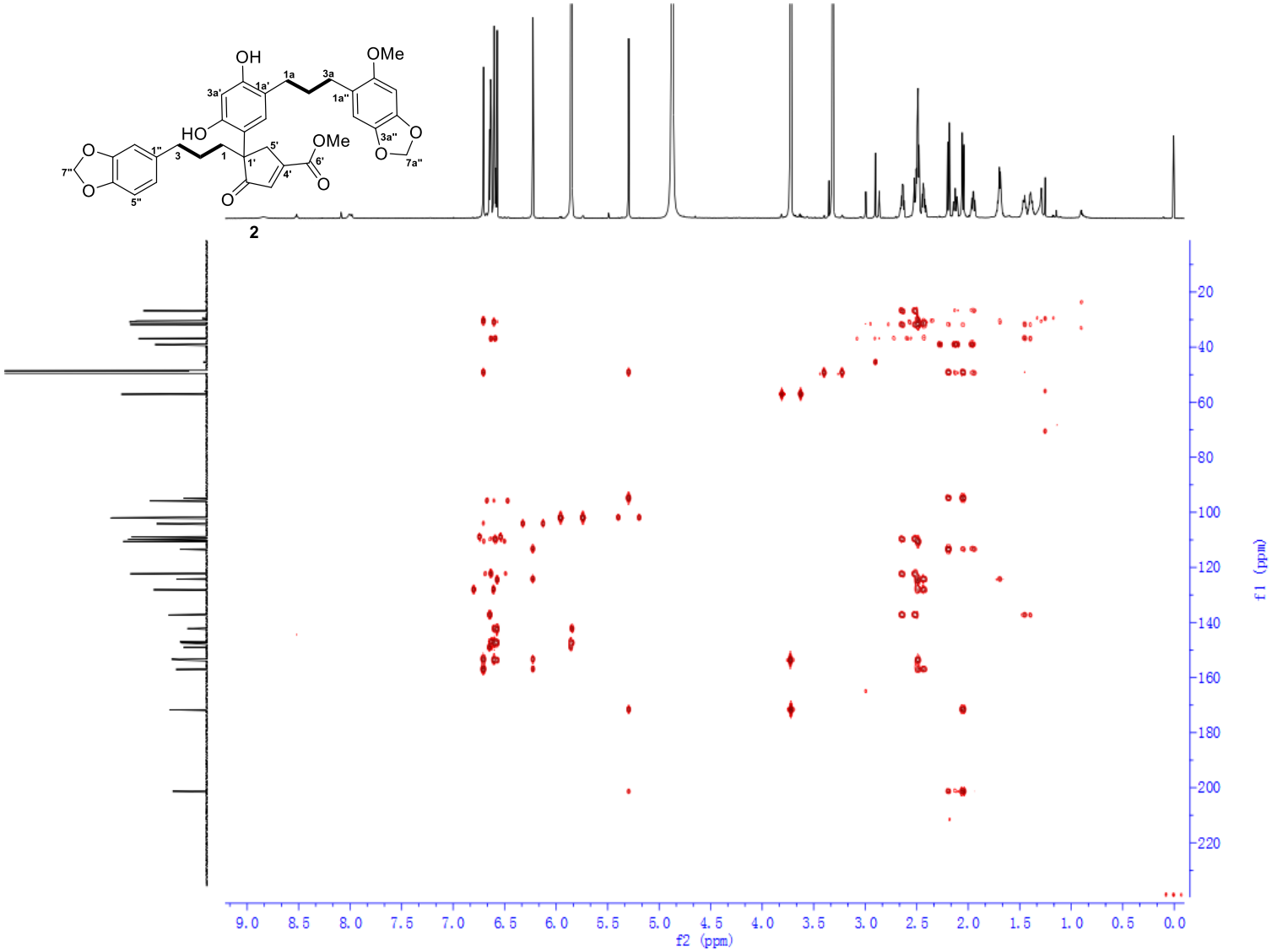

Figure S43. HMBC spectrum of compound **2**

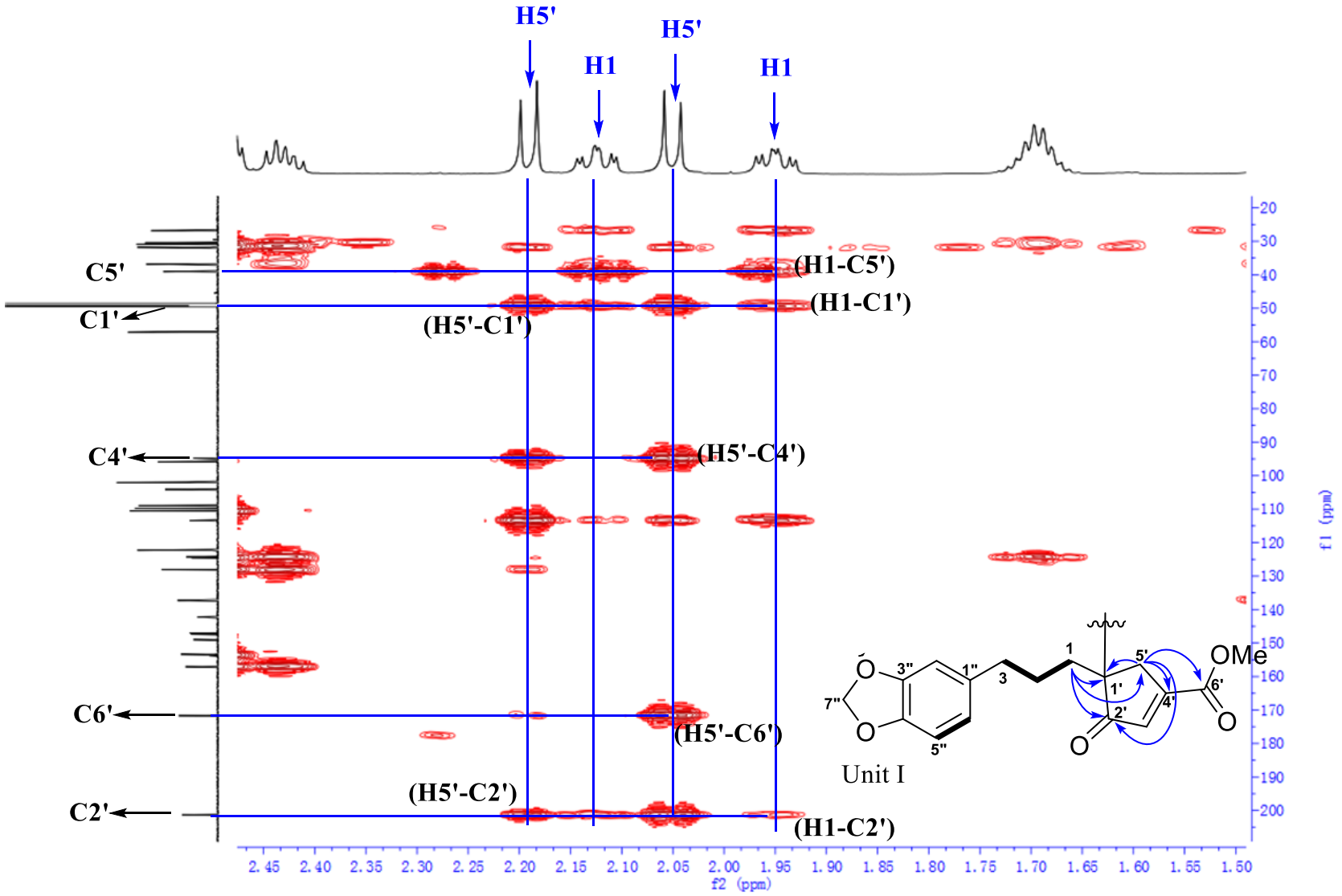

Figure S44. Key HMBC spectrum (δ_H 1.50-2.45 and δ_C 20-200) of unit I in compound **2**

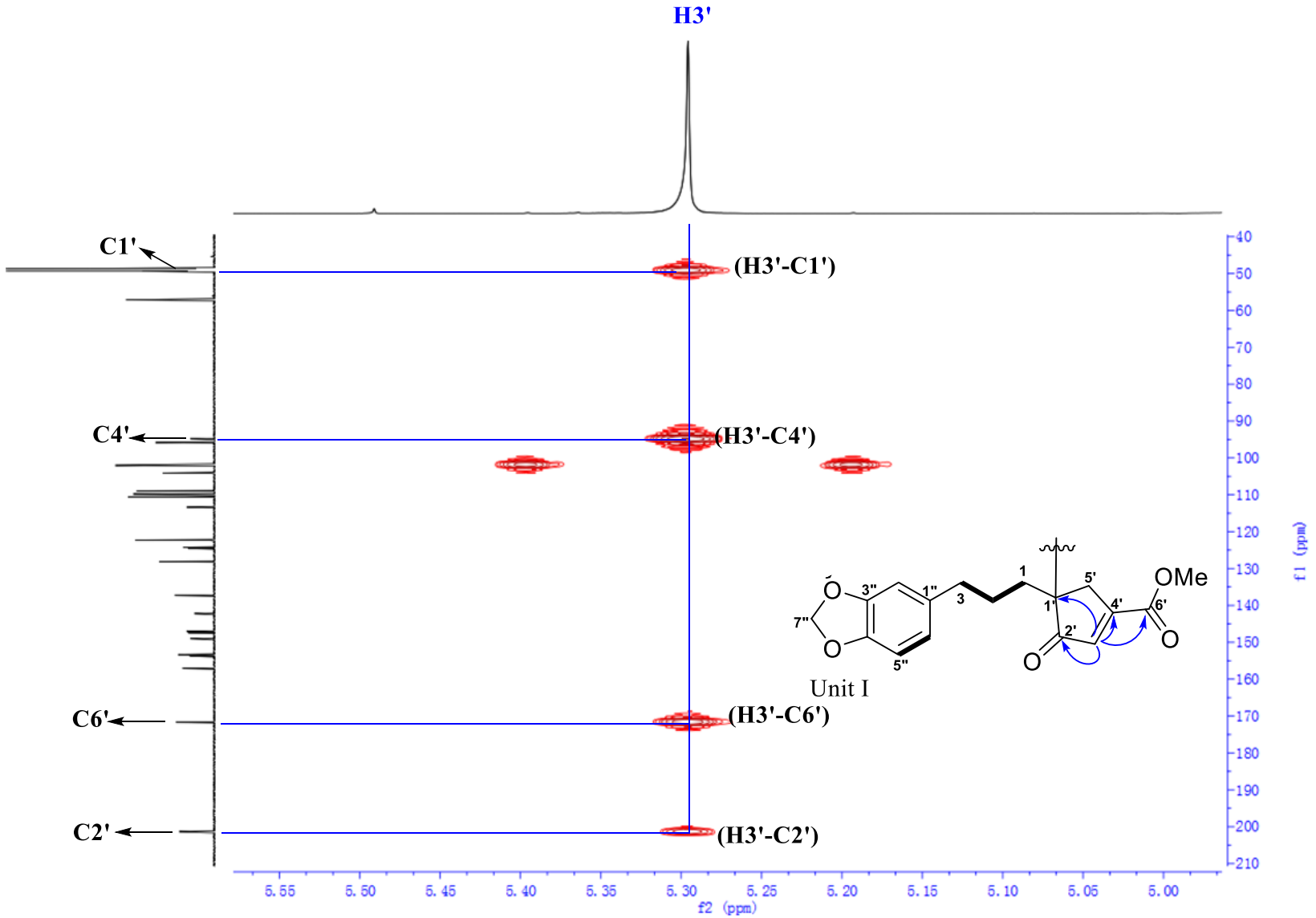

Figure S45. Key HMBC spectrum (δ_H 5.00-5.55 and δ_C 40-210) of unit I in compound **2**

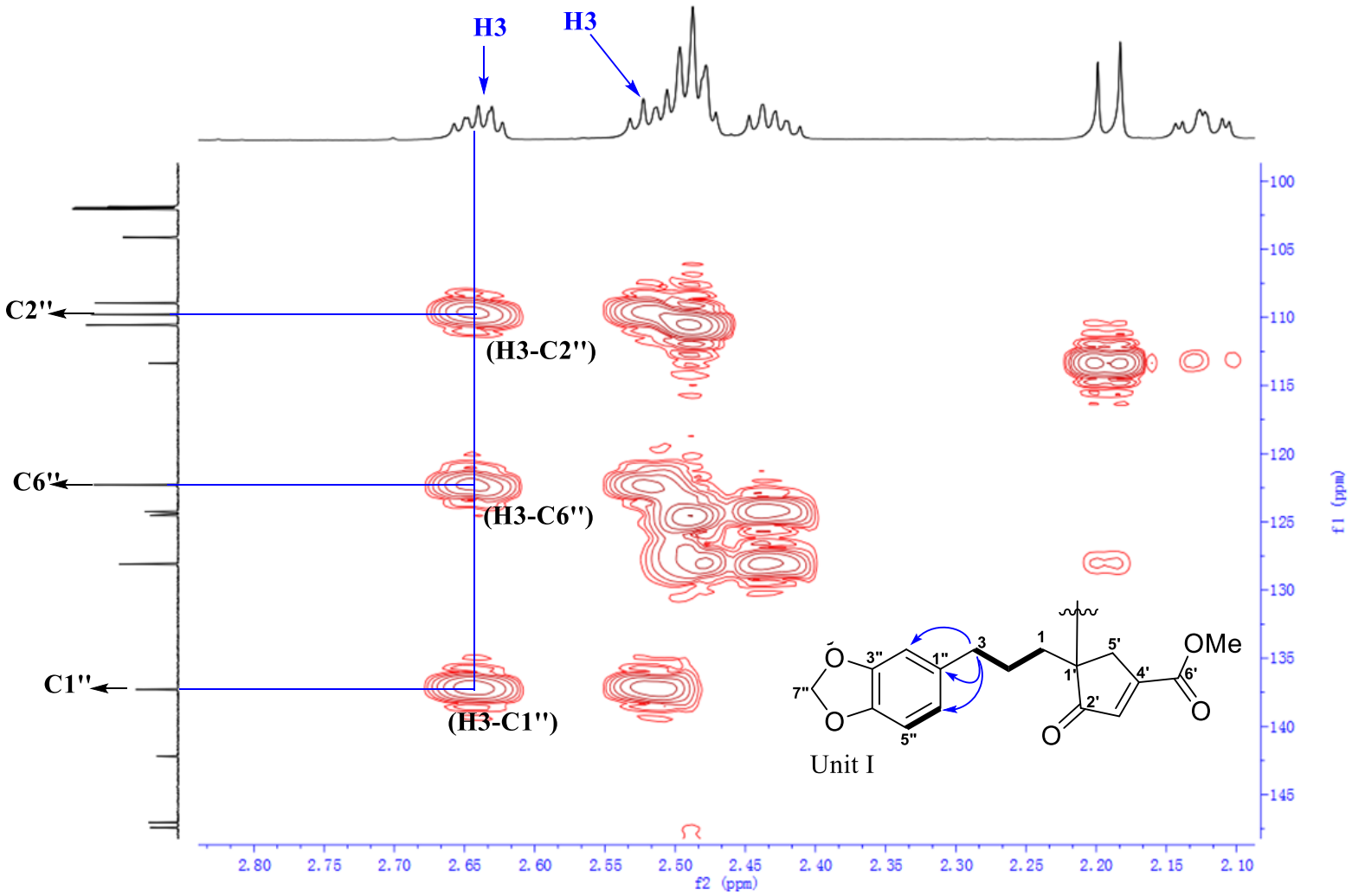

Figure S46. Key HMBC spectrum (δ_H 2.10-2.80 and δ_C 100-145) of unit I in compound **2**

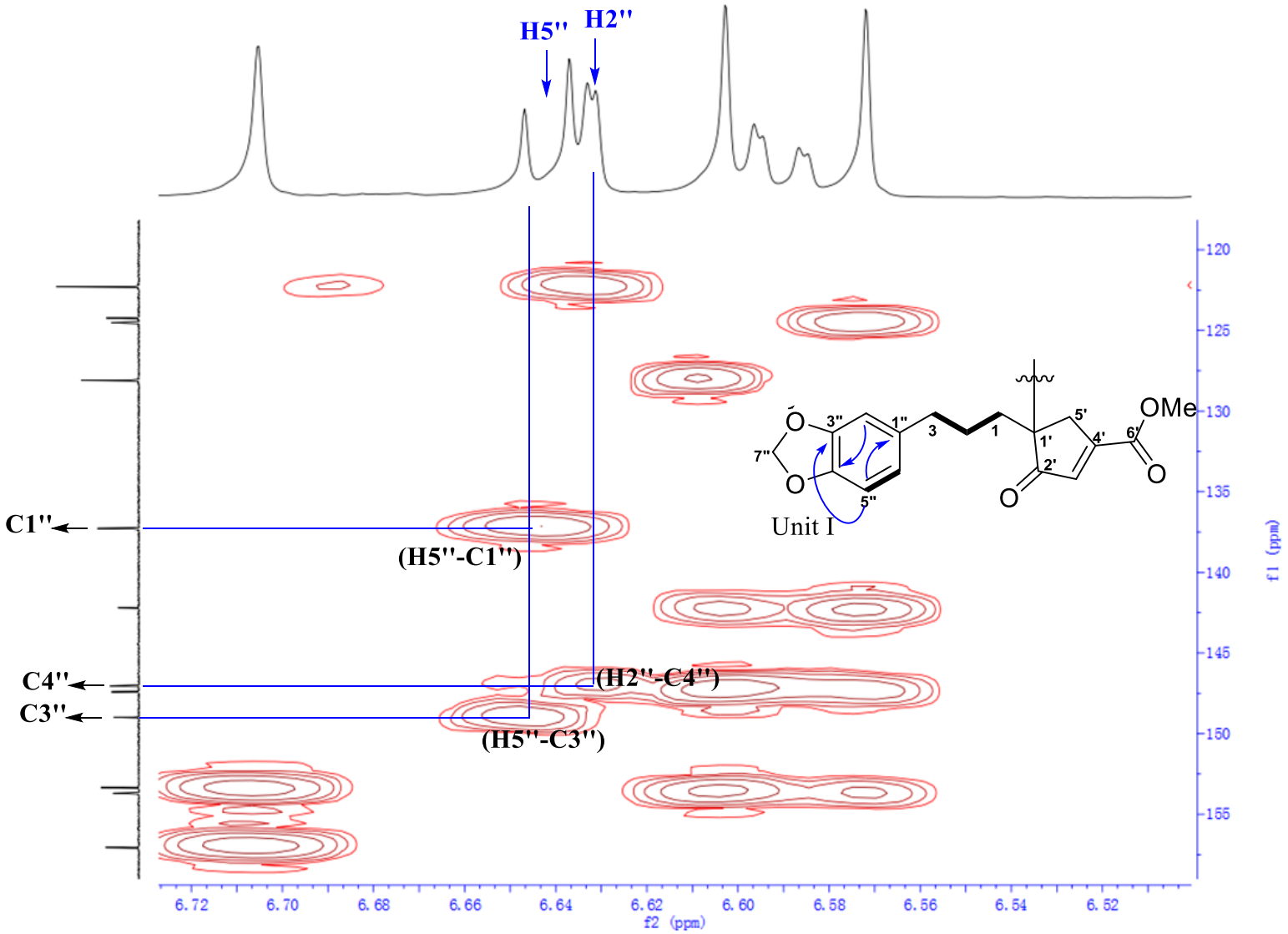

Figure S47. Key HMBC spectrum (δ_H 6.52-6.72 and δ_C 120-160) of unit I in compound **2**

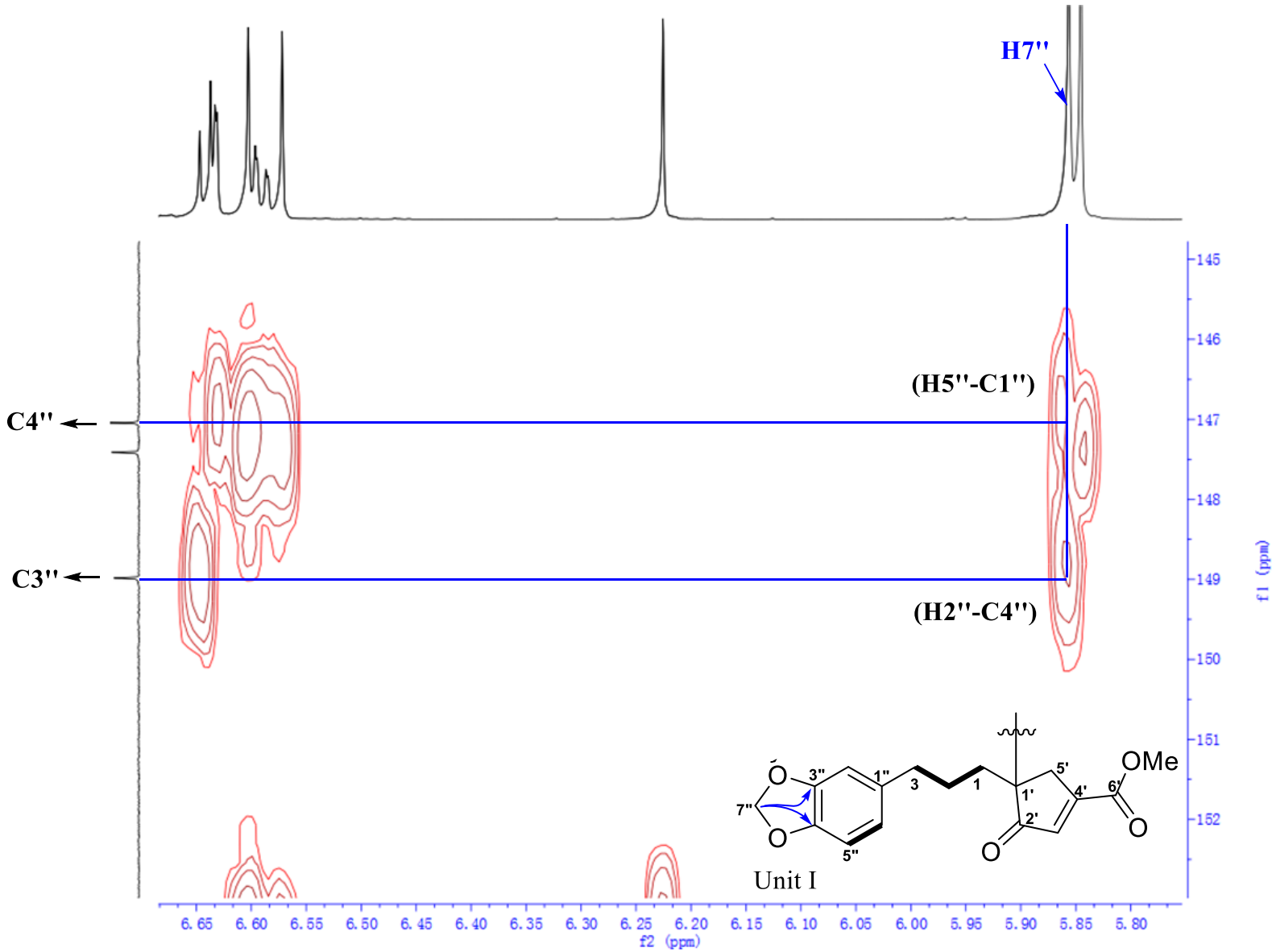

Figure S48. Key HMBC spectrum (δ_H 5.80-6.65 and δ_C 145-152) of unit I in compound **2**

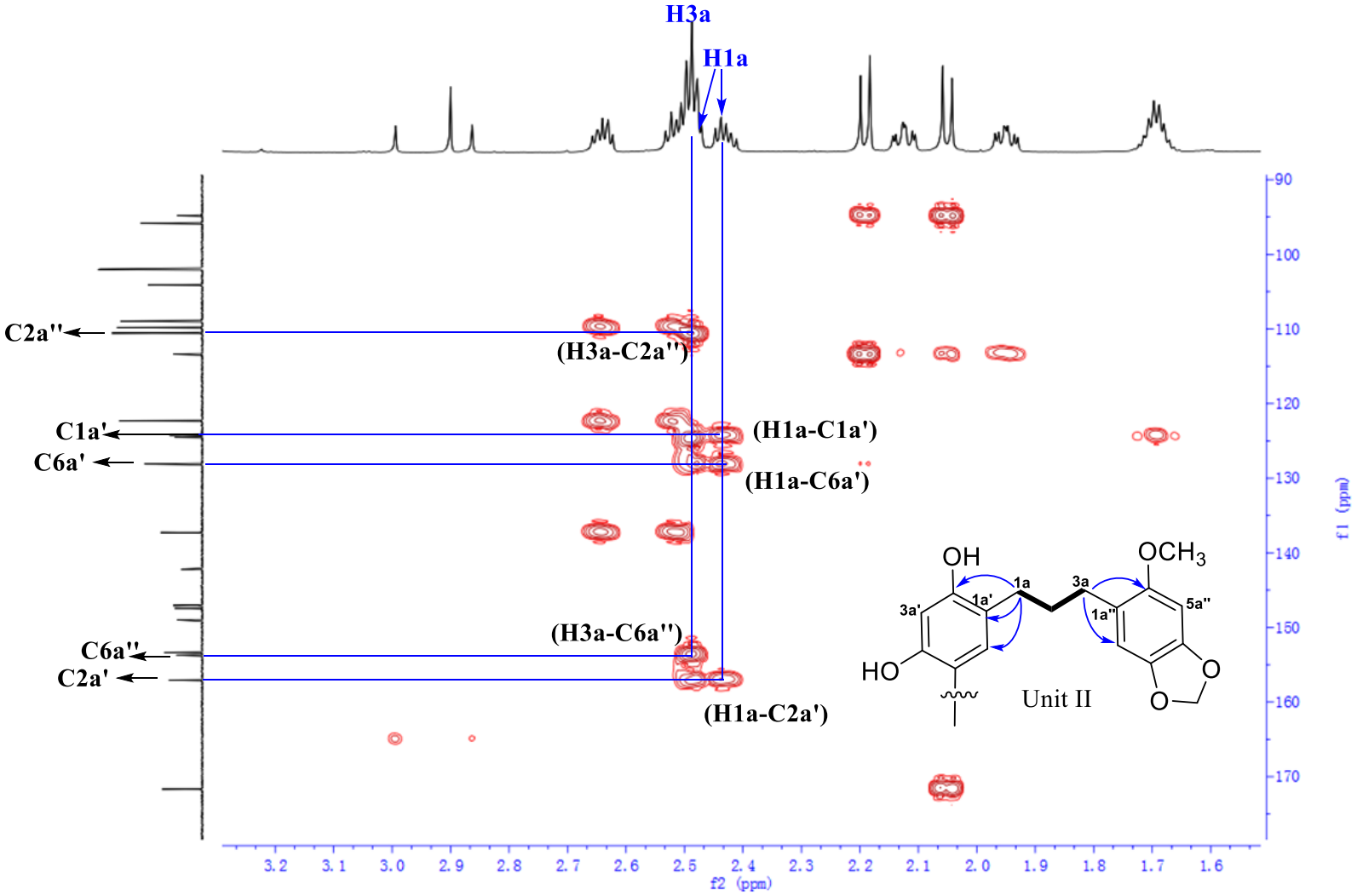

Figure S49. Key HMBC spectrum (δ_H 1.60-3.20 and δ_C 90-170) of unit II in compound **2**

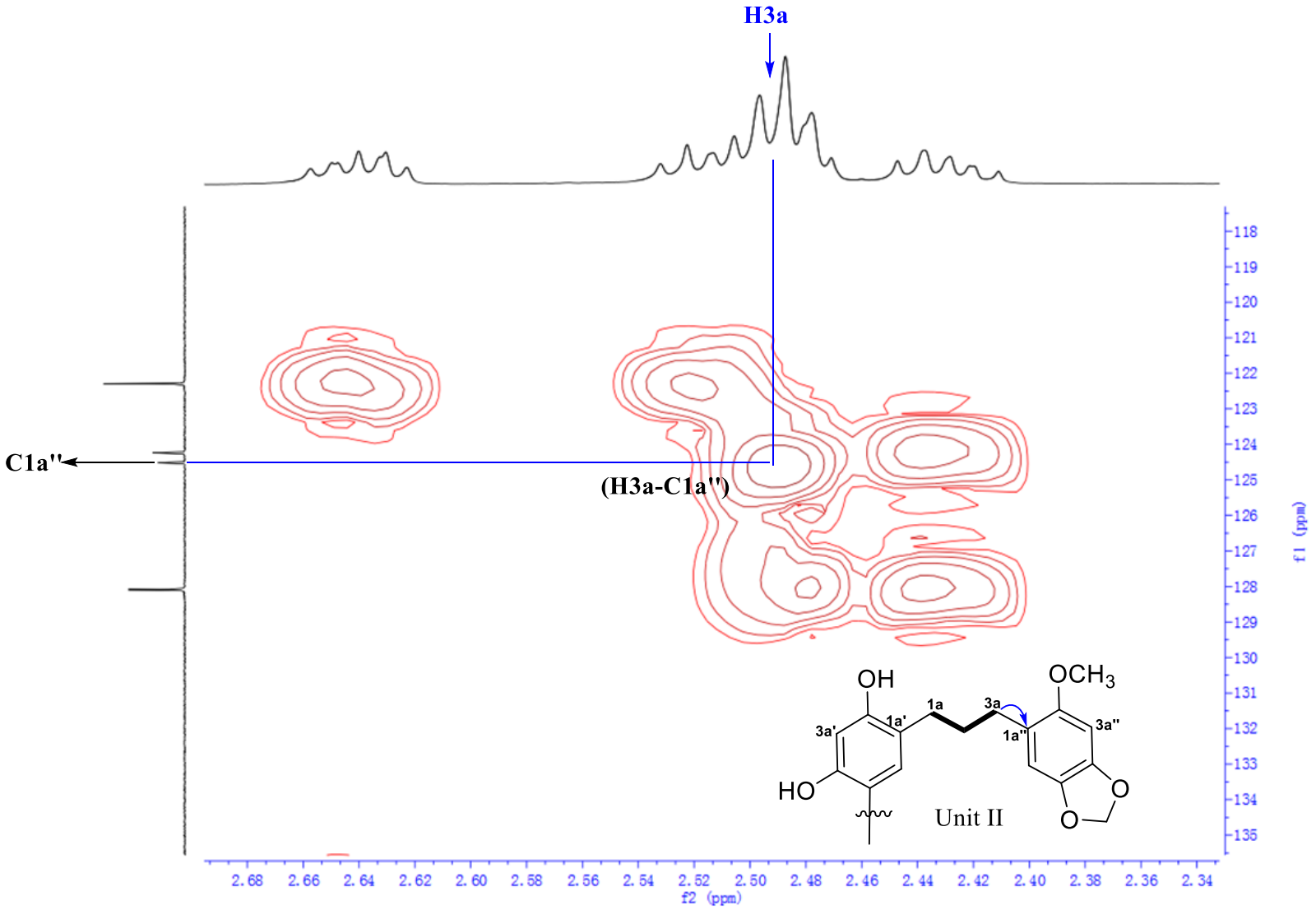

Figure S50. Key HMBC spectrum (δ_H 2.34-2.68 and δ_C 118-135) of unit II in compound **2**

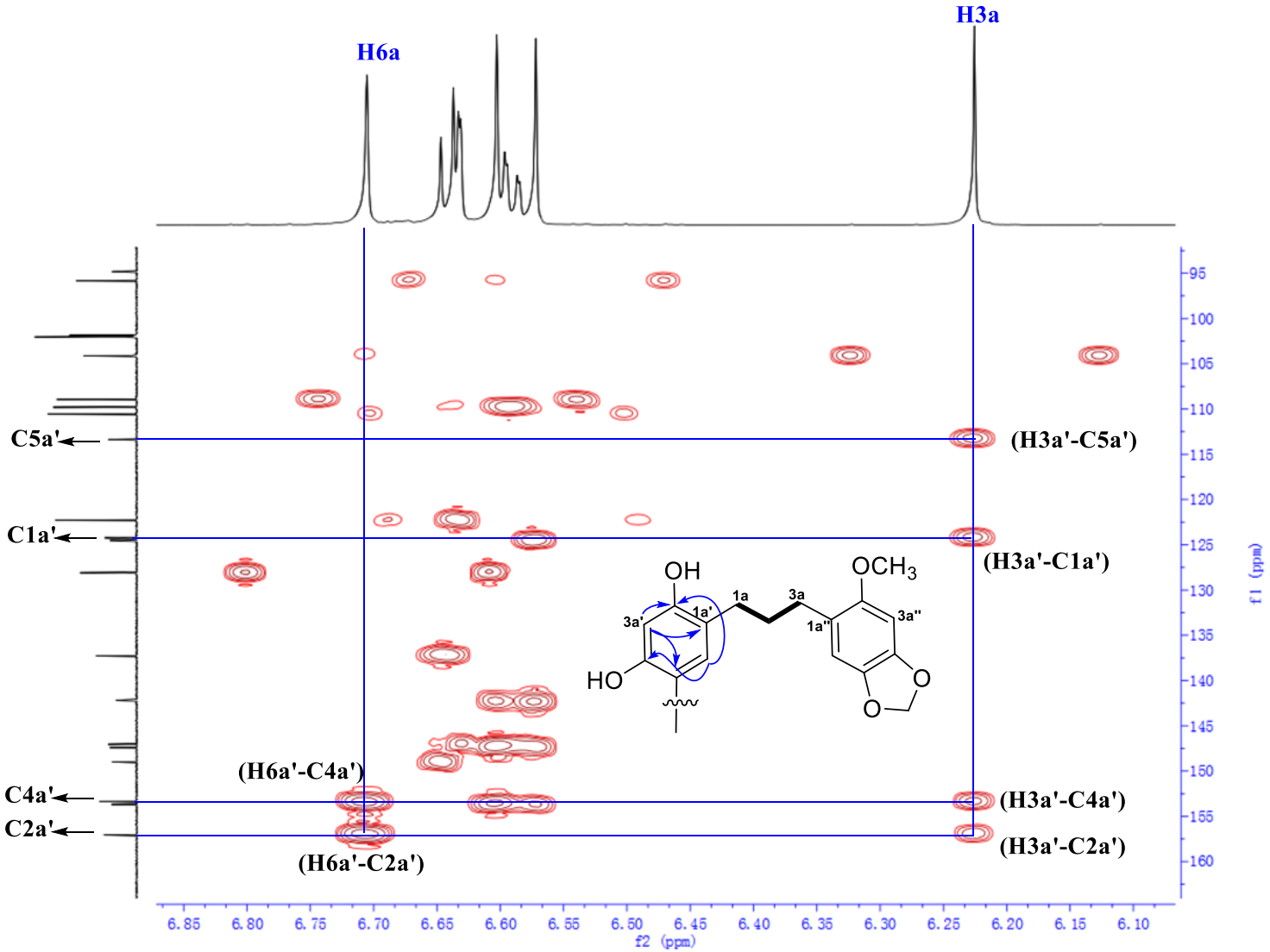

Figure S51. Key HMBC spectrum (δ_H 6.10-6.85 and δ_C 95-160) of unit II in compound **2**

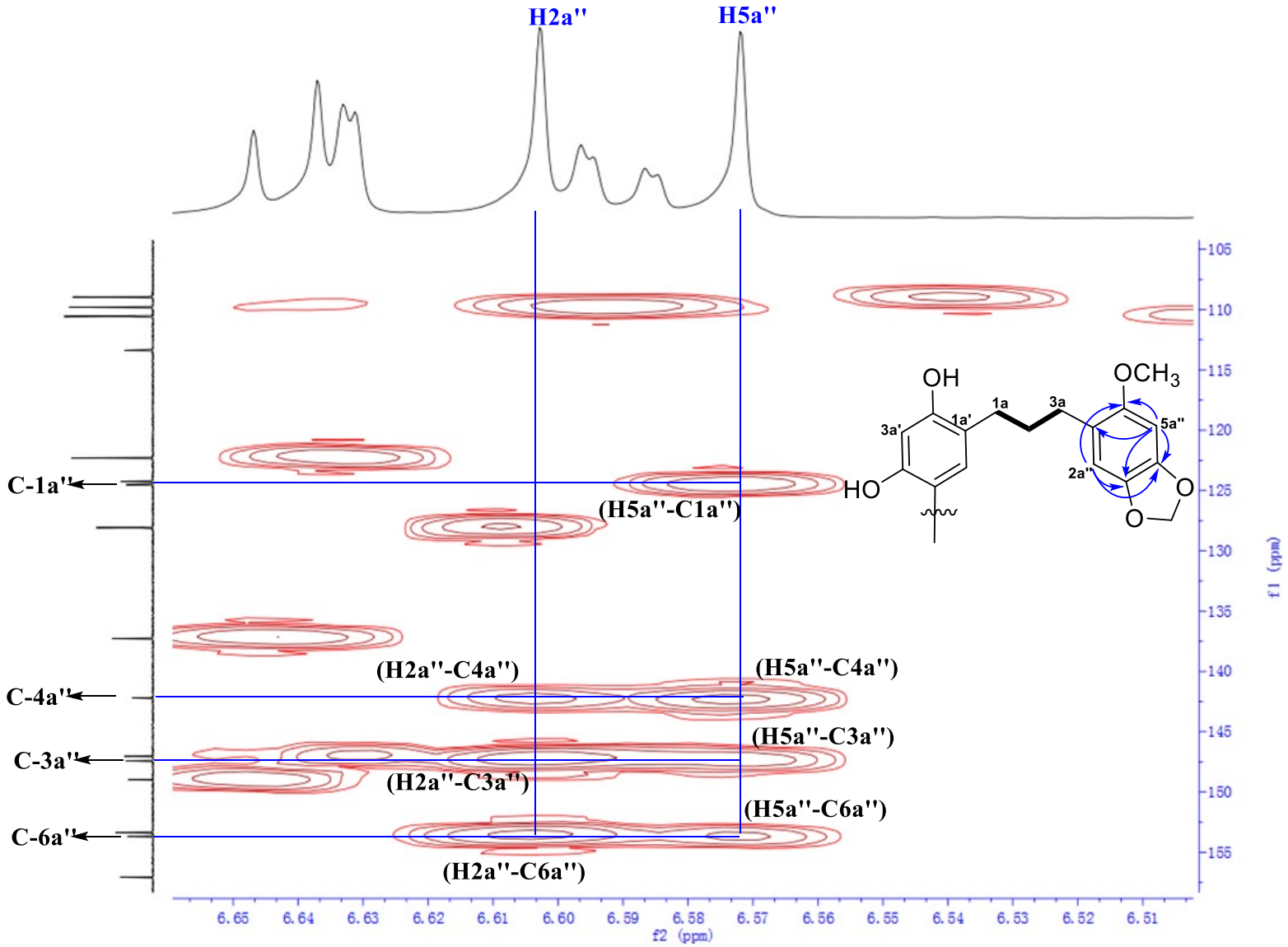

Figure S52. Key HMBC spectrum (δ_H 6.51-6.65 and δ_C 105-155) of unit II in compound **2**

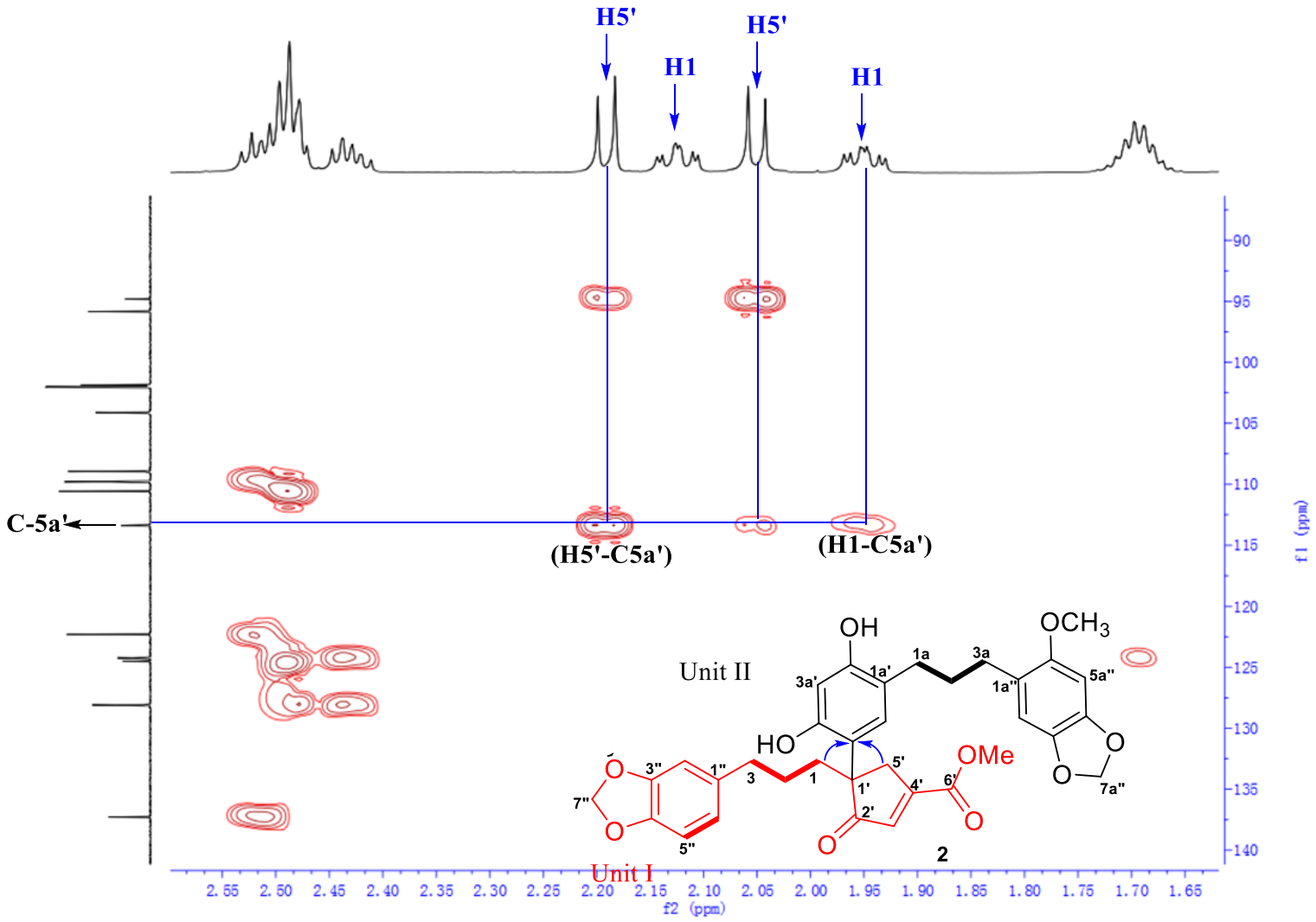

Figure S53. Key HMBC spectrum (δ_H 1.65-2.55 and δ_C 90-140) of compound **2**

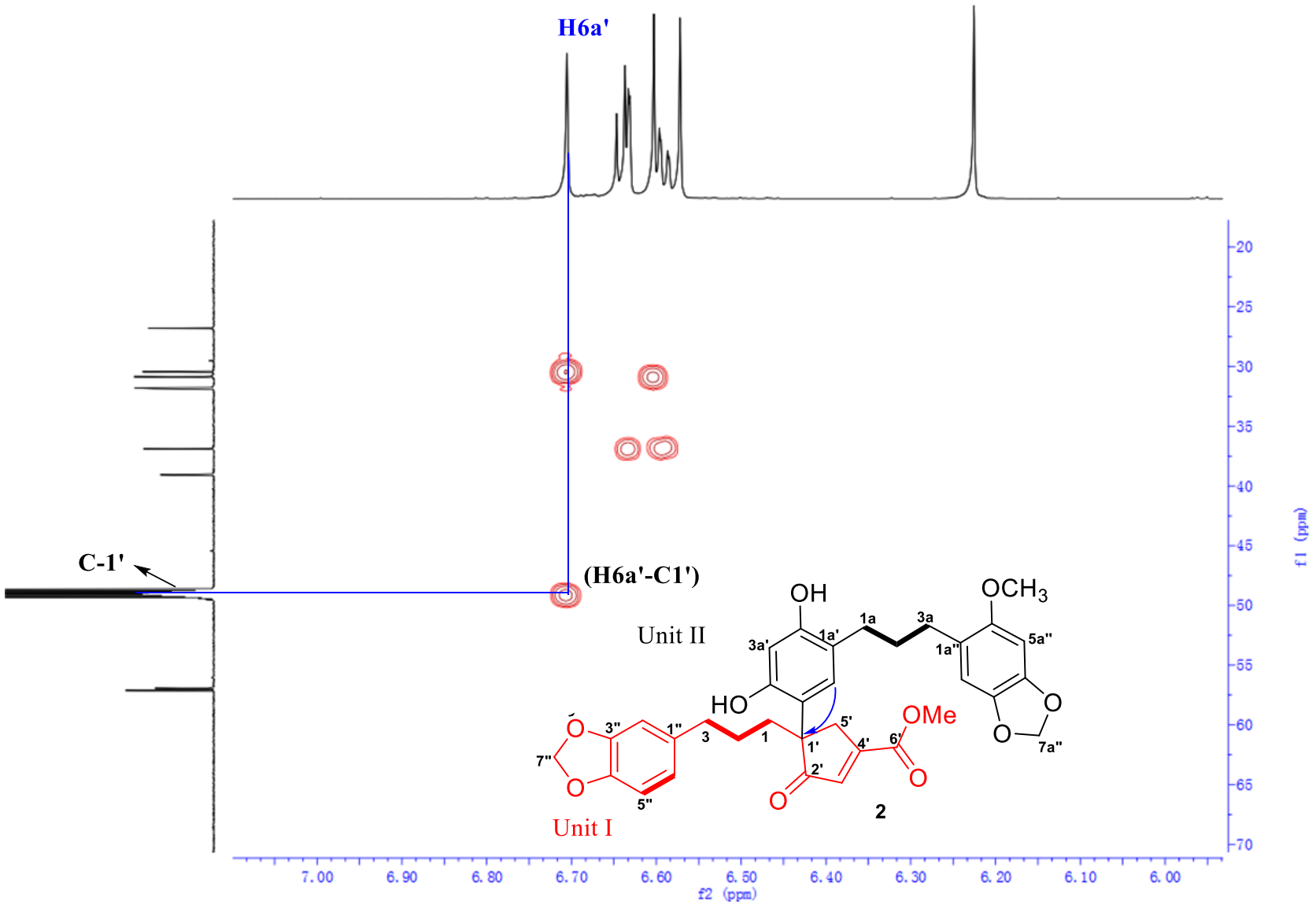

Figure S54. Key HMBC spectrum (δ_H 6.00-7.00 and δ_C 20-70) of compound **2**

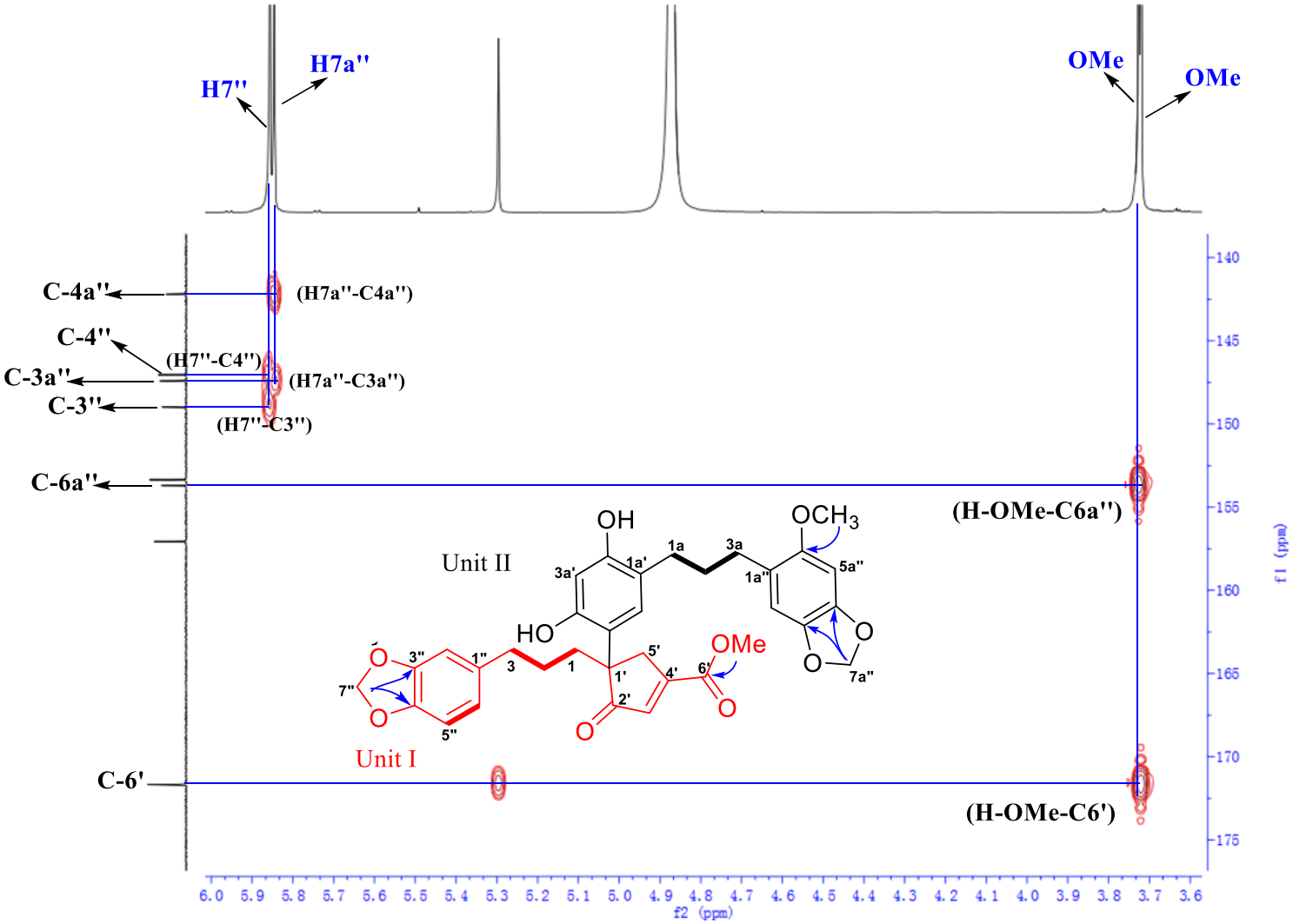

Figure S55. Key HMBC spectrum (δ_H 3.60-6.00 and δ_C 140-175) of compound **2**

User Spectra

Fragmentor Voltage	Collision Energy	Ionization Mode
135	0	ESI

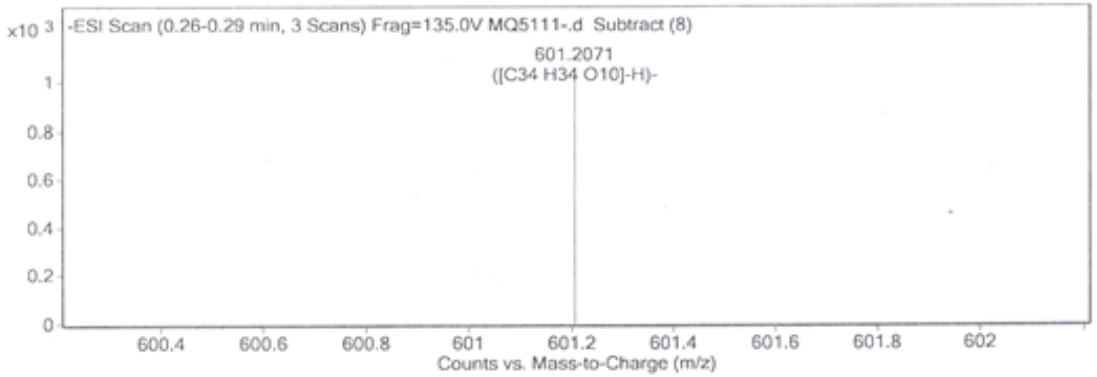

Peak List

m/z	z	Abund
184.9874	1	2830.51
205.1596	1	6582.36
250.1446	1	3091.27
255.2322	1	7408.83
279.1231	1	3459.85
413.1957	1	3521.71
449.1734	1	7411.48
499.1709	1	2672.65

Formula Calculator Element Limits

Element	Min	Max
C	3	60
H	0	120
O	0	30

Formula Calculator Results

Formula	CalculatedMass	CalculatedMz	Mz	Diff. (mDa)	Diff. (ppm)	DBE
C34 H34 O10	602.2152	601.2079	601.2071	0.2	0.3	18.0000

--- End Of Report ---

Figure S56. HRESI of compound **2**

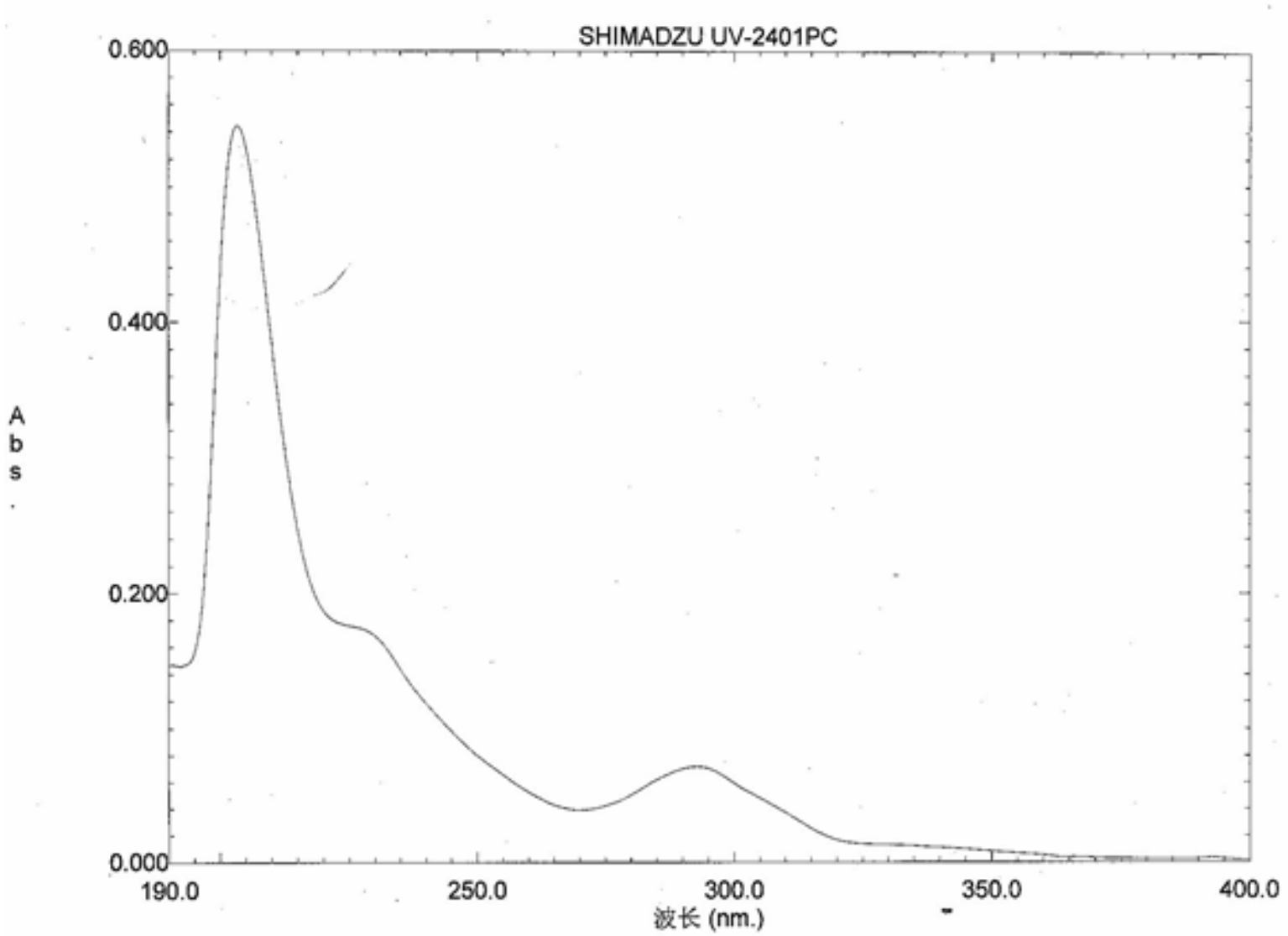

Figure S57. UV spectrum of compound **2**

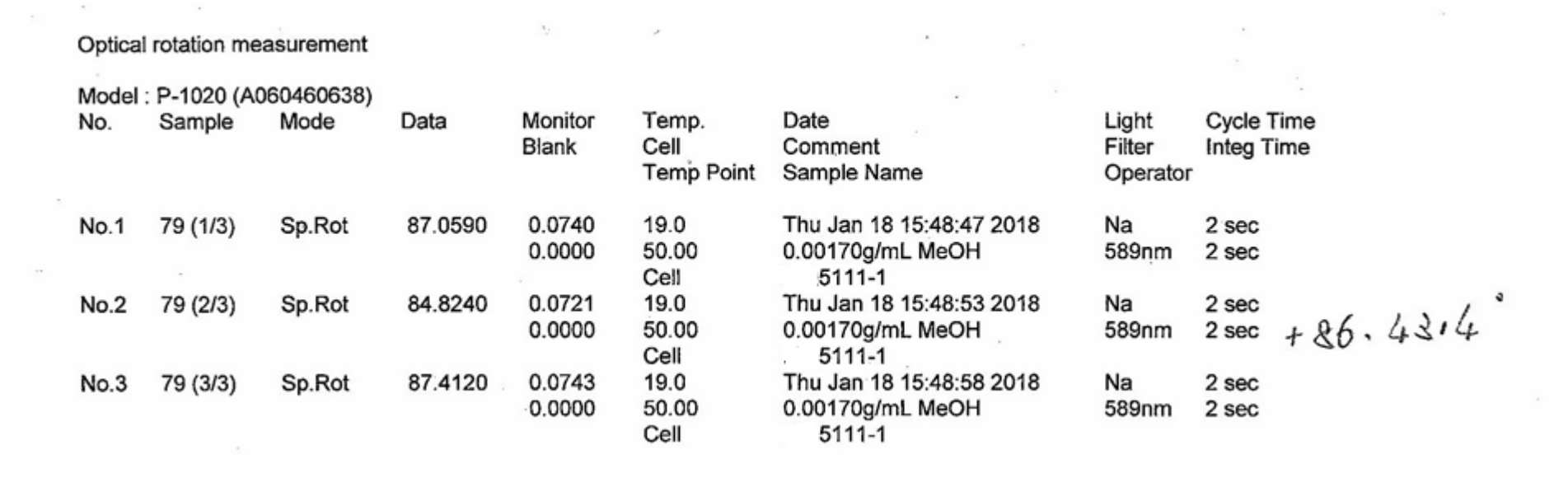

Optical rotation measurement

Model : P-1020 (A060460638)

No.	Sample	Mode	Data	Monitor Blank	Temp. Cell Temp Point	Date Comment Sample Name	Light Filter Operator	Cycle Time Integ Time
No.1	79 (1/3)	Sp.Rot	87.0590	0.0740 0.0000	19.0 50.00 Cell	Thu Jan 18 15:48:47 2018 0.00170g/mL MeOH 5111-1	Na 589nm	2 sec 2 sec
No.2	79 (2/3)	Sp.Rot	84.8240	0.0721 0.0000	19.0 50.00 Cell	Thu Jan 18 15:48:53 2018 0.00170g/mL MeOH 5111-1	Na 589nm	2 sec 2 sec
No.3	79 (3/3)	Sp.Rot	87.4120	0.0743 0.0000	19.0 50.00 Cell	Thu Jan 18 15:48:58 2018 0.00170g/mL MeOH 5111-1	Na 589nm	2 sec 2 sec

+86.434°

Figure S58. ORD of compound **(+)-2**

Optical rotation measurement

Model : P-1020 (A060460638)

No.	Sample	Mode	Data	Monitor Blank	Temp. Cell Temp Point	Date Comment Sample Name	Light Filter Operator	Cycle Time Integ Time
No.1	81 (1/3)	Sp.Rot	-121.8330	-0.0731 0.0000	18.8 50.00 Cell	Thu Jan 18 16:07:21 2018 0.00120g/mL MeOH 5111-2	Na 589nm	2 sec 2 sec
No.2	81 (2/3)	Sp.Rot	-125.1670	-0.0751 0.0000	18.8 50.00 Cell	Thu Jan 18 16:07:26 2018 0.00120g/mL MeOH 5111-2	Na 589nm	2 sec 2 sec
No.3	81 (3/3)	Sp.Rot	-125.0000	-0.0750 0.0000	18.8 50.00 Cell	Thu Jan 18 16:07:31 2018 0.00120g/mL MeOH 5111-2	Na 589nm	2 sec 2 sec

−124.0000°

Figure S59. ORD of compound **(-)-2**

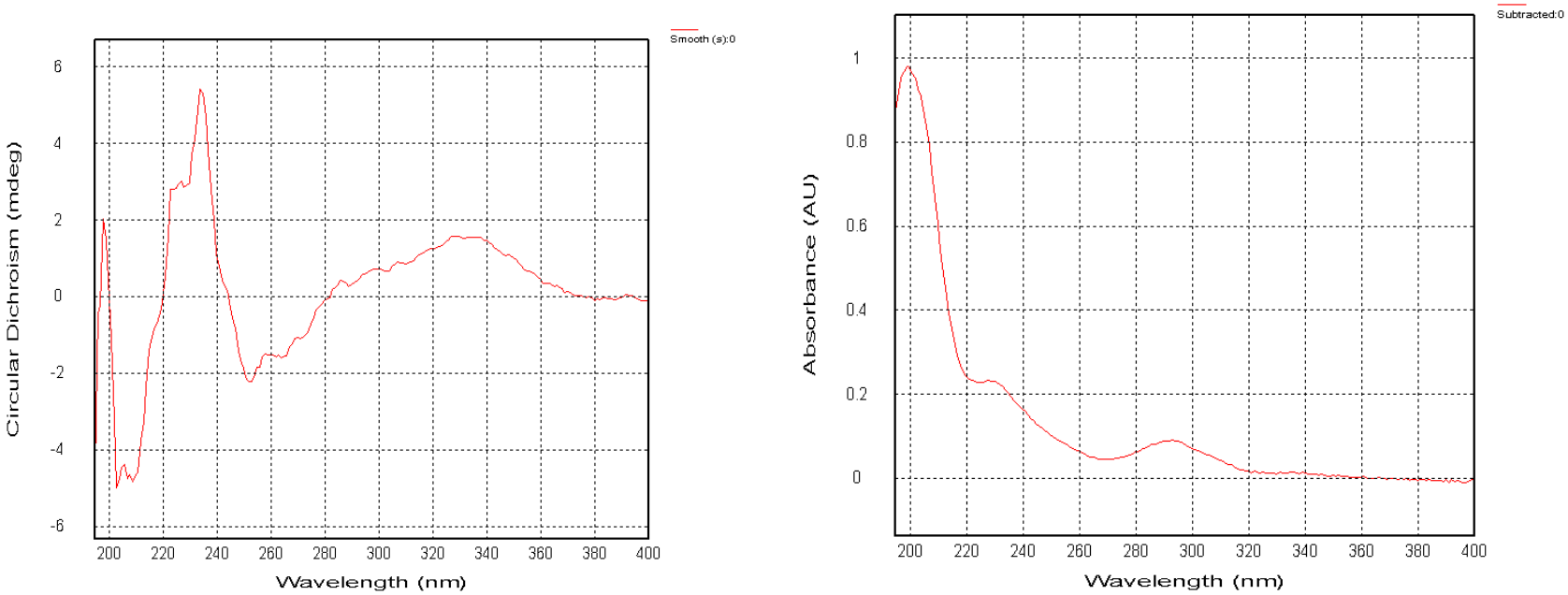

Figure S60. CD spectrum of compound **(+)-2**

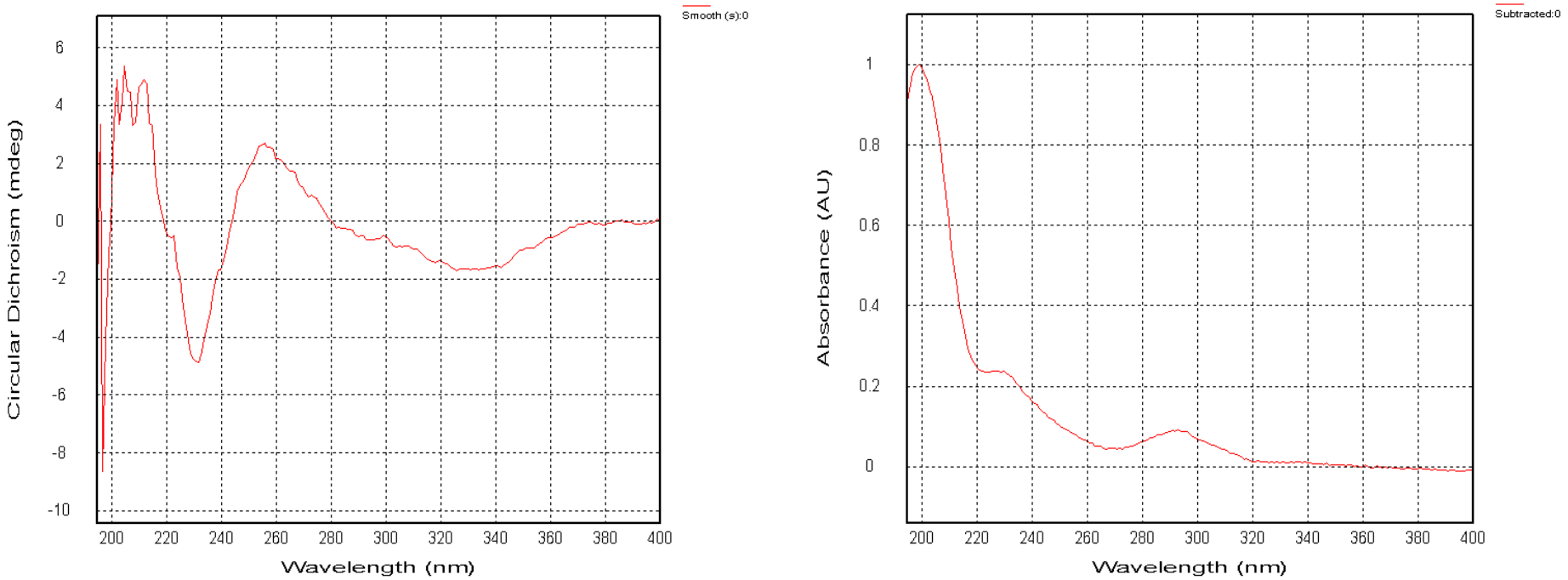

Figure S61. CD spectrum of compound **(-)-2**

Reference

1. Morris, G. M.; Huey, R.; Lindstrom, W.; Sanner, M. F.; Belew, R. K.; Goodsell, D. S.; Olson, A. J., AutoDock4 and AutoDockTools4: Automated docking with selective receptor flexibility. *Journal of Computational Chemistry* **2009,** *30* (16), 2785-2791.

2. (a) Giardina, G.; Montioli, R.; Gianni, S.; Cellini, B.; Paiardini, A.; Voltattorni, C. B.; Cutruzzolà, F., Open conformation of human DOPA decarboxylase reveals the mechanism of PLP addition to Group II decarboxylases. *Proceedings of the National Academy of Sciences* **2011,** *108* (51), 20514-20519; (b) Ren, J.; Zhang, Y.; Jin, H.; Yu, J.; Zhou, Y.; Wu, F.; Zhang, W., Novel Inhibitors of Human DOPA Decarboxylase Extracted from Euonymus glabra Roxb. *ACS Chemical Biology* **2014,** *9* (4), 897-903.

3. Zhou, Y.; Yu, J.; Lei, X.; Wu, J.; Niu, Q.; Zhang, Y.; Liu, H.; Christen, P.; Gehring, H.; Wu, F., High-throughput tandem-microwell assay identifies inhibitors of the hydrogen sulfide signaling pathway. *Chemical Communications* **2013,** *49* (100), 11782-11784.